THE EFFECT OF SURFACE CHEMISTRY AND POROSITY OF ACTIVATED CARBONS ON THE ADSORPTION OF TRACES OF ODORIFEROUS COMPOUNDS

By

YEHYA A. ELSAYED

A dissertation submitted to the Graduate Faculty of Chemistry in partial fulfillment of the requirements for the degree of Doctor of Philosophy at The Graduate School and University Center of The City University of New York

2006

UMI Number: 3213174

ProQuest Information and Learning Company
300 North Zeeb Road
P.O. Box 1346
Ann Arbor, MI 48106-1346

This manuscript has been read and accepted for the Graduate Faculty in Chemistry in satisfaction of the dissertation requirement for the degree of Doctor of Philosophy.

01/24/06	Prof. Teresa J. Bandosz
Date	Chair of Examining Committee
01/31/06	Prof. Gerald W. Koeppl
Date	Executive Officer

Prof. Teresa Bandosz

Prof. Ronald Birke

Prof. David Locke

THE CITY UNIVERSITY OF NEW YORK
The Graduate School and University Center of
The City University of New York

Abstract

THE EFFECT OF SURFACE CHEMISTRY AND POROSITY OF ACTIVATED CARBONS ON THE ADSORPTION OF TRACES OF ODORIFEROUS COMPOUNDS

by

Yehya A. Elsayed

Advisor: Professor Teresa J. Bandosz

The odor of human sweat has its origin in such substances as acetaldehyde, valeric acid and ethylmethylamine (EMA). As adsorbents for these compounds, three activated carbons of coal origin and wood origin were used in this study. The surface of the initial samples was modified using oxidation with nitric acid or impregnation with urea followed by heat treatment at 723K and 1223K. Boehm and potentiometric titrations, thermal analysis and diffuse reflectance FTIR were used to characterize the surface chemistry. Adsorption of acetaldehyde from the vapor phase was studied using inverse gas chromatography (IGC) and thermal analysis (TA). The results showed that hydrogen bonding and dispersive interactions contribute to the heat of acetaldehyde adsorption. At very low surface coverage acetaldehyde tends to adsorb in the small pores whereas with increasing surface coverage, acetaldehyde starts to adsorb in larger pores where functional groups contribute to the adsorption process. Adsorption of valeric acid and ethylmethylamine from aqueous solutions was measured at 333 K and 299 K, respectively. The calculated isotherms showed good fits to the Freundlich equation. Specific acid-base interactions governed the adsorption of both compounds from aqueous solution at low concentrations. At higher concentrations, the volume of small micropores

(< 10 Å) determined the capacity of carbons toward the valeric acid removal whereas the surface chemistry of activated carbons played the predominant role in case of EMA adsorption. The density of surface basic groups controlled amount of valeric acid strongly adsorbed whereas in the case of EMA the amount strongly adsorbed increased with an increase in the amount of strong acidic groups on the surface. In the case of adsorption from vapor phase under dry conditions, dispersive interactions and hydrogen bonding control the adsorption process of valeric acid while dipole-dipole, hydrogen bonding or specific acid-base interactions govern the mechanism for EMA adsorption. The presence of strong acidic groups not only increases the amount of EMA adsorbed but also promotes the incorporation of nitrogen into the surface when heat treatment is applied. In adsorption of EMA from humid air stream, water adsorbs preferably via hydrogen bonding and thus hinders EMA adsorption.

Acknowledgments

I would like to express my first, and most earnest, acknowledgment to my advisor and chair of my special Committee, Professor Teresa Bandosz. Words of thanks and appreciation will not be enough to compensate for the support and encouragement that she provided to me throughout my doctoral study. I would like to thank her for spending the time guiding me in my research, providing all the possible help to resolve the obstacles that I have met in the last five years. This thesis would have been impossible to be completed without her editorial and academic advices.

I would also like to thank my Committee members Professors Ronald Birke and David Locke for their guidance, support, helpful discussion and their valuable comments. I am grateful to them for sharing their valuable time in spite of their busy schedules.

I am truly grateful to all of those who helped me working towards finishing my Ph.D., and they are many. I wish to express my special gratitude to Professors Stanley Radel and Michael Weiner for their guidance and support when I came to City College. Without their help, I might not have had the opportunity to start my Ph.D.

I wish to express my special thanks to all my friends and my colleagues at City College of New York for all the discussions, cooperation and for the wonderful time we have shared. All of them deserve my heartfelt thanks and gratitudes specially Anna Kleyman for her love and care, Issa Salame, Svetlana Bashkova, Danh Nguyen-Thanh, and Deon Hines.

I am very grateful for the continuous help, love and encouragement of my parents, brothers, sisters and their families.

Especially, I would like to express my loving gratitude to the special person in my life, for her patience, understanding and support throughout the past years. She is a never-ending source of love and inspiration to me.

Table of Contents **Page**

List of Tables **Page**

List of Figures **Page**

CHAPTER 1
INTRODUCTION

1.1 Background

Adsorption of odoriferous pollutants from environment is nowadays of great importance to scientific community due to the effects of those pollutants on the ecosystem, and their noxious smell and toxicity. Besides pollutants introduced into the ecosystem from industry there are numerous natural sources of air contamination. One of them is the bodies of living organisms where body fluids are produced and then volatilized to the atmosphere. Air contamination by components of human emissions such as sweat becomes an important issue in clean rooms where sophisticated electronic instruments are produced, in confined species such as submarines, and ICU room in the hospitals. Some of the sweat components which are responsible for the unpleasant odor are acetaldehyde, valeric acid and ethylmethylamine (EMA).

To remove such species, several factors should be taken into consideration. These include the nature of the adsorbent and adsorbate along with adsorption conditions. Adsorbent characteristics consist of both structural parameters and surface chemistry. Examples include the surface area, pore size distribution, ash content, hydrophobicity, in addition to the type and amount of surface functional groups. On the other hand, the

nature of the adsorbate depends on the size of the molecule, hydrophobicity, its polarity and chemical nature. The adsorption conditions involve the temperature, the nature of the solvent (when applicable), and the presence of other competing species for the adsorption sites.

Removal of pollutants and contaminants from air and water on activated carbons is a well-known method used to clean the environment and prevent its pollution [1-3]. At present, activated carbon is one of the most promising solid adsorbents used to remove such compounds, owing to its commercial availability, high adsorptive capacity, surface chemistry and structural features including a high surface area and the presence of small pores, similar in sizes to the molecules to be removed [1, 3, 4]. In order to study the adsorption of these odoriferous compounds on activated carbons, characterizations of surface chemistry (quantitative and qualitative analysis of the surface functional groups) and structural parameters (pore size distribution, pore volume and surface area) of the activated carbon sorbents have to be carried out.

There are several experimental techniques that are applied to characterize the surface and to obtain information about the structural features and surface chemistry of activated carbons. Many of these techniques may not provide direct information due to the complexity of the carbon surface. The most commonly employed method for determining the pore size distribution of activated carbons involves the adsorption of gases and vapors such as nitrogen or carbon dioxide.

The surface chemistry of activated carbons can be analyzed using "wet" and "dry" methods of analysis. The most common "wet" methods are Boehm titration (amount of surface acid and basic groups) [5] and potentiometric titration (proton binding curves and pK_a distribution) [6-8] which provide qualitative and quantitative information about the carbon surface groups. These techniques work well when applied to oxygen groups on the surface. They classify acidic groups as phenols, lactones, and carboxylic acids, while neglecting other forms of acidic functional groups present on the surface. "Dry" methods are also used and include diffuse reflectance FTIR (DRIFTS) [9, 10], X-ray photoelectron spectroscopy (XPS) [11, 12], thermal analysis (TA) [13] and temperature programmed desorption (TPD) [14, 15]. The disadvantage of the dry methods is that they neither can

be applied directly for quantitative analysis (XPS and DRIFTS) [12] nor do provide direct qualitative information on the carbon surface chemistry (TPD) [14, 15].

1.2 Research Objectives and Scope

The main objective of this work is to develop a mechanism for adsorption of acetaldehyde, valeric acid and ethylmethylamine on activated carbons. This is achieved by studying their adsorption on various activated carbons with different levels of surface modifications. Surface characterization of the raw and modified activated carbons is included along with the adsorption studies from the vapor phase and liquid phase of the above mentioned compounds. The work is expected to have various impacts toward expanding the application of activated carbons as human odor adsorbents.

Scientific impact:

The research is expected to provide the fundamentals of body odor components adsorption on activated carbons. We expect our work to throw new light on a number of unanswered questions regarding activated carbons as deodorants: (i) What is the mechanism by which adsorption /immobilization occurs? (ii) How do the functionality, surface acidity, and arrangement of oxygenated and nitrogen-containing sites on the surface affect adsorption? (iii) What are the optimum density, type, and geometric arrangement of sites that give a maximum adsorption? (iv) How do temperature, pore width, and pore volume affect the adsorption process? At present no fundamental mechanism of the process is described. In addition, we expect the work to lead to improved methods for the surface characterization of carbons as deodorants and filters.

Applied impact:

There is a great interest in the chemical, cosmetics, gas, pharmaceutical, and high tech industries in the behavior of activated carbons as adsorbents of specific odor molecules. Body odor is inevitable. It can disturb human productivity and have an impact on the lifetime of sophisticated computers. All of this has generated much research on odor control. The Intellectual Property Network [16] lists 2,450,531 patents related to various methods and devices to remove odors. Defining the features of carbons useful for

removal of body odor can enhance the performance of already working inventions and indicate new, still uninvented, approaches.

CHAPTER 2

LITERATURE REVIEW

Adsorption phenomena have been used for a long time to perform various separation or purification processes. The success or failure of an adsorption process depends on how the solid performs in both equilibrium and kinetic conditions [17]. The first controls the adsorptive capacity while the second is related to finding the way of adsorbate molecules to the interior of a surface area or micropore volume. Thus a good solid adsorbent is the one that provides sufficient adsorptive capacity as well as good kinetics. An adsorbent that satisfies these two requirements must be a porous solid having a reasonably high surface area and micropore volume. It must have also a reasonably large pore network allowing the transport of molecules to the interior. In other words, the porous solid must have a combination of pore ranges mainly in the micropore (small pores) and mesopore (larger pores) ranges. Among the adsorbents used in industry, activated carbon is the most versatile because of its high surface area and micropore volume [17].

2.1 Activated Carbon

Activated carbons have been widely used as adsorbents in purification systems for centuries [1, 2, 18]. They are obtained by carbonization of organic matter-rich precursors at high temperature followed by activation [19]. Activation creates pores in the structure. Activated carbons have been commercially produced from a broad variety of carbon-containing starting materials such as coconut shells, paper-mill waste, wood char, carbon

black, sawdust, coal and petroleum coke [18]. They can be prepared by physical or chemical activation. Physical activation is based on the reaction of various forms of chars at elevated temperatures with steam, carbon dioxide, carbon monoxide, or oxygen. In chemical activation, chars are chemically activated during carbonization with activating agents at various temperatures. The most common activation agents are phosphoric acid, ammonium hydrogen phosphate and potassium hydroxide. Various activation methods result in diversity in pore size distribution and surface chemistry of a carbon material. These surface properties of activated carbons are responsible for their adsorptive capacities. There are at least three primary variables in the activation of carbon which can affect the surface chemical and structural properties and consequently the adsorptive properties of activated carbon products. They are: (1) the nature of the starting material; (2) the composition of the activation atmosphere; and (3) the time and temperature of the activation processes. Based on the resulting surface properties, some activated carbons will be favored over other carbons in their application as adsorbents.

The development of porous activated carbons with a high surface area and thus adsorption capacity is associated primarily with the degree of burn off of starting materials. Various activated carbons with different pore size distribution have been produced. These pores range in size from few angstroms (Å) to a few hundred angstroms. The pore sizes are divided into three main groups: micropores, mesopores, and macropores. Micropores are pores that are less than 20 Å in size; mesopores are pores with the size of 20 Å– 500Å; macropores are pores larger than 500 Å.

A three dimensional model to describe activated carbons structure was suggested by Stoeckli (Figure 1) [20]. This model describes activated carbons as a loose packing of graphene layers of curved aromatic rings between which slit-shaped micropores are believed to exist [21]. The larger pores (meso- and macropores) result from voids between aggregates. It was found that highly microporous carbons are obtained from coal, petroleum pitch, or coconut shells, whereas mesoporous activated carbons having low mechanical stability and low density have their origin in wood as an organic precursor [22].

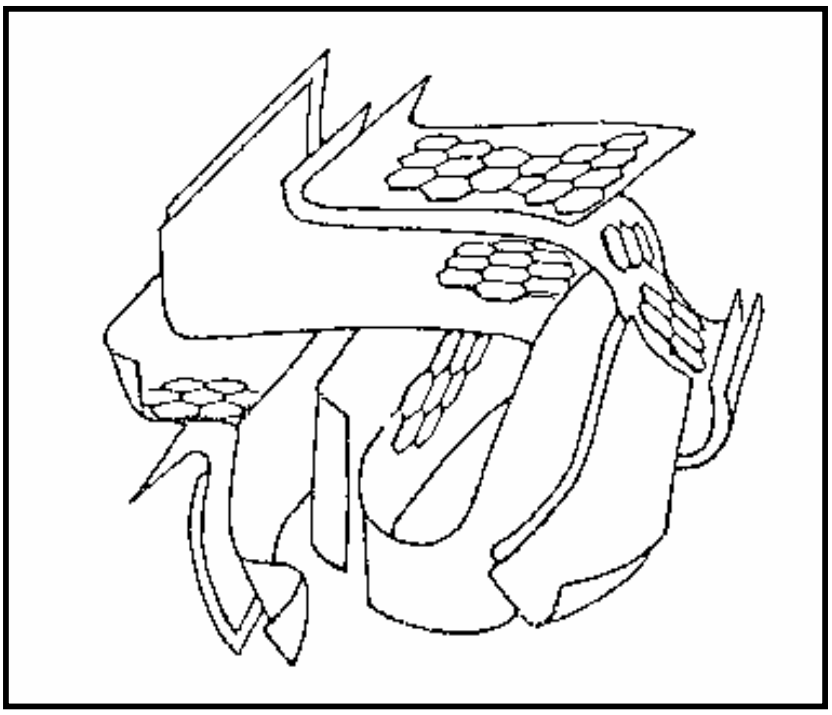

Figure 1: Schematic structure of an active carbon [20].

As mentioned above, both porosity and surface chemistry are responsible for the adsorptive nature of the material. It is important to mention then that surface of carbon is not totally hydrophobic from the chemical point of view. The chemical nature of the activated carbon surface is more complex than its pore network and determines its chemical heterogeneity. This heterogeneity results from the presence of heteroatoms other than carbon in the activated carbon matrix [5]. The heteroatoms include oxygen, nitrogen, sulfur and phosphorus. They usually exist in the form of organic functional groups at the edges of the graphene layers. The origin of these heteroatoms is in the nature of the organic precursors (nitrogen, oxygen and sulfur), in the chemistry of activation processes (oxygen and phosphorus), in the storage conditions (oxygen), and in the further modification processes (oxygen and nitrogen) [23].

Mostly, activated carbons are made from raw materials which are usually rich in oxygen and therefore many oxygen functionalities are expected to exist on the surface. Also, the presence of oxygen functionalities is always expected as a result of self-oxidation [2] or the method of activation. A variety of different oxygen functional groups can exist on the carbon surface. Figure 2 shows some examples of the IR- active oxygen

functionalities found on the surface [10, 24]. They include chromene, carboxylic acids, phenols, pyrones, carbonyls, ethers and lactones.

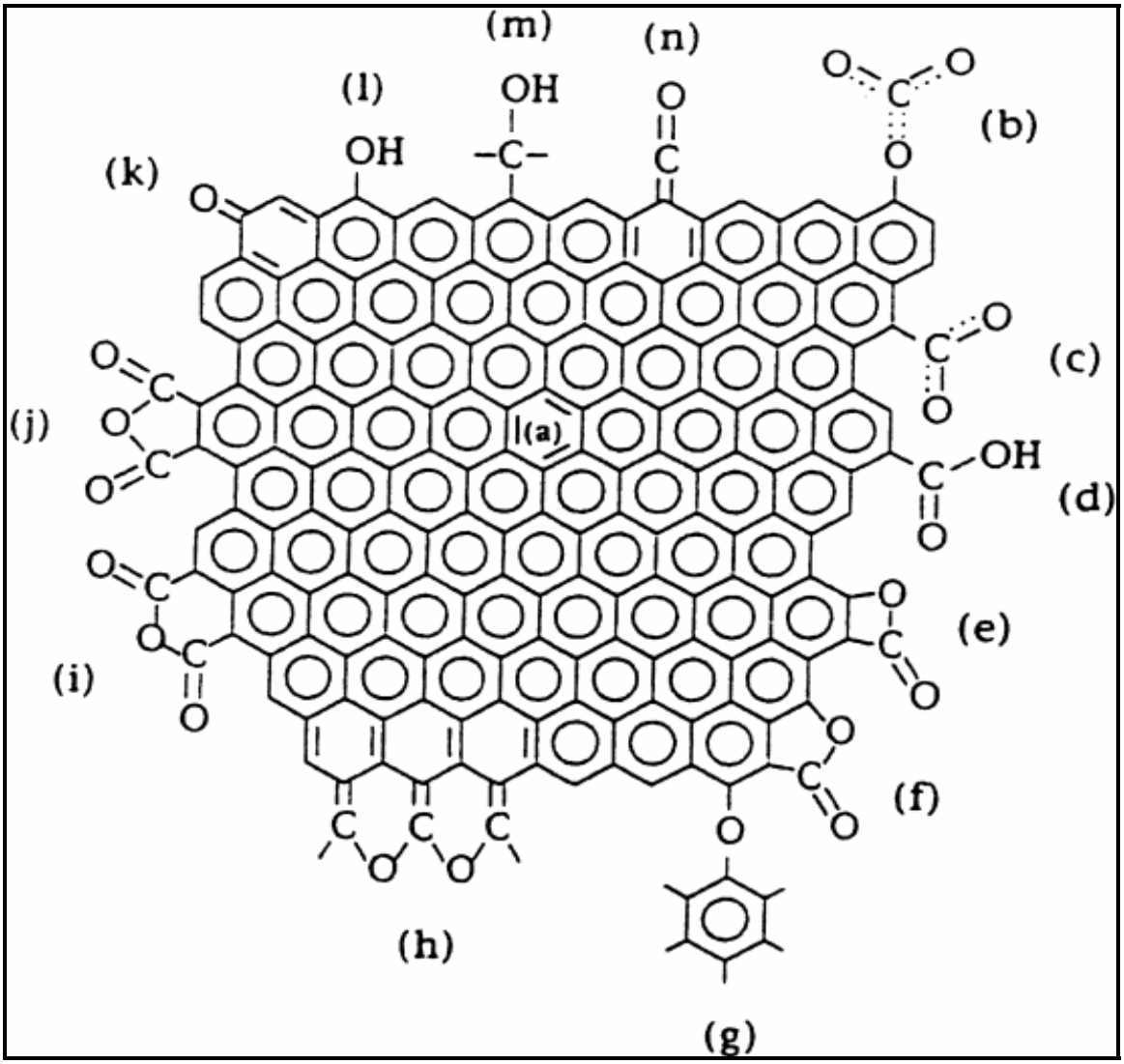

Figure 2: IR-active functionalities on carbon surfaces: (a) aromatic C C stretching; (b) and (c) carboxyl-carbonates; (d) carboxylic acid; (e) lactone (4-membered ring); (f) lactone (5-membered ring); (g) ether bridge; (h) cyclic ethers; (i) cyclic anhydride (6-membered ring); (j) cyclic anhydride (5-membered ring); (k) quinone; (l) phenol; (m) alcohol; and (n) ketene [10, 24].

One of the most common methods to introduce nitrogen groups into the surface is urea impregnation followed by heat treatment at different temperatures [25-28]. As shown in Figure 3, this modification introduces nitrogen in the form of amines, amides, imides, pyridine and nitro groups [25-28]. It is worth mentioning that the presence of

heteroatoms such as oxygen and nitrogen determines the acidity and basicity of the activated carbon surface [4, 5].

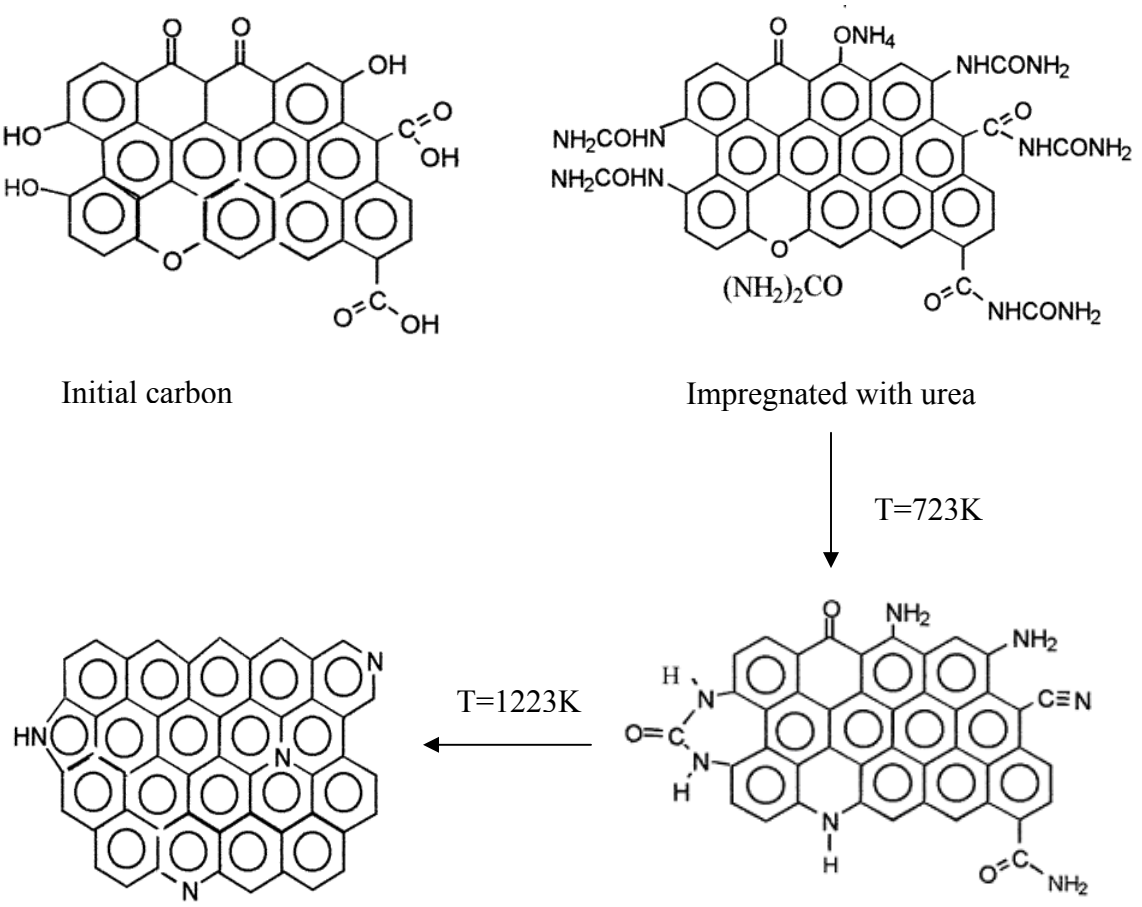

Figure 3: Schematic representation of changes in surface chemistry of carbons due to saturation with urea and heat treatment [28].

2.2 Adsorption Processes

Adsorption processes are classified and defined according to the mode of interaction between the adsorbate molecules and the surface of activated carbon. In their efforts to define the modes of interaction on adsorption, Garten and Weiss [18] classified adsorption processes as physical and chemical in their nature. Adsorption was denoted as physical adsorption if it occurs via dipole-dipole interaction, hydrogen bonding, or van der Waals forces. According to Garten and Weiss chemical adsorption refers to adsorption by electrostatic forces, ionic and covalent bonds. There are currently two defined mechanisms of physical adsorption on the surface of activated carbons [29-34]:

dispersive interactions and specific interactions. The dispersive forces and thus the adsorption strength is expected to increase as the size of pores becomes closer to the diameter of the adsorbate molecule due to the overlapping of adsorption potential [29-33]. On the other hand, the presence of heteroatoms has a significant effect on the adsorption of polar species via specific interactions such as hydrogen bonding, dipole-dipole and specific Lewis acid–base interactions [34]. Heteroatoms can catalytically affect the conversion of adsorbed species as in the case of hydrogen sulfide adsorption [13, 28]. In addition, chemical groups may also have an effect on the sorption of non-polar molecules by creating obstacles for physical adsorption and preventing the molecule from occupying the most energetically favorable position on the surface [35].

The strength of adsorption processes covers a wide range of bond energies representing the different physical and chemical interactions [18]. Adsorption is always exothermic with an observed net decrease in the enthalpy, ΔH, of the process. This is because surface adsorption, regardless of the energy of the interaction, must always proceed with a negative free-energy change, ΔG, as well as a decrease in entropy, ΔS. This decrease at a particular temperature T is defined by the general equation:

$$\Delta H = \Delta G + T\Delta S \tag{1}$$

Physical adsorption is a relatively weak adsorptive interaction process which is assumed to proceed rapidly with a zero or negligible activation energy and is completely thermodynamically reversible [36]. The attractive forces in physical adsorption processes are represented by the types of interactions responsible for the condensation of a gas, and involve net energies that are typically 5-40 KJ/mol related to factors like molecular mass and polarity. Conversely, chemical adsorption or chemisorption may or may not have finite activation energy and may or may not proceed rapidly [37]. Some chemisorption reactions involve a thermodynamically irreversible step. The net enthalpies for chemisorption processes vary over a range from 8 kJ/mol to 800 kJ/mol depending on the chemical bond strength [18]. The nature of this bond may lie anywhere between the extremes of virtually complete ionic or complete covalent character. Since chemisorption processes are often characterized by chemical reactions, a chemical specificity between

the sorbate and the sorbent is required. This chemical specificity requires a clean or at least reactive surface. In some cases, chemisorption may be accompanied by physical adsorption onto the chemisorbed layer when solution is involved.

Although physical adsorption and chemisorption can be differentiated based on the net enthalpy change values, difficulties start to arise in case of adsorption from aqueous solution, mainly when the net enthalpy-change are in the range 8-60 KJ/mol [18]. Adsorption energies in this range are hard to be classified as either physical or chemical adsorption based on the energy of interaction alone. Often the lack of knowledge about the chemistry of the specific activated carbon surface itself, make it harder to differentiate between these two types of adsorption.

In adsorption from a gas phase, activated carbons act as well-defined systems of pores and the adsorption in these pores is classified as physical. Physical adsorption processes from a gas phase may involve multilayer formation of the sorbate molecules [38] while chemisorption results in only monolayer formation [38]. In adsorption from solution, the interaction of the solute molecules with the solvent molecules is usually significantly greater than their attraction with each other, so that after the formation of the first monolayer on a surface, multilayer formation usually does not take place. This type of interaction does not occur in gas-phase systems. The result of this general lack of multilayer formation for adsorption from solution makes it impossible to use the surface coverage parameters alone as a method of distinguishing between physical adsorption and chemisorption. In most of the recent studies, adsorption processes from solution are classified as specific when they involve direct interactions.

The specific interaction of the adsorbates with the carbon surface groups is also affected when adsorption occurs from solution. Although oxidation of activated carbons is expected to increase the removal of polar organic compounds from the gaseous phase by enhancing the specific interactions [39, 40], it was found that presence of acidic groups reduces the adsorption of polar and non polar organic compounds from aqueous solution [40-44]. This is due to the preferential adsorption of water onto carbon surfaces containing oxygen and nitrogen groups [40-44]. Water can adsorb via hydrogen bonding on oxygen-containing groups, which is followed by clustering of additional water molecules at these sites [4, 45]. The resulting water clusters can prevent an adsorbate

access to hydrophobic sites, mainly in micropores, thus reducing the interaction energy between the adsorbate molecule and the adsorbent surface. The extent of the competition between water and polar adsorbate for adsorption sites depends on the chemistry of these active sites, their location on the surface and the strength of hydrogen bonding between water and those surface sites. Therefore, the higher is the ability of the adsorbate to strongly bond to the surface groups and thus compete with water more effectively, the more important is the specific nature of an adsorption process.

2.2.1 Acetaldehyde

Acetaldehyde, also called ethanal, is an aldehyde with the formula CH_3CHO. Pure acetaldehyde is a colorless and flammable liquid with pungent, fruity odor and is miscible in water. Its vapor pressure is 740 mmHg at 293K, boiling point 293.8 K and odor threshold 0.21 ppm. Acetaldehyde is the first and most toxic poison formed during ethanol metabolismT in the body. It was reported [46] that more than 90% of the ingested ethanol is metabolized in the body into acetaldehyde and acetate. Acetaldehyde is classified as a probable carcinogen. It is unstable in air and undergoes autopolymerization with metals or acids.

Besides its presence in human sweat, acetaldehyde is also a component of tobacco smoke and automobile exhaust gas. Since acetaldehyde is odoriferous at very low concentrations and stimulates the skin, eyes, nose, and respiratory tract, an effective removal method is needed. Cal and co-workers [47] examined the use of activated carbon cloths (ACC) to remove low concentrations of acetaldehyde, acetone, benzene, and methyl ethyl ketone from air. The main goal of their work was to produce filtration systems for indoor air environments, industrial gas streams, and spray paint booths. Adsorption isotherms were measured for acetaldehyde, acetone, benzene and water vapor samples. For the 10-1000 ppmv concentration range examined, benzene exhibited the highest adsorption capacity, followed by acetone and then acetaldehyde. Water vapor adsorption was not significant except at high relative humidities (>50%). The Dubinin-Radushkevich (DR) equation [48] was used to describe the physical adsorption and to predict the equilibrium adsorption capacities of the organic compounds examined in that study. The DR equation is represented by:

$$W = W_0 \exp - (A / \hat{a} E_0)^2 \quad (2)$$

where W (mg/g) is the adsorption capacity, W_0 (mg/g) is the total volume of the micropores accessible to the given adsorbate, *A* (kJ/mol) is the differential molar work and is equal to RT ln(P/P_0), â is the affinity coefficient, and E_0 (kJ/mol) is the characteristic adsorption energy. The DR equation was used to extend the adsorption capacity characterization for adsorbates from 100 ppbv to 10 000 ppmv range using the experimental data obtained in the 10-1000 ppmv concentration range [47]. Applying Dubinin-Radushkevich approach, Cal and coworkers found that the adsorption capacity obtained for acetaldehyde was far smaller than the adsorption capacities of the other compounds. That was related mainly to the high vapor pressure of acetaldehyde at 298 K.

Cal [49] also studied the effect of oxidation and amination on the adsorption capacities of acetaldehyde, acetone, benzene, and methyl ethyl ketone from air. The results showed that oxidation of activated carbons enhanced the physical adsorption of acetaldehyde, acetone and water vapor. An increase in the acetaldehyde adsorption capacity on the oxidized carbon was attributed to an increase in dipole interactions and the number of hydrogen bonds that form between acetaldehyde molecules and the additional carboxylic groups present on the oxidized carbons. This effect appeared to be the most pronounced at lower adsorbate concentrations, and diminished at higher adsorbate concentrations when the larger adsorbent pores begin to fill. Nitrogen-containing activated carbons showed improved acetaldehyde adsorption capacity over untreated samples. Cal and co-workers explained that increase by the interactions of acetaldehyde with the basic groups and a change in the pore structure as a result of modifications.

Rong and co-workers [50] studied the effect of air oxidation and heat treatment on the adsorption of formaldehyde on rayon-based activated carbon fibers (ACFs). They found that samples oxidized at the temperature range of 723–1123 K showed a remarkable increase in the adsorption rate. Heat treatment resulted in an increase in the pore volume and surface area of the carbon samples under study. This increase was favorable for formaldehyde adsorption. The amount of oxygen-containing functional groups also increased on the surface of the oxidized samples which was expected to have

an important influence the adsorption behavior. Rong and coworkers also found that the adsorption capacities were higher after air oxidation of the ACFs. In their final conclusion, they related an increase in the adsorption capacity and breakthrough times for formaldehyde to the cooperative effect of dipole- dipole interaction, hydrogen bonding, an increase in the specific surface area, and the increased total pore volume of the modified ACFs.

Adsorption of formaldehyde on activated carbons was also studied by of Domingo-Garcia and co-workers [51]. They found that formaldehyde is strongly adsorbed with isosteric heat between 15-33 kJ/mol. The retention volumes obtained in that study increased with an increase in the surface areas of activated carbons.

Recently, Hayashi and co-workers [52] studied the acetaldehyde adsorption capacities on activated carbons impregnated with various amines. They found that the adsorption capacity of impregnated activated carbons is influenced by the steric structure of impregnants as well as their acidity. The adsorption capacities of activated carbons impregnated with 2-aminoethanol, morpholine, aniline, *m*-anisidine, *p*-anisidine, *p*-phenetidine, *m*-toluidine, and *p*-toluidine increased linearly with an increase in the amount of impregnation. The activated carbons impregnated with these amines remove acetaldehyde via the following condensation reaction:

$$R\text{-}NH_2 + CH_3CHO \rightarrow R\text{-}N{=}CHCH_3 + H_2O \qquad (3)$$

On the other hand, activated carbons impregnated with *p*-aminophenol, *p*-nitroaniline, and *p*-phenylenediamine did not adsorb acetaldehyde, indicating that these amines do not react with acetaldehyde on the activated carbon surface.

The activated carbon impregnated with aminobenzenesulfonic acid differed from that impregnated with the other amines in the acetaldehyde adsorption mechanism [52]. In case of aminobenzenesulfonic acid, a Doebner- Miller reaction was involved. This reaction takes place only under acidic conditions, where a molecule of aromatic amines reacts with two molecules of aldehydes. Aminobenzenesulfonic acids were not only the reactant but also the acid catalyst in the removal of acetaldehyde. The obtained results showed that p-aminobenzenesulfonic acid reacted with acetaldehyde without steric

hindrance. The proposed reaction scheme between aminobenzenesulfonic acids impregnated on the activated carbon and acetaldehyde is as follows:

$$2CH_3CHO \xrightarrow{H^+} CHCH_3{=}CHCHO + H_2O \quad (4)$$

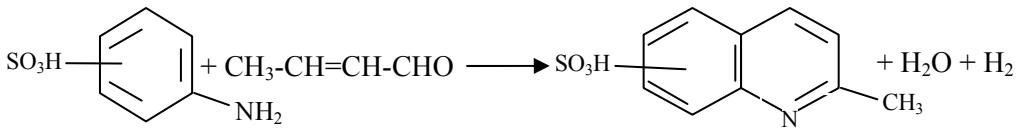

(5)

In the first step, two molecules of acetaldehyde condense to form crotonaldehyde by acid-catalyzed aldol condensation on the surface of activated carbon, where aminobenzenesulfonic acids serve as the acid catalyst for this reaction. Then crotonaldehyde reacts with aminobenzenesulfonic acids to form 2-methylquinoline derivatives in the second reaction. Because the second reaction is hindered for the *o*- and *m*-aminobenzenesulfonic acids compared to *p*-aminobenzenesulfonic acid, the reactivities of *o*- and *m*-aminobenzenesulfonic acids are lower than that of *p*-aminobenzenesulfonic acid which showed to be the most suitable impregnation for the chemisorption of acetaldehyde.

To our best knowledge the heat of acetaldehyde adsorption on activated carbon has not been reported. We expect it to be greater than the heat of ethane adsorption and smaller than that of acetone. The heats of adsorption for these compounds on nonporous carbon blacks were investigated by Avgul and Kiselev and their values were 15 kJ/mol for ethane and 35 kJ/mol for ethanol [34]. On the porous materials, the heats are expected to be twice greater reaching about 30 kJ/mol for ethane and 70 kJ/mol for acetone [33]. On the other hand, the heat of formaldehyde adsorption on various activated carbons was found to be between 15-33 kJ/mol [51]. Following this, and Avgul's and Kiselev's evaluation of the heat of one CH_3 moiety on nonporous carbon black to be equal to 9 kJ/mol [34], the heat of acetaldehyde obtained on microporous carbons should be in the range of 33-51 kJ/mol. When contribution of hydrogen bonding exists, the heat should be even greater of about 10 kJ/mol [34].

2.2.2 Valeric Acid

International Occupational Safety and Health Information Centre (CIS) classifies valeric acid as a corrosive liquid and harmful to aquatic life. Valeric acid, with the chemical formula $CH_3(CH_2)_2COOH$, is a colorless liquid with a characteristic smell identical to the smell of sweat or stinking socks. Its odor threshold was reported to be 0.015 ppm. CIS summarized its main physical properties which include: vapor pressure 0.02 kPa at 293 K, solubility in water 2.4 g/100mL and boiling point about 460 K.

Although there are many papers published describing the role of the activated carbons in the adsorption of weak electrolytes and nonelectrolytes from aqueous solution [18], little is mentioned about valeric acid adsorption [18, 53-62]. In brief, most of those papers studied the adsorption of aliphatic acid from solutions on different adsorbents. The polarity of solvents and adsorbents used varied between one study and another. Most of the results were interpreted based on Traube's Rule on surface tensions of aqueous solutions of organic solutes. Traube found that surface activity increases strongly and regularly as any series is ascended. Because surface activity is related to adsorption at the interface, Traube's Rule had been expressed in terms of the regular increase in the strength of adsorption of successive members, as measured by the work required to remove one mole from the surface layer to the bulk of the solution [53].

In 1926, Freundlich studied the adsorption of lower fatty acids from aqueous solutions on charcoal [54]. By applying the Traube's Rule [53], he found an increasing adsorption with increasing chain length. Similar results were obtained by Landt and Knop for the adsorption of lower fatty acids from aqueous solution on ash-free sugar charcoal [55]. In 1974, analogous behavior was obtained by Parkash [56] on a series of lower aliphatic acids (formic to caproic) adsorbed from aqueous solutions on activated carbon. The adsorption appeared to increase regularly as one ascends the homologous series following the Traube's rule behavior; however, of all the surface area available for N_2 adsorption, only a fraction of it was available for adsorption of the aliphatic acids. Wang and coworkers [57] presented the adsorption data for five pure carboxylic acid systems (acetic acid, propionic acid, n-butyric acid, n-hexanoic acid, and n-heptanoic acid) at three different temperatures, 278, 298, and 313 K. For an equilibrium concentration of 0.1 M, the uptake of the acids was about 37% greater than the uptake found by Parkash

[56] for the same adsorbent. The greater uptake was attributed to the more extensive acid pretreatment of the carbon in the preparation step prior to the experiments. Examination of the adsorption data showed that the adsorption of lower aliphatic acids from aqueous solutions increases with an increasing chain length. Their result agrees with Traube's rule since the addition of a $-CH_2$ group to the aliphatic acid molecule reduces its solubility in water.

However, the reversal of Traube's Rule is expected for adsorption of aliphatic acids from a relatively non-polar solvent on a polar solid adsorbent. This was verified by Holmes and McKelvey [58], who studied the adsorption of fatty acids from toluene by silica gel. The same behavior was confirmed by Nekrassow [59], when he studied the adsorption of fatty acids from aqueous solution by charcoal prepared under strongly oxidizing conditions. Nekrassow attributed that reversal behavior to the polar nature of the charcoal. He assumed an increase in the water uptake as a result of the competition for the active sites on the surface. A different explanation of Nekrassow results was given by Bruns [60]. According to him, the reversal might have been due to the exclusion of larger molecules from very narrow pores rather than to the polarity of the surface.

Furthermore, Hansen and co-workers [61, 62] investigated the adsorption of lower fatty acids and alcohols from hydrocarbon solvents and from their binary aqueous solutions by a series of relatively non-porous carbons (carbon black and several graphites). It was found that the adsorption isotherms of organic acids on carbon were superimposable on each other when the amounts adsorbed were plotted versus the reduced concentration. The reduced concentration is defined as the actual solute concentration in the bulk solution divided by its solubility at the temperature of the measurement. Hansen and co-workers pointed out that the work required to remove the solute from the solution as a pure substance depends only on the absolute activity, λ, of the solute ($\lambda = \exp(\mu/RT)$, where μ is the chemical potential, R is the gas constant and T is the thermodynamic temperature). Moreover, if the adsorbent acted on the same functional group, congruency of adsorption isotherms in a homologous series when plotted as functions of reduced concentration was not surprising. They concluded that the relative adsorption of members in a homologous series on non-porous adsorbents is determined primarily by solute activity. This principle furnished not only a rational basis

for Traube's rule but also for inversion of Traube's rule. According to Hansen and co-workers [61, 62], the reversal in the adsorption of the lower fatty acids and alcohols from hydrocarbon solvents, was obtained because the activity coefficients decrease on ascending the series.

Adsorption of lauric and stearic acid on carbon blacks and on activated carbon from aqueous solution was also studied by Weatherburn and coworkers [63, 64]. It was found that the behavior of higher fatty acid is similar to that of lower acids in exhibiting an isotherm that follows the Freundlich equation.

It was also pointed out in the literature that orientations adopted by the molecules of the adsorbate are of importance since the orientation may considerably alter the number of molecules that can occupy a unit area of the adsorbent surface [18]. A valeric acid molecule adsorbed with its hydrocarbon chain parallel to the surface should occupy more area compared to the situation when the chain is perpendicular to the surface. It was found that during adsorption of mixed vapors of fatty acid and water, the fatty acid molecules are adsorbed with the hydrocarbon chain parallel to the surface due to their high affinity to the graphene plates [65]. This orientation is assumed to be adopted for adsorption from aqueous solution [65].

The effect of temperature on adsorption from solution was also studied [18, 59]. Since the adsorption reaction is exothermic, an increase in temperature drives the adsorption isotherm towards a lower surface coverage for a given equilibrium concentration [66]. This behavior was demonstrated by Wang and co-workers [57] for the adsorption of lower aliphatic acids from aqueous solution at three different temperatures (278, 298 and 313 K). They found that the uptake of all acids decreased as the temperature increased. This decrease in the uptake with an increase in temperature corresponds to the weakening of the attractive forces between the solute and the solid surface. It may correspond also to an increase in solubility of the solute in the solvent. Thus if the solute is regarded as distributed between the adsorbed layer and the solution in a partition equilibrium, the position of equilibrium is displaced in favour of the solution as the temperature rises.

As a summary of the work done before, several factors have been found to affect the adsorption of valeric acid. These include the porosity and surface chemistry of the

adsorbent, the nature of the solvent, and the temperature at which adsorption studies were done. It was further found that the adsorption process of valeric acid from aqueous solution on activated carbons depends on the porosity of the carbon and the chemical nature of the carbon surface.

2.2.3 Ethylmethylamine

Aliphatic amines can be found in many wastewater effluents from industry, agriculture, pharmaceutical manufacturing, and food processing. Amines can induce toxicological responses that are relevant in biochemical treatment processes, as well as in natural waters. Ethylmethylamine (EMA) is a colorless liquid with strong ammoniacal odor. Its main physical properties include: boiling point 309 K, vapor pressure 8.53 psi at 293 K, odor threshold about 0.504 mg/m^3, pH around 12.3 and complete miscibility with water. Alkylamines are important intermediates in the chemical industry for the synthesis of nitrogen-containing organic compounds.

While nothing is mentioned in the literature about ethylmethylamine adsorption on activated carbon, a little is mentioned on the other amine molecules interactions with the carbon surfaces. Amines have a free electron pair on the nitrogen atom and are willing to accept a proton to form quaternary salts. Therefore, they are Lewis bases, as well as nucleophiles. The strength of their basicity depends upon the attached substituents. Electron withdrawing groups such as halides and aromatic compounds decrease their basicity, while electron donating groups such as alkyl groups increase it as long as they are not so large to interfere with the lone pair. The presence of methyl- and ethyl- alkyl groups which are electron donating groups, make ethylmethylamine a stronger base than ammonia itself. More recently, Ellison and co-workers [67] studied the adsorption of ammonia and trimethylamine on single-walled carbon nanotubes (SWNTs). They reported that NH_3 adsorbs via both its lone pair and its H atoms. IR data suggested that NH_3 adsorbs by interacting with multiple nanotubes within a bundle of SWNTs. Unexpectedly, trimethylamine, a compound similar to NH_3, was not adsorbed at room temperature. It was hypothesized that the size of trimethylamine prevents it from entering the grooves between nanotubes in the sample, whereas NH_3 is small enough to enter the grooves and interact with multiple nanotubes.

Up to this day, the most detailed work done on alkylamines adsorption on activated carbons was by Pérez-Mendoza and co-workers [68]. They studied the adsorption of mono-, di- and trimethylamine (MMA, DMA and TMA) on carbon materials at zero surface coverage by using inverse gas-solid chromatography (IGSC). The adsorbents used in their study had different textural characteristics and chemical surface groups. They tried to relate these surface properties to different types of interactions with the adsorbates. Since methylamines are polar molecules, they were expected to interact with the surface groups of the carbon materials through dipole-dipole, acid-base or hydrogen bond interactions, producing the so-called specific interactions. At the same time, interaction with the surface through London dispersion forces, or nonspecific interactions was also expected.

In order to find the type of interactions controlling the adsorption process, Pérez-Mendoza and coworkers used a method proposed by Donnet and co-workers [69] which compares the standard free energies of adsorption for molecules (n-alkanes, n-C4 to n-C7) interacting through dispersive forces (nonspecific) to those of molecules capable of specific interactions (methylamines). From the plot of the variation in the standard free energy of adsorption ΔG^o versus $(h\nu_L)^{1/2}\alpha_L$, where h is Planck's constant, ν_L is the characteristic vibration energies of the adsorbate, and α_L is the deformation polarizabilities, a straight reference line was obtained for n-alkanes. The values of ΔG^o of methylamines, mainly MMA, were located above this line which indicates specific interactions.

Moreover, it was found that the standard free energy decreased from MMA to TMA. These results lead to a conclusion that adsorption of methylamines on the carbon materials takes place via a mixed mechanism composed of nonspecific and specific interactions. The former was almost negligible in MMA and was predominant in TMA. Conversely, the latter was very important in MMA. Specific interactions were weak in DMA and TMA cases, following the same trend as the dipolar moment of the adsorbates: MMA > DMA > TMA. Pérez-Mendoza and co-worker pointed out that if the specific interactions were controlled by the basic character of the adsorbates then adsorption should be favored in the order: DMA > MMA > TMA since this is the trend of their K_b. Therefore, although specific interactions could be the result of acid-base or dipole-dipole

forces, the experimental data supported the second type. For this reason, none of the acidic chemical surface groups was preferred by the adsorbates.

Based on the literature review, EMA was expected to be adsorbed and a few thoughts were formulated toward understanding the role of surface features governing the adsorption process. Taking into account the nature of adsorbent and adsorbate, the adsorption strength is expected to increase as the size of pores become closer to the adsorbate molecule diameter due to the overlapping of the adsorption potential [30-32, 70]. Surface groups should also affect the adsorption of EMA due to the possibility of hydrogen bonding with the polar groups in the carbon matrix.

CHAPTER 3
EXPERIMENTAL SECTION

3.1 Choice of Carbons

Three activated carbons were chosen for this study. They are as follows: BPL 4x10 (Calgon, bituminous coal origin), MVP 4x10 (Norit, bituminous coal origin), and BAX 1500 (Westvaco, wood origin) [71]. These carbons are referred to as BPL, MVP and BAX respectively. Before experiments, the initial carbons were washed in a Soxhlet apparatus to remove water-soluble species. The carbon samples chosen are expected to differ in both the surface chemistry and the pore size distribution due to differences in their origins and the methods of activation [7, 72].

The choice of carbons was governed by their properties. BPL is a bituminous coal-based virgin granular activated carbon used in vapor phase applications. It has a particle and internal pore size distribution allowing for rapid adsorption kinetics at medium to low differential pressure drop across the carbon bed. Because of its surface area, density, and strength characteristics, BPL can be reactivated for reuse, eliminating disposal problems. MVP is a granular activated carbon produced by steam activation of selected grades of bituminous coal. As a result of a unique patented activation process and stringent quality control, it offers excellent adsorption properties and is recommended for removal of impurities from water and industrial process applications.

BAX is a low temperature wood based carbon, prepared by chemical activation with phosphoric acid [71].

3.2 **Modification of Carbons**

The initial carbons used in this study were modified by oxidation and urea modification methods. The modified carbons were prepared several times during this work. It is important to mention that full reproducibility of results on the same carbon after modification is impossible; however the trends are in good qualitative and quantitative agreements.

3.2.1 *Oxidation*

Oxidation of the carbon samples were carried out with nitric acid. The procedure was as follows: 10 grams of the initial sample was mixed with 100 ml of 15 N (73%) HNO_3 [13, 76]. The suspension was stirred for 24 hours (acetaldehyde study) and 20 hours (valeric acid and ethylmethylamine studies) followed by washing in a Soxhlet apparatus to remove any excess of oxidizing agent and water-soluble compounds. The oxidized samples were continuously washed until constant pH was reached. After oxidation, the samples are referred to as BAXO, BPLO and MVPO.

Oxidation is expected to introduce significant amounts of oxygen-containing functional groups into the surface, which might affect the adsorption process of the compounds of interests. The effect of oxidation on carbons of different origin is assumed to be reflected in a spectrum of groups and their surface densities.

3.2.2 *Urea Impregnation Followed by Heat Treatment*

Carbon samples were impregnated with urea (H_2NCONH_2) (saturated solution). The suspension were stirred overnight then the carbons were heated at 723 or 1223 K for 50 minutes (acetaldehyde study) and 1 hour (valeric acid and ethylmethylamine studies) in nitrogen atmosphere at the rate of 10 K/min in order to introduce nitrogen groups [28, 75]. After modification, the samples were washed with distilled water in a Soxhlet apparatus until constant pH was reached. This step was done to remove any excess of urea decomposition products and any water-soluble compounds. The urea modified

carbons are referred to as BAXN1, BPLN1, BAXN2 and BPLN2. N1 and N2 stand for heating temperature of 723 K and 1223 K, respectively. To exclude the effects of changed surface nature as a result of heat treatment, another sample of BAX carbon was heated in nitrogen at 1223 K at the same conditions as its urea-modified counterpart. It is referred to as BAXHT.

At 723K nitrogen is expected to be in the form of -NH and -NH_2, amides or NH_4^+ species [28]. These surface groups decompose at around 873 K and some nitrogen is likely converted to aromatic nitrogen species built into the carbon matrix [28]. At 1223 K, the majority of nitrogen incorporated into the carbon matrix is in a pyridine-like configuration [28, 75].

3.3 Choice of Odoriferous Compounds

The three volatile organic compounds described above were studied: Acetaldehyde, valeric acid, and ethylmethylamine. The purities of these compounds were 99%, 99% and 97%, respectively as obtained from Aldrich and Acros Organics suppliers. These compounds were chosen because of their major contribution to human odor owing to their chemical functionality [73]

3.4 Study of Surface Chemistry of Carbons

3.4.1 *Boehm Titration*

One gram portions of carbon sample were placed in 50 ml of 0.05N of the following solutions: sodium hydroxide, sodium carbonate, sodium bicarbonate and hydrochloric acid. The vials were sealed and shaken for 24 h. The samples were filtered and then 10 mL of each filtrate was pipetted out and the excess of base or acid was titrated with 0.1N HCl or NaOH, respectively. The number of acidic sites of various types were calculated under the assumption that NaOH neutralizes carboxyl, phenolic, and lactonic groups; Na_2CO_3 carboxyl and lactonic; and $NaHCO_3$ only carboxyl groups [5, 72]. In case of urea modified carbons, Boehm titration was also applied. With these carbons, only the total number of acidic and basic groups can be calculated. This is because acidic groups cannot be classified as carboxylic, lactonic and phenolic due to presence of protonated nitrogen containing organic groups (NH_3^+ and NH^+) which can

have similar pK_a to carboxylic acids [76]. The total number of acidic and basic groups is calculated using a similar procedure. One gram portions of carbon sample were placed in 50 ml of 0.05N of the sodium hydroxide and hydrochloric acid solutions. The vials were sealed and shaken for 24 h. The samples were filtered and then 10 mL of each filtrate was pipetted out and the excess of base or acid was titrated with 0.1N HCl or NaOH, respectively.

3.4.2 *Potentiometric Titration*

The potentiometric titration measurements were performed with a DMS Titrino 716 automatic titrator: Metrohm, Brinkmann Instruments, Westbury, NY, USA. The experiment was performed by placing 0.100 g samples in a container thermostatted at 298 K with 50 mL of 0.01 M $NaNO_3$. The suspensions were stirred and equilibrated overnight in saturated N_2 gas environment to eliminate any interference by dissolved CO_2. Prior to the experiment the suspensions were made acidic by adding measured volumes of 0.1N HCl to lower the pH to around 3. NaOH was used as titrant. Titration curves representing the variation in pH with the volume of 0.1N NaOH added were obtained. The carbon suspension was stirred throughout the measurement. Because of the buffering effect of water at pH < 3 and > 11, experiments were carried out in the pH range 3-11 [4, 6, 7, 77].

It is assumed that the system under study consists of acidic sites characterized by their acidity constants, K_a [12]. The population of sites can be described by a continuous pK_a distribution, f (pK_a). The experimental data was transformed into a proton binding isotherm, Q(pH), which represents the total amount of protonated sites. Q(pH) is related to the pK_a distribution by the following integral equation:

$$Q(pH) = \int_{-\infty}^{+\infty} q(pH, pK_a) f(pK_a) dpK_a \qquad (6)$$

From this equation, the distribution of acidity constants f(pK_a) and their population can be obtained. The solution of the equation is obtained using the numerical procedure SAIEUS (Solution of Adsorption Integral Equation Using Splines) [78]. Based on the spectrum of acidity constants, pK_a, and the history of the carbon samples (origin,

activation method, chemical modification), the detailed surface chemistry is evaluated.

3.4.3 pH Measurement

0.4 g of dry carbon powder was added to 20 ml of water and the suspension was stirred overnight to reach equilibrium. Then the samples were filtered and the pH of the filtrates was measured.

3.4.4 FTIR

A Nicolet Impact 410 FT-IR instrument equipped with a diffuse reflectance unit was used to collect IR spectra. The instrument resolution was set at 4 cm^{-1}. Carbon powder was placed in a micro-sample holder. Before each measurement, the background was collected, and automatically subtracted from the sample spectrum.

IR spectra provide very important qualitative fingerprint type information about the surface. As an example, the presence of stretching vibrations characteristic bands at 1275 cm^{-1} , 1700 cm^{-1} and at 1580 cm^{-1} indicate the presence of a carboxylic group. A band at 3400-3600 cm^{-1} is an indication of the presence of phenolic groups [9]. The presence of bands between 2500 and 3500 cm^{-1} is linked to the presence of N-H bonds. Bands in the range 3200-3500 cm^{-1} are characteristic of ─NH, ─NH_2, ─NH_3 groups present on the surface, while bands at around 1500 and 1600 cm^{-1} are related to vibrations from pyridines and amides [79].

3.4.5 Thermal Analysis

A TA Instrument Thermal Analyzer was used to carry out thermal analysis. The instrument settings were: heating rate 10 K/min, and nitrogen atmosphere at flow rate of 100 mL/min. Approximately 20 mg of a ground carbon sample was used for each measurement. Thermogravimetric (TG) and Differential thermogravimetric (DTG) curves were obtained. TG curves provide the % weight loss caused by the decomposition of surface functional groups as a result of heating. DTG curves are obtained from TG curves. The position of the peaks on DTG curves is related to the thermal stability of the surface groups. It was found that carboxylic acid sites decompose to CO_2 between 473 and 873 K whereas at temperature higher than 873 K weak acids, phenols and basic

groups decompose to CO [14,15]. The decomposition of amine-like groups (NH, and NH_2) is expected to be in the range between 673-1173 K [80, 81].

3.4.6 CHN Elemental Analysis

CHN analysis was carried out by Huffman Laboratories, Golden CO.

3.5 Characterization of the Pore Structure

3.5.1 Sorption of Nitrogen

A (Micromeritics, Norcross, GA, USA) ASAP 2010 was used to measure nitrogen adsorption isotherms at 77 K. Before the experiment, the samples were heated at 393 K and then outgassed under a vacuum to constant pressure of 10^{-5} torr. Characterization of pore sizes and pore structure were accomplished using Density Functional Theory (DFT) [82, 85]. This method is based on the concept that the free energy of an inhomogeneous fluid can be expressed as a function of $\rho(r)$, which is the spatial variation of the average one-body density. DFT works under the assumption that the experimental isotherm can be expressed as the sum of the convolution of a kernel function which represents the isotherm of an ideal homoporous adsorbent with a frequency distribution of pore sizes. The convolution is done by fitting the experimental isotherms into combinations of pre-existing isotherms for various pore sizes until the best fit is obtained. DFT provides an accurate method for describing inhomogeneous systems like activated carbons. Using DFT, specific surface area (S_{DFT}), total pore volume (V_t), micropore volume (V_{mic}), volume of pores less than 10Å ($V_{<10Å}$) were calculated [82, 85]. These data was used to calculate the average pore size (L). Moreover, the surface areas, $S_{BET,}$ were also calculated using the BET method. The characteristic energy of adsorption (E^o) was obtained using Dubinin-Astakhov equation [31].

3.6 Sorption of Odoriferous Substances from Vapor Phase Using IGC

Gas chromatography is called inverse gas chromatography (IGC) when it is applied to study the adsorption on a solid stationary phase [7, 86-88]. The chromatographic experiments were performed with an SRI 8610 (SRI, Torrance, CA, USA) equipped with a flame ionization detector. Stainless steel columns (2.17 mm in diameter) were filled

with dry carbon particles of size ranging from 0.2 to 0.4 mm. The difference in the column weight before and after filling gives the mass of the carbon adsorbent. Helium was used as a carrier gas and methane as a non-retained species. The flow rate was measured at the outlet of each column and was corrected for pressure drop across the column. The samples were conditioned at 473 K in the chromatographic column under helium gas flow over night prior to the measurements.

3.6.1 Inverse Gas Chromatography at Infinite Dilution

This method is based on the study of physical adsorption of appropriate molecular probes by mean of chromatographic (dynamic) experiments. In infinite dilution chromatography only very small amounts of solutes are injected. The peaks on the chromatogram are symmetrical (Figure 4) since Henry's Law describes the sorption process [88].

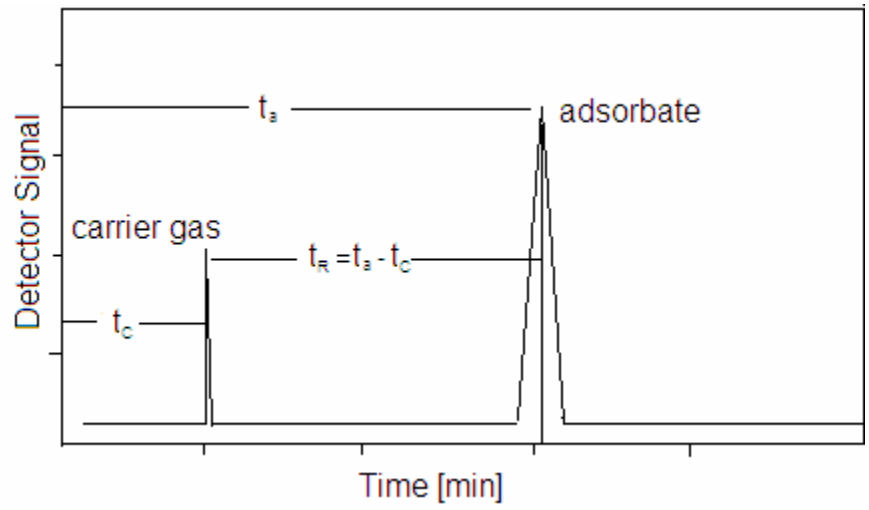

Figure 4: Typical elution peaks represents inverse gas chromatography at infinite dilution (t_a and t_c are the measured retention times for the adsorbed and nonadsorbed species respectively).

Under infinite dilution conditions, only interactions between the adsorbate molecules and the surface occur. The retention time is independent of the amount injected. The retention volume, V_N:

$$V_N = F \cdot t_R \cdot J \tag{7}$$

Where F is the flow rate of the carrier gas measured at the column outlet, t_R is the corrected retention time of the adsorbate, and J is the James-Martin compressibility correction factor [86-88].

When the retention volume of the adsorbate vapor is measured at different temperatures, the enthalpy of adsorption, ΔH^o, can be calculated from the temperature dependence of the retention volume:

$$\Delta H^o = -R \frac{\partial \ln(V_N / T)}{\partial (1/T)} \tag{8}$$

Where R and T represent the gas constant and the temperature in Kelvin, respectively. The isosteric heat of adsorption is

$$Q_{st} = -\Delta H^o \tag{9}$$

3.6.2 Inverse Gas Chromatography at Finite Concentrations

In this method, a known volume of liquid adsorbate was injected into the column containing the activated carbon. From the adsorbate peak on the chromatogram, the adsorption isotherm can be determined using the characteristic point elution method [84, 87-92]. This method is frequently used because of its rapidity and its direct application on the chromatograms without any further adaptation. In characteristic point elution method, the isotherm can be determined from a single chromatogram. At finite concentrations, the peaks are not symmetrical and the retention volume alters with the change in the adsorbate concentration. The characteristic point elution method gives good results if the front or rear profiles of the peaks for varied sample volumes overlap (Figure 5).

In the characteristic point elution method, the chromatogram is divided into i segments parallel to the base line (Figure 6). Thus, equilibrium pressure, P_i, corresponding to i points on the isotherm can be calculated.

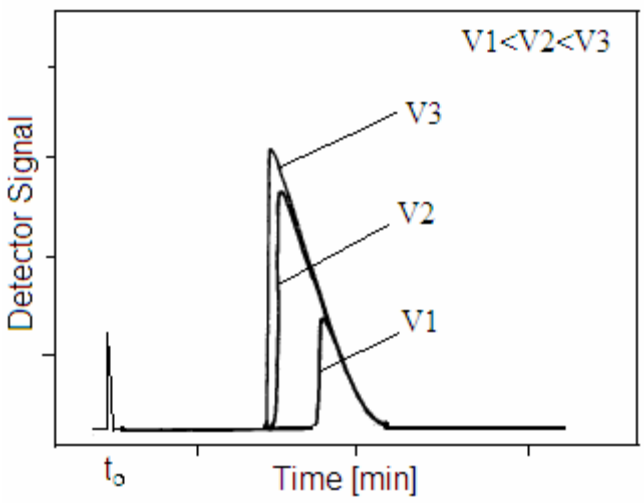

Figure 5: Chromatograms for various sample volumes (V1, V2, V3) for inverse gas chromatography at finite concentration.

The total amount of solute adsorbed on the solid support is calculated from the following formula:

$$q = \frac{F_c}{m} k \int_0^h (t - t_0) dh \tag{10}$$

where, q is the amount adsorbed , F_c is the corrected flow of helium gas through the column [87], m is the weight of the adsorbent, and t and t_o are the retention times of adsorbates and non-adsorbed species (methane), k is a proportionality constant between the height of the peak h_i and the corresponding concentration at that height, C_i.

Dividing the chromatographic peak into i portions, the concentration representing each height, C_i can be obtained [90, 91]:

$$C_i = \frac{n \,.\, h_i}{F_c \cdot S_{peak}} \tag{11}$$

n is the amount injected, S_{peak} is the area of the chromatographic peak. The amount adsorbed at different portions is calculated using the following equation:

$$q_i = \frac{n \,.\, S_i}{F_c \cdot S_{peak}} \tag{12}$$

where S_i is the area at h_i and S_{peak} is the peak area.

The concentration and pressure are related through the following expression:

$$P_i = C_i \cdot R \cdot T \tag{13}$$

where R is the gas constant and T is the temperature in Kelvins .

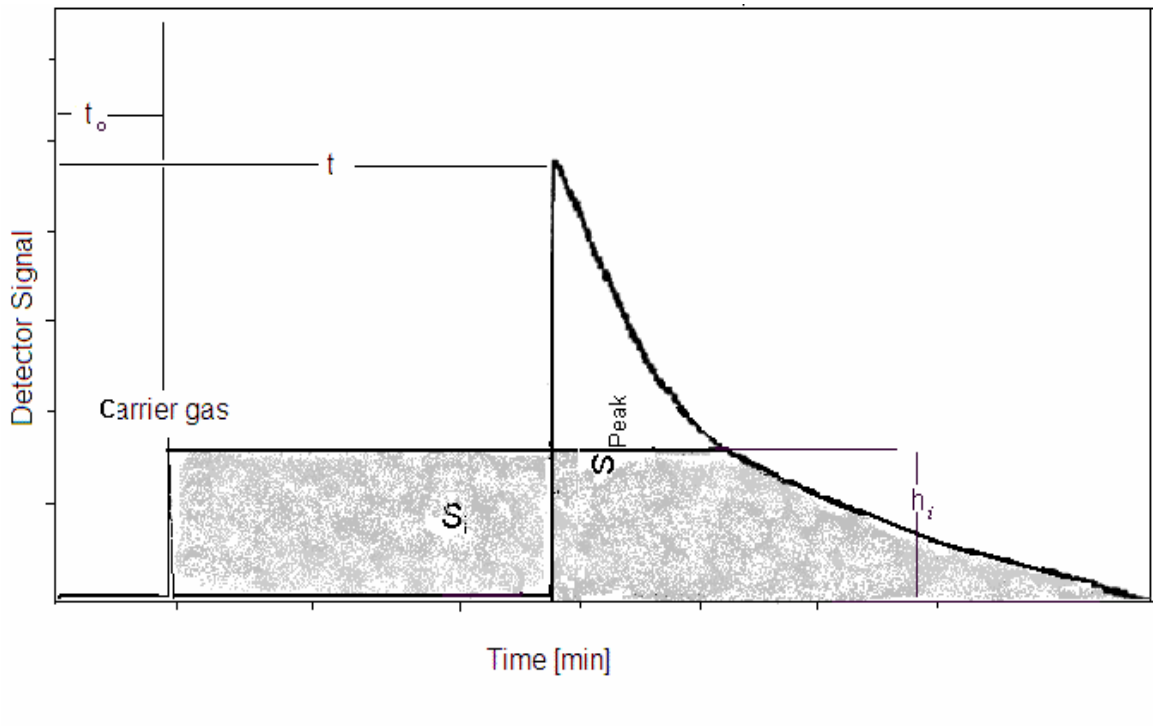

Figure 6: IGC at finite concentration: characteristic point elution method.

Before each experiment the column was conditioned by heating it to 488 K for 12 hours, under helium flow, to remove impurities form the carbon surface. The column used was a 1.0 meter long and 3 mm in diameter. The amount of valeric acid injected ranged from 5 to 20µl. Temperatures of the measurements were between 473 K and 488 K.

3.7 Adsorption of Odoriferous Substances from Vapor Phase

In this experiment, a beaker containing 10mL adsorbate liquid was placed in a dessicator along with several small weighing dishes containing 1g of a powdered carbon samples each. The carbons were kept in the liquid vapor atmosphere for a period of time until equilibrium was reached.

TG/DTG curves were obtained for each carbon sample before and after adsorption. By plotting the differences in the curves between initial and exposed carbons, characteristic peaks related to the desorption and decomposition of species on the surface of carbon can be obtained. The intensities and positions of these peaks provide information about the type of interactions and the strenght of adsorption on the surface of carbon

3.8 Adsorption of EMA and Valeric Acid from Aqueous Solution

The equilibrium adsorption isotherms for EMA and valeric acid from an aqueous solution on activated carbons were measured at 299 K and 333 K respectively. Different amounts of carbons in a range between 0.05g and 1 g were weighed and added into different bottles containing 40 ml of the EMA or valeric acid aqueous solution of 350 ppm. All the solutions were prepared with deionized water. The bottles were then sealed and placed in a shaking bath and allowed to shake for 24 hours for EMA and 72 hours for valeric acid at a rate of 55 RPM. Then the suspensions were filtered and saved for further analysis. A Shimadzu GC- MS QP5050 gas chromatograph equipped with a mass spectrometer (Shimadzu, Columbia, MD, U.S.A.) was used to determine the concentration of EMA and valeric acid in the filtrates. The separation was done on a XTI-5 (95 % dimethyl-5% diphenyl polysiloxane) capillary column 30 m in length and 0.25 mm in diameter manufactured by Restek (Restek, Bellefonte, PA, U.S.A.).
The amount adsorbed is calculated from the following formula:

$$q_e = \frac{V.\Delta C}{m} \tag{14}$$

$$\Delta C = (C_o - C_e) \tag{15}$$

where q_e is the amount of adsorbate adsorbed per gram of adsorbent, V is the volume of the liquid phase, C_o is the concentration of the solute in the bulk phase before it comes in contact with the adsorbent, C_e is the concentration of the solute in the bulk phase at equilibrium, and m is the mass of the adsorbent. The change in the volume of the bulk liquid phase is negligible because the solute concentration is very small and the volume occupied by the adsorbent is also very small. The amount of adsorbate in each sample is calculated using a previously determined calibration curve.

In most of the adsorption studies a constant adsorbent dose, mass of adsorbent per volume solution, is used while the initial solution concentration varies. Other studies [45, 93-96] changed the adsorbent dose while keeping the initial concentration constant. In those studies, it was clearly shown that changing the adsorbent dose affects the adsorption capacity with overestimated capacities resulting from lower- dose isotherms. As adsorbent dose varies, the amount adsorbed per unit area varies in accordance with the adsorption capacity. A unique isotherm for a series of different doses was attained by normalizing the amount of the adsorbate in solution at equilibrium with the dose of adsorbent, such that the amount of adsorbate in solution is expressed as an adsorbate mass per a unit mass of an adsorbent, instead of concentration units.

The obtained isotherms were fitted into the modified form of the Freundlich single solute isotherm, which has the following equation [56, 97-99]:

$$q_e = K_F \cdot (A_e)^n \tag{16}$$

where q_e is the amount of EMA and valeric acid adsorbed per unit gram of adsorbent, A_e is the amount of the adsorbate at equilibrium (calculated from the concentration and volume) per unit weight of the adsorbent, K_F is considered as the capacity factor while the exponential term n represents the heterogeneity of the site energies and is related to the magnitude of the adsorption driving force. The fitting range for A_e was from 1 to 200 mg / gram of carbon.

3.9 Breakthrough Measurements for EMA

Breakthrough tests under dynamic conditions were carried out in order to obtain

more information about the adsorption mechanism. From the adsorbate breakthrough time, the service life of the activated carbon filter can be predicted. Breakthrough experiments for EMA vapors were carried out at room temperature with inlet concentration of 1000 ppm EMA and an arbitrary breakthrough concentration of 5 ppm. The air flow was adjusted to 10 L/min with a relative humidity of 70%. The bed diameter was 4 cm, and bed depth was adjusted to obtain a filter of either 20g or 30g of carbon. In order to evaluate the influence of the moisture, the breakthrough experiments were also performed in dry air.

A number of semi-empirical models for predicting breakthrough times have been proposed in the past. These include the Mecklenburg [100] the Wheeler–Jonas (WJ) [101-103], and the Yoon–Nelson [104] equations. All these equations are based on the mass balance between the quantity of vapor entering the carbon bed and the sum of the quantities adsorbed in and penetrating the bed. Among these equations, the Wheeler–Jonas equation [103, 105,106] has been widely used by several research groups over the past decades to estimate breakthrough times of organic vapors for filter beds filled with granular activated carbon (GAC).

3.9.1 Theoretical

The Wheeler–Jonas equation (eq.17) is a well-known predictive equation to estimate the breakthrough times of physisorbed organic vapors on activated carbon beds [102, 105-107]. The prediction is based solely on the measurable and readily available macroscopic parameters:

$$t_b = \frac{M \,.\, W_e}{Q \cdot C_{in}} - \frac{\rho_b \,.\, W_e}{k_v \cdot C_{in}} \ln\left[\frac{C_{in} - C_{out}}{C_{out}}\right] \tag{17}$$

where t_b is the breakthrough time to reach C_{out} (min); C_{in} is the vapor inlet concentration in air (g/cm^3); C_{out} is the chosen breakthrough concentration (g/cm^3); M is the weight of the carbon bed (g); W_e is the equilibrium adsorption capacity (g/g_{carbon}); Q is the volumetric flow rate (cm^3 /min); ρ_b - the bulk density of the carbon bed (g_{carbon}/cm^3); and k_v is the overall adsorption rate coefficient (min^{-1}). Two unknown parameters, W_e and k_v,

in this equation need to be calculated. Several models were derived which allow calculations of these parameters without any prior breakthrough experiment [108-111]. W_e is normally estimated from the Dubinin–Radushkevich equation [108].

$$W_e = W_o \cdot d_L . \exp\left[-\frac{B . T^2}{\beta^2} \log^2\left(\frac{C_s}{C_{in}} \right) \right] \tag{18}$$

W_e is the static adsorption capacity (g/g_{carbon}); W_o is the micropore volume (cm^3/g); d_L is the liquid density (g/cm^3); B is a structural constant of the carbon; β is the affinity coefficient of the organic vapor; T is the adsorption temperature (K); C_s is the saturation vapor concentration (ppm); C_{in} is the vapor inlet concentration (ppm). The only unknown parameters in this equation are W_o and B. They can be derived from nitrogen adsorption isotherms at 77 K.

Calculation of the overall adsorption rate coefficient, k_v, is more complex. For organic compounds, k_v is mainly linked to the effects of surface diffusion. The most recent equation to calculate the value of k_v is by using the following semi-empirical equation [110].

$$k_v = 800 . \beta^{0.33} . V_L^{0.75} . d_p^{-1.5} . \sqrt{\left(\frac{W_e}{M_W} \right)} \tag{19}$$

k_v is the overall adsorption rate coefficient (min^{-1}); W_e is the adsorption equilibrium capacity (g/g_{carbon}); M_w is the molecular weight of the vapor (g/mole); d_p is the average diameter of the carbon particle (cm); β is the affinity coefficient of the organic vapor and V_L is the linear velocity through the bed (cm/s).

Experimentally, different breakthrough times can be obtained by varying the weight of the carbon bed (varying only M). A plot of breakthrough time versus carbon bed weight, should yield a straight line that allows calculating W_e and k_v using the slope and the intercept.

3.10 Water Uptake Measurement

Water uptake was measured gravimetrically. The carbon was put into contact with a constant air stream at 293 ± 2 K, with a fixed humidity of 70 ± 3 % RH. The sample was weighed at regular intervals until no more weight change (i.e. less than 10^{-5} g) could be detected.

3.11 Elemental Nitrogen Analysis

The content of nitrogen was determined in the samples before and after EMA adsorption/thermal treatment. Prior to analysis, the samples were prepared under the same condition of thermal analysis by heating in nitrogen atmosphere to 1223 K. Elemental N analysis was carried out by Huffman Laboratories, Golden CO.

CHAPTER 4

RESULTS and DISCUSSION

4.1 Acetaldehyde

4.1.1 Surface Structure Characterization

Sorption of Nitrogen Results

Surface structure is the most important parameter in studying the adsorption on activated carbon of trace concentrations of small molecules. As described above, the carbons used in this study are of different origins. They are also prepared by different activation methods and thus expected to have different pore structure. Nitrogen adsorption isotherms are presented in Figures 7, 8 and 9.

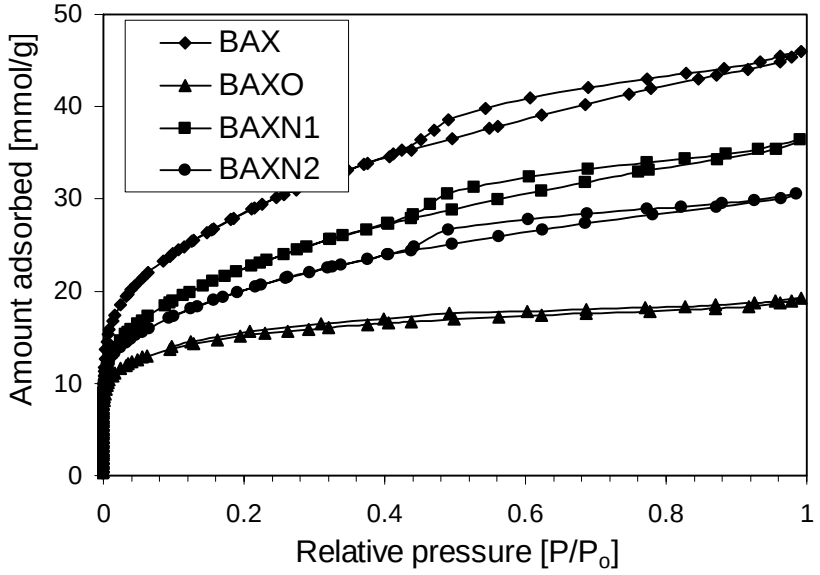

Figure 7: Nitrogen adsorption isotherms on BAX series of carbons.

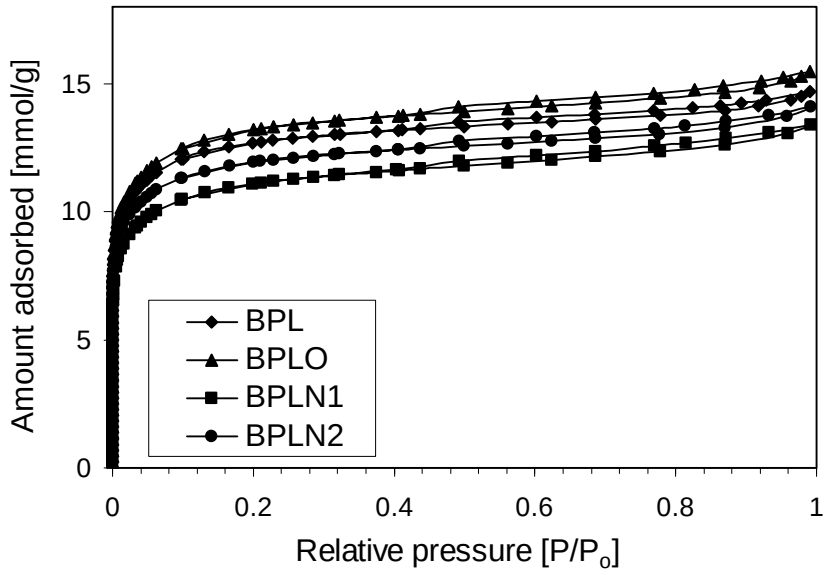

Figure 8: Nitrogen adsorption isotherms on BPL series of carbons.

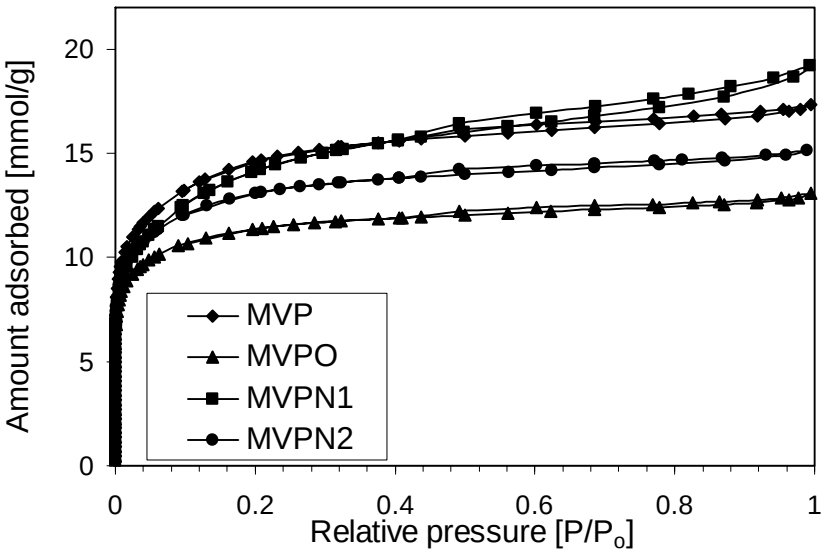

Figure 9: Nitrogen adsorption isotherms on MVP series of carbons.

The shape of the curves indicates that BPL and MVP are predominantly microporous sorbents whereas in the case of BAX some mesoporosity exists [3, 28, 71]. After oxidation, the nitrogen uptake decreased for most samples indicating a decrease in the pore volume. The only exception is for BPL carbon after oxidation where the nitrogen uptake didn't show any noticeable change. The most susceptible to change after oxidation is BAX, which is expected for wood-origin carbons [112,113]. After modification with urea and heat treatment at 723 K, the nitrogen uptake decreased on all samples. Further decrease is also noticed for the samples heat treated at 1223 K. However, for BPL after treatment at 1223 K the nitrogen uptake increased compared to that treated at 723 K likely due to the decomposition of amine-like groups blocking the pore entrances.

The pore size distributions (PSDs) obtained from nitrogen adsorption isotherms [82, 83] are presented in Figure 10. Based on the shapes of these figures, the carbons used in this study show significant differences in their porous structure. The BPL sample is the microporous one whereas BAX has a significant contribution of mesopores. The MVP carbon has a porous structure intermediate between those of BPL and BAX. Comparison of the plots clearly shows that the carbons studied have different susceptibilities toward oxidation. The most resistant to oxidation is BPL, the least resistant is BAX. In the case of the former sorbent, oxidation only slightly decreased the adsorption capacity leaving the pore structure almost intact. On the other hand, in the case of BAX carbon after oxidation, BAXO, the pore structure is significantly altered. It is worth noting that mesopores are greatly affected and their volume significantly decreased. In the case of MVP material the contribution of very small micropores (smaller than 10Å) increased after oxidation with a noticeable decrease in the volume of larger micropores and mesopores. After urea treatment, either at low or high temperature, the volumes of micropores (10-20 Å) and mesopores decreased. The volume of very small micropores, smaller than 10 Å, seems to increase mainly on carbons modified at 1223K.

The structural parameters such as surface areas, S_{DFT} and S_{BET}, micropore volume,$V_{<20Å}$, volume of pores smaller than 10 Å ($V_{<10\ Å}$) and the total pore volume along with the characteristic energy of adsorption E^o, were calculated from the isotherms and are summarized in Table 1.

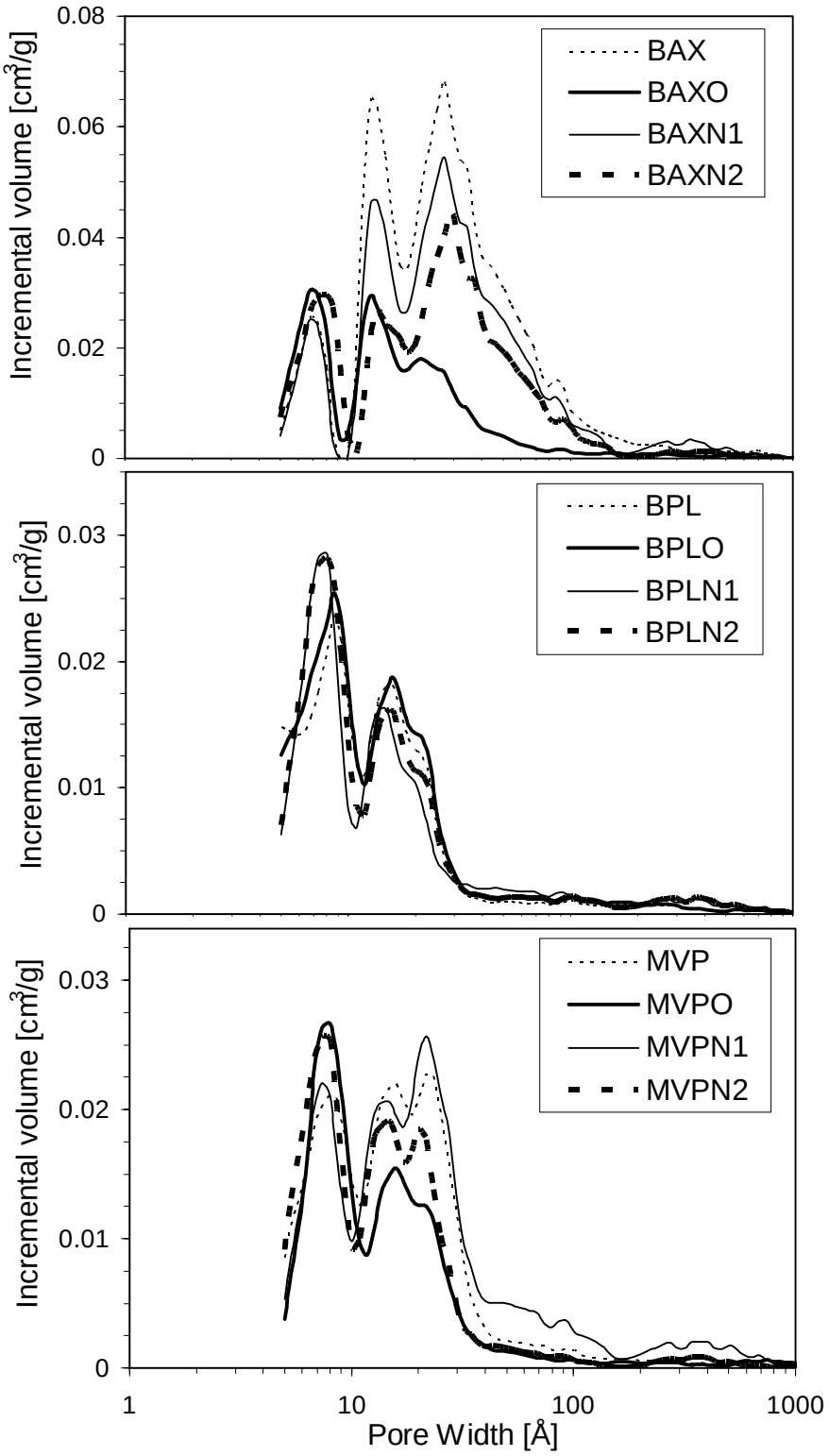

Figure 10: Pore Size Distribution on BAX, BPL and MVP series of carbon.

Table 1: Structural Parameters calculated from nitrogen adsorption isotherms.

Sample	S_{BET} [m^2/g]	V_t [cm^3/g)]	$V_{(<20\ A)}$ [cm^3/g]	$V_{(<10\ A)}$ [cm^3/g]	L [Å]	E^o [kJ/mol]
BAX	2266±84	1.339	0.528±0.010	0.123±0.003	12.98	15.62
BAXO	1105±41	0.521	0.362±0.007	0.174±0.004	10.96	19.55
BAXN1	1775±66	1.033	0.380±0.007	0.075±0.002	12.71	16.41
BAXN2	1558±58	0.852	0.387±0.007	0.120±0.003	11.02	18.55
BPL	901±33	0.376	0.319±0.006	0.186±0.005	10.38	21.10
BPLO	938±34	0.404	0.337±0.006	0.201±0.005	10.30	20.81
BPLN1	787±29	0.370	0.293±0.005	0.182±0.004	10.83	20.19
BPLN2	846±31	0.388	0.320±0.006	0.206±0.005	9.93	21.22
MVP	1059±39	0.483	0.355±0.007	0.176±0.004	10.79	19.01
MVPO	812±30	0.365	0.300±0.005	0.184±0.004	10.23	20.55
MVPN1	1049±39	0.540	0.318±0.006	0.146±0.003	11.07	18.81
MVPN2	936±35	0.417	0.330±0.006	0.180±0.004	10.65	19.60

It is clearly seen that BAX has the highest surface area. This is due to its having the largest pore volume. In the case of PBL these parameters are the smallest. After oxidation the volumes of pores for BAX and MVP carbons decreased. This decrease is the most pronounced for the BAXO sample. In the case of this carbon the total pore volume decreased almost threefold. In the case of BPL the structural parameters are not altered significantly. The volume of micropores and pores smaller than 10 Å decreased after urea modification, especially for BAX and MVP modified at 723 K. After urea treatment at 1223 K the volumes of pores smaller than 10 Å increased compared to the initial carbons as a result of the decomposition of amine type groups. In the case of

BAXN2 the pore volumes and surface areas are smaller than those for the initial materials due to an increase in the degree of carbonization as a result of heat treatment [28].

4.1.2 Surface Chemistry Characterization

Oxidation and urea modification are expected to affect the surface chemistry of carbons [18, 23, 24, 28, 38]. The direct effect of oxidation is usually an increase in the surface acidity due to the formation of oxygen containing groups such as carboxylic, lactonic and phenolic groups. Urea modifications result in the introduction of nitrogen groups into the surface which are basic in their chemical nature.

Boehm Titration Results

Table 2 presents the results obtained from Boehm titrations along with the pH values of the carbon surfaces. For urea-modified carbons we do not classify acidic groups as carboxylic, lactonic and phenolic. This is due to the fact that nitrogen-containing organic groups after protonation, especially the amine-like ones, may have the pK_a similar to those for carboxylic acids [76]. The data reported indicate that the initial carbons differ in their acidity as a result of the activation method and organic precursor [2]. The total number of groups and their distributions within various categories result in different values of the surface pH. Although the three carbons have average surface pH values close to neutral, BAX is the most acidic. This is expected for a phosphoric acid-activated carbon [71]. In the cases of BPL and MVP, although the total numbers of groups are similar, the distributions of species are different. The latter material contains more strong acids than the BPL sample, which has a noticeable contribution of phenols.

After oxidation the amounts of surface oxygen groups increased for all carbons; however, the overall effects of oxidation differ. As found from the nitrogen adsorption results, the most resistant to oxidation is BPL and the least is BAX. It is interesting that after oxidation MVPO and BPLO resemble each other. The reason for this may be in their common organic precursor, bituminous coal. The number of acidic groups increased threefolds on all carbons after oxidation. It is worth to note that the number of acidic groups introduced into BAX carbon after oxidation increased significantly. This increase

is reflected in the pH value which shows a significant decrease. Moreover, after oxidation the basic groups on this carbon are no longer present.

Table 2: Results of Boehm titration (mmol/g).

Sample	pH	Carboxylic	Lactonic	Phenolic	Acidic	Basic	Total
BAX	6.55	0.255	0.140	0.367	0.763±0.033	0.363±0.199	1.125
BAXO	3.71	1.616	0.448	0.328	2.392±0.104	0.000±0.000	2.392
BAXN1	6.92	---	---	---	0.718±0.031	0.563±0.031	1.281
BAXN2	7.1	---	---	---	0.678±0.029	0.595±0.032	1.272
BPL	7.54	0.000	0.025	0.163	0.188±0.008	0.450±0.024	0.638
BPLO	6.10	0.255	0.166	0.292	0.713±0.031	0.225±0.012	0.938
BPLN1	6.78	---	---	---	0.167±0.007	0.507±0.027	0.674
BPLN2	6.99	---	---	---	0.178±0.008	0.675±0.037	0.853
MVP	7.34	0.038	0.038	0.099	0.175±0.008	0.438±0.024	0.613
MVPO	6.23	0.255	0.179	0.279	0.713±0.031	0.225±0.012	0.938
MVPN1	6.90	---	---	---	0.238±0.010	0.413±0.022	0.651
MVPN2	7.36	---	---	---	0.231±0.010	0.413±0.022	0.644

The incorporation of nitrogen is expected to have an effect on the changes in the overall chemistry of the surface [28]. After modification with urea and heat treatment at 723 K or 1223 K, the surface chemistry seen by Boehm titration did not change significantly. The amount of basic groups increased for BAX, which indicates that even after heating at 723 K, the chemistry of the carbon matrix changes. It is noteworthy that BAX is a low temperature carbonized wood material, which is expected to increase the degree of carbonization after heating, especially at 1223K [28]. This increase is related to

the removal of aliphatic chains and oxygen-containing groups. When urea is present, incorporation of nitrogen heteroatoms within the matrix occurs [28]. A noticeable change in the number of basic groups (30% increase) is also found for BPLN2. It is worth mentioning that the number of acidic groups does not show any significant change. It is interesting that the changes in pH values of surfaces after urea modifications do not follow the direct changes in the number of basic groups. This is likely related to the fact that the acidity represented here by the pH value consists of the average number and strength of groups dissociating in water. For BAX carbon the pH increased after urea treatment. Based on a previous study, this carbon is the most vulnerable to this kind of modifications owing to its low degree of carbonization [78].

Table 3: Results of Boehm titration (molecules/nm^2).

Sample	Carboxylic	Lactonic	Phenolic	Acidic	Basic	Total
BAX	0.068	0.037	0.098	0.203	0.096	0.299
BAXO	0.880	0.244	0.179	1.303	0.000	1.303
BAXN1	---	---	---	0.244	0.191	0.435
BAXN2	---	---	---	0.262	0.230	0.492
BPL	0.000	0.017	0.109	0.126	0.300	0.426
BPLO	0.164	0.107	0.187	0.458	0.144	0.602
BPLN1	---	---	---	0.128	0.389	0.517
BPLN2	---	---	---	0.127	0.480	0.607
MVP	0.022	0.022	0.056	0.100	0.249	0.349
MVPO	0.189	0.133	0.207	0.529	0.167	0.696
MVPN1	---	---	---	0.137	0.237	0.374
MVPN2	---	---	---	0.148	0.265	0.413

For comparison and correlation purposes, the results of Boehm titrations were also calculated in terms of density of groups, defined as the number of molecules per square nanometer of the surface. The results are presented in Table 3. It is interesting that the density of acidic groups increased significantly after oxidation and, to a less extent, on the urea-modified carbons. Oxidation decreased the density of basic groups on the surface while their number increased after urea modification at 1223 K.

Potentiometric Titration Results

The changes in the degree of surface acidity were also studied using potentiometric titration. The proton binding curves (Figures 11, 12 and 13) were deconvoluted using the numerical SAIEUS procedure (Solution of Adsorption Integral Equation Using Splines) [78]. From proton binding curves, the pH_{PZC} could be estimated [115]. Those values shift from 6.5 for the initial BAX carbon to around 2 after its oxidation, from 8.1 for BPL to 5.6 for the BPLO, and from 8.7 for MVP to less than 3 for MVPO. After modifications with urea, the pH_{PZC} values for all series of carbons show a shift toward more basic values. This shift after urea modification was most pronounced for BPL and MVP series.

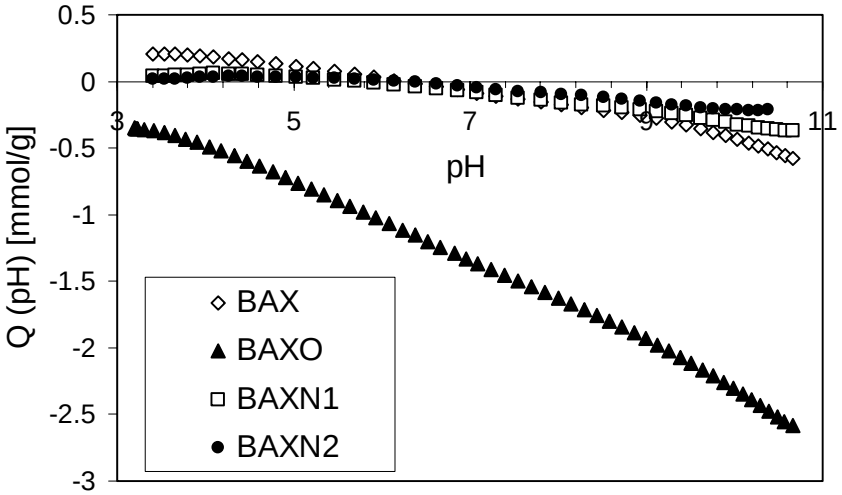

Figure 11: Proton binding curves for BAX carbon series.

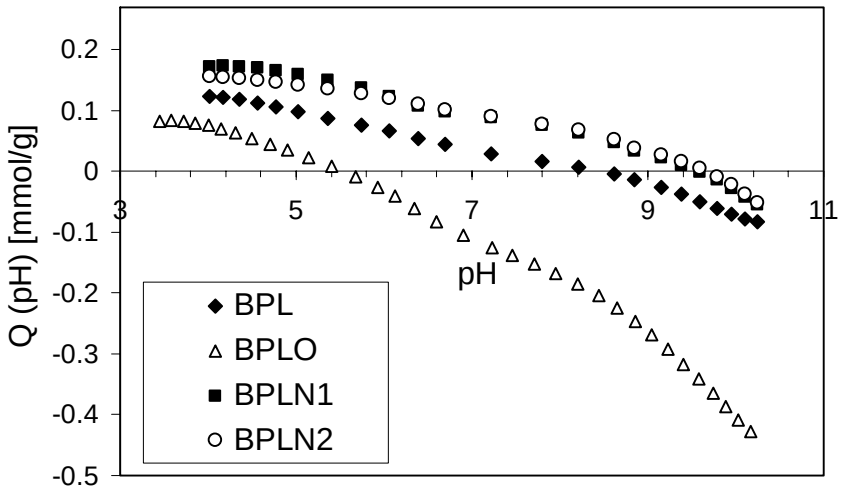

Figure 12: Proton binding curves for BPL carbon series.

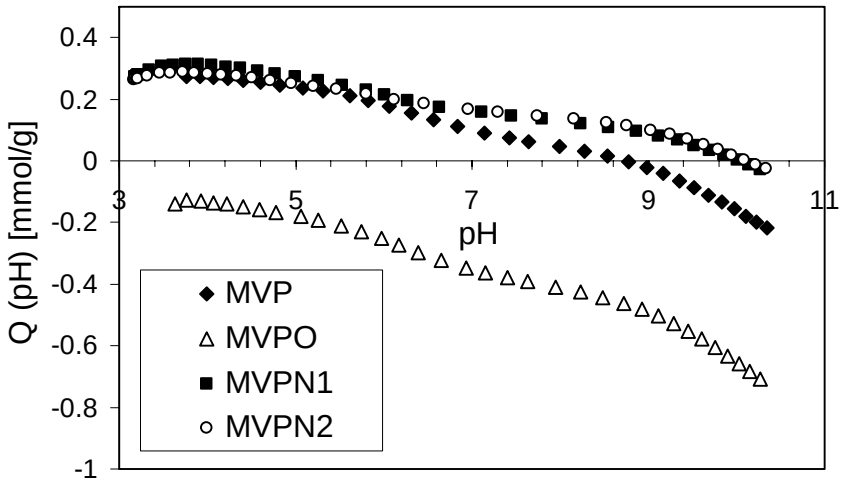

Figure 13: Proton binding curves for MVP carbon series.

By solving the integral equation, the distributions of acidity constants (f (pK_a)) were obtained. Because of the buffering effect of water at pH < 3 and > 11 only species with pK_a between 3 and 11 are analyzed by this method [115]. Based on the previous studies [76, 89], the groups with pK_a< 8 are classified as carboxylic acids and those with pK_a> 8 are classified as phenols and quinones. As described previously, NH_3^+ and NH^+ ionic groups can be also found in this range [76]. The distributions of acidity constants

are presented in Figure 14. Moreover, the amounts of species calculated by integration of each peak and the peak positions are collected in Table 4. Analysis of the pK_a distributions reveals similar trends to the ones observed from the Boehm titrations. The most acidic and the most heterogeneous is BAX, whereas MVP and BPL are similar to each other. The effects of oxidation are the most pronounced for BAXO and least pronounced for BPLO where the intensities of only two peaks representing species having pK_a at about 6.2 and 9.3 increased. In the case of MVP the intensities of all peaks increased. As shown in Figure 15, a good correlation (R^2 ~0.97) is observed between the densities (molecules/nm^2) of the total groups on the initial and oxidized carbons calculated from both titrations methods. The variation from 1 in the slope and the correlation coefficient is related to the slightly different conditions of experiments and limitations of potentiometric titration below pK_a 3 and above pK_a 11. The advantage of potentiometric titration is in the distinct distribution of species having pK_a in the range between 3 and 11 [7].

After modification with urea and heat treatment at 723 K, the pKa's of the species are not changed for BAX and BPL carbons, however the intensity of some peaks as those at pK_a about 6 and 7.5 decreased. In the case of MVP, the shift in the peaks at pK_a 6.5 and 8.5 is noticed and the possible overlap of those peaks at pK_a's between 8.5 and 11. Further heat treatment results in the formation of a very heterogeneous surface with a broad distribution of species not resolved even using the rigorous regularization method. In the case of PBL carbons the effects of urea modifications at 1223 K were similar to those for BAX. The only notable difference is a presence of a peak at pK_a about 5 for BPLN2 and disappearance of the species having pK_a around 6. The shift in the position of the peaks was also noticed on MVP carbon after treatment at 1223 K indicating the presence of different groups on the surface.

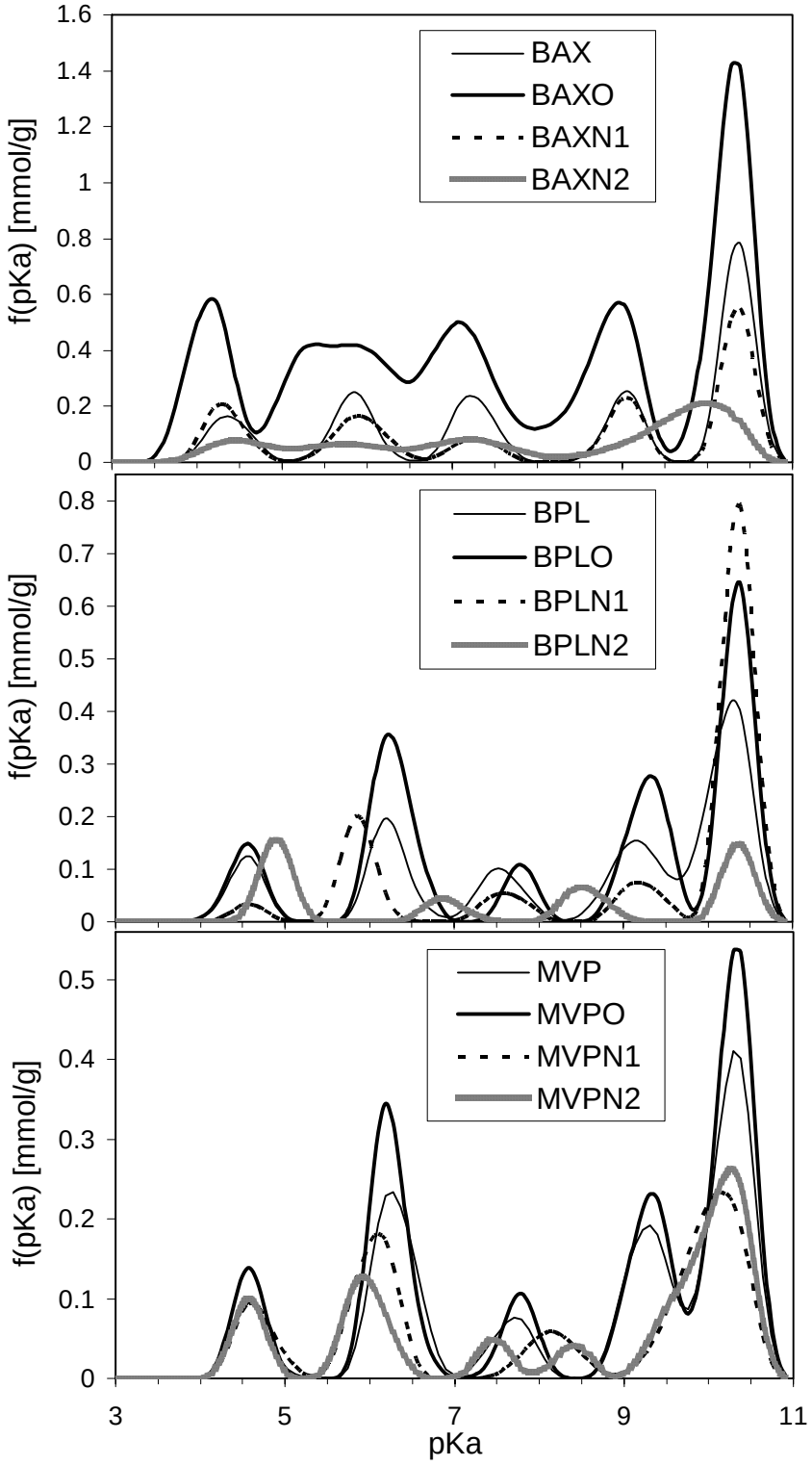

Figure 14: Distribution of acidity constants on BAX, BPL and MVP carbon series.

Table 4: Results of potentiometric titration: Peak position and the number of group (in parentheses; molecules/nm^2).

Sample	Pk_a4-5	pK_a5-6	pK_a6-7	pK_a7-8	pK_a8-9	pK_a9-10	pK_a10-11	Total
BAX	4.38 (0.028)	5.86 (0.041)	---	7.26 (0.039)	---	9.02 (0.037)	10.35 (0.102)	(0.247)
BAXO	4.16 (0.221)	5.64 (0.323)	---	7.09 (0.029)	8.82 (0.261)	---	10.28 (0.453)	(1.547)
BAXN1	4.33 (0.041)	5.93 (0.042)	---	7.28 (0.020)	---	9.02 (0.043)	10.36 (0.091)	(0.237)
BAXN2	4.47 (0.028)	5.74 (0.033)	---	7.29 (0.040)	---	9.76 (0.105)	---	(0.206)
BPL	4.53 (0.043)	---	6.23 (0.074)	7.56 (0.044)	---	9.22 (0.089)	10.26 (0.174)	(0.424)
BPLO	4.53 (0.050))	---	6.27 (0.139)	7.78 (0.034)	---	9.28 (0.112)	10.35 (0.202)	(0.537)
BPLN1	4.57 (0.012)	5.87 (0.077)	---	7.61 (0.027)	---	9.21 (0.038)	10.36 (0.294)	(0.448)
BPLN2	4.89 (0.054)	---	6.91 (0.019)	---	8.55 (0.030)	---	10.36 (0.050)	(0.153)
MVP	4.60 (0.028)	---	6.29 (0.085)	7.67 (0.028)	---	9.30 (0.079)	10.28 (0.138)	(0.358)
MVPO	4.57 (0.050)	---	6.23 (0.139)	7.76 (0.040)	---	9.31 (0.114)	10.3 (0.226)	(0.569)
MVPN1	4.65 (0.032)	---	6.06 (0.067)	---	8.16 (0.026)	---	10.03 (0.124)	(0.249)
MVPN2	4.58 (0.031)	5.97 (0.051)	---	7.49 (0.016)	8.42 (0.014)	---	10.06 (0.149)	(0.261)

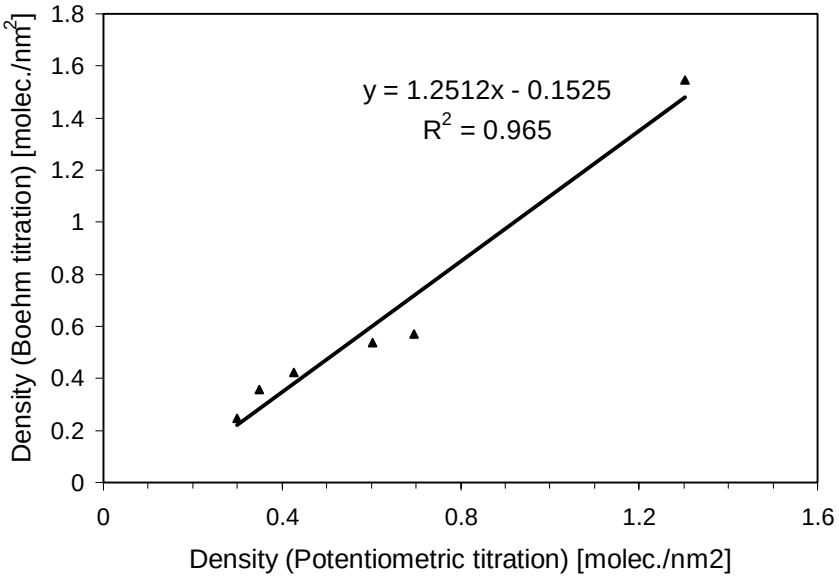

Figure 15: Relationship between the density of all groups calculated from Boehm and and potentiometric titration.

Thermal Analysis Results

Surface chemistry of carbons was also analyzed based on DTG curves obtained in nitrogen (Figure 16) [14, 15]. The peaks on the curves represent the weight loss due to the decomposition of surface groups. As well established using temperature programmed desorption (TPD), carboxylic acid groups decompose to CO_2 between 473 and 873 K whereas at temperature higher than 873 K weak acid, phenol and basic groups decompose to CO [14, 15]. For all our samples after oxidation an increase in the weight loss due to the decomposition of oxygen groups is noticed. Differences in thermal stability are also found for the initial samples. As seen from the curves, the effects of oxidation are the most pronounced for BAX carbon where a significant amount of oxygen-containing groups was introduced into the carbon matrix. The effects of oxidation are similar in the cases of BPL and MVP carbons.

A significant increase in weight loss above 673 K and 873 K is found for all samples after urea modification at 723 K. The effect of urea modification is also manifested between 873 K and 1073 K; however, the intensity of these peaks is much

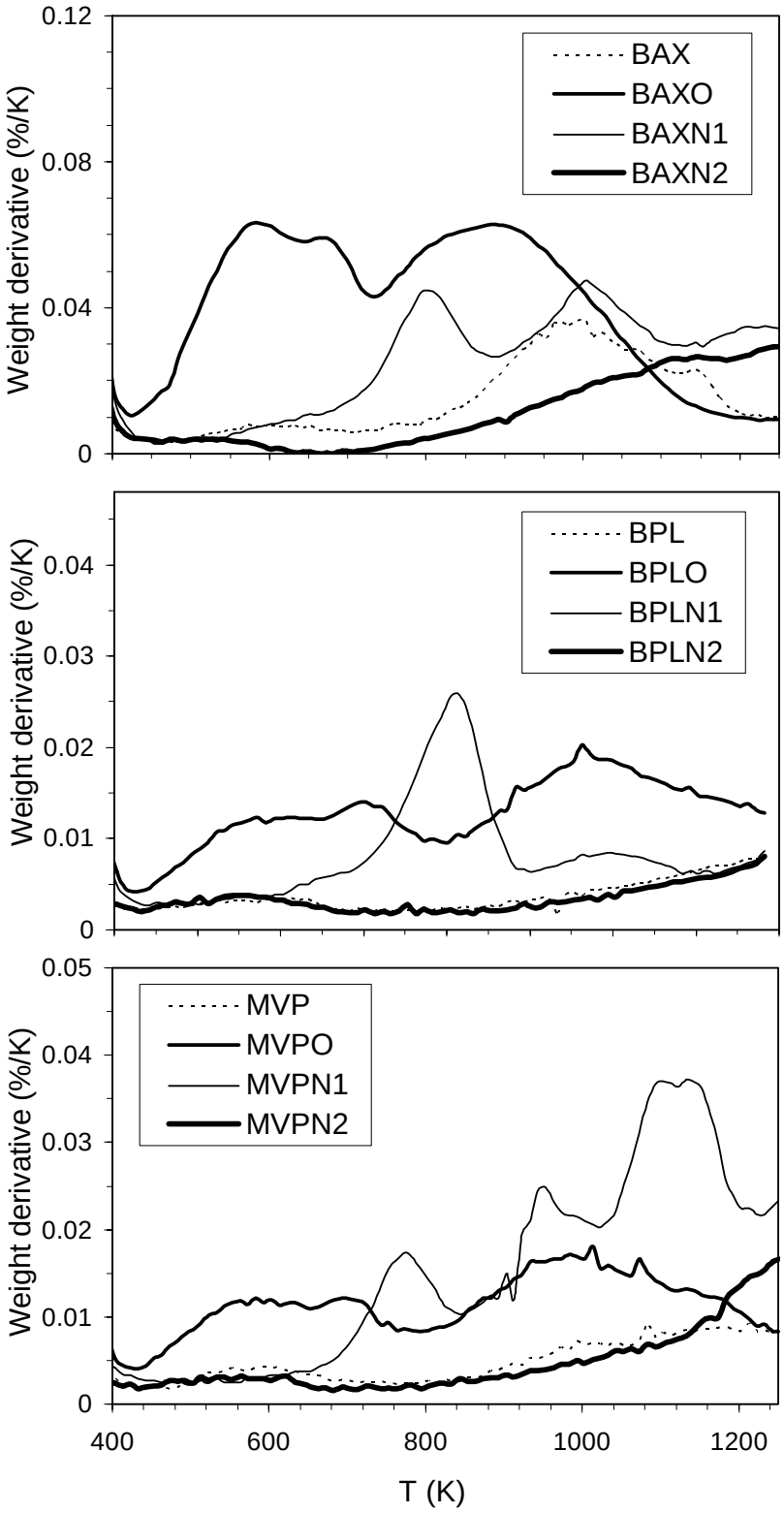

Figure 16: DTG curves in nitrogen for BAX, BPL and MVP carbon series.

smaller for BPLN1 in this range. Since the samples were heat treated at 723 K, the peaks on DTG curves likely represent the decomposition of amine type groups (-NH and -NH_2) incorporated into the carbon matrices [80, 81]. In the case of the BPLN1 and MVPN1 samples a well-defined peak is found between 1023 K and 1223 K, which suggests high degree of heterogeneity of nitrogen-containing surface groups. After treatment at 1223 K the surface of these two carbons is almost featureless and resembles the initial material. On the other hand, the surface of BAX is different. The broad peak between 873K and 1173 K observed for the initial sample disappears and surface seems to be more stable. This is the effect of graphitization at 1223 K, which resulted in an increase in the degree of aromatization and likely in incorporation of nitrogen containing species.

FTIR Results

DRIFT spectra are presented in Figures 17, 18 and 19. Although in using DRIFTS it is difficult to obtain quantitative information about carbon surface chemistry, it shows the trend in surface modifications. For BAX carbon, due to its low degree of aromatization, well-defined adsorption bands at 1730, 1620 and 1260 cm^{-1} are noticed. According to Zawadzki [9], they represent C=O, C⋯O, and C…O stretching vibrations related to the presence of carboxylic groups. Those bands are not found in the cases of BPL and MVP due to their high degree of aromatization. After oxidation of BAX the intensities of bands related to the presence of oxygen-containing groups increase. For other samples the DRIFTS results were inconclusive.

After treatment with urea, the spectra show characteristic bands in the ranges 1500-1600 cm^{-1} and 3500-3600 cm^{-1} which can be related to the presence of nitrogen in the form of amides and amines. Any band around 1600 cm^{-1} represents the vibration of pyridine [79] while the bands related to N-H bonds vibration can be detected in the range 3200-3550 cm^{-1} [79]. The main nitrogenated functional groups introduced into the carbon samples by the reaction with urea are found to be amides and amines mixed in a band around 3550 cm^{-1} and amides 1550 cm^{-1}. Unfortunately, the IR analysis cannot give more accurate results concerning the nature of the functional groups formed after modification.

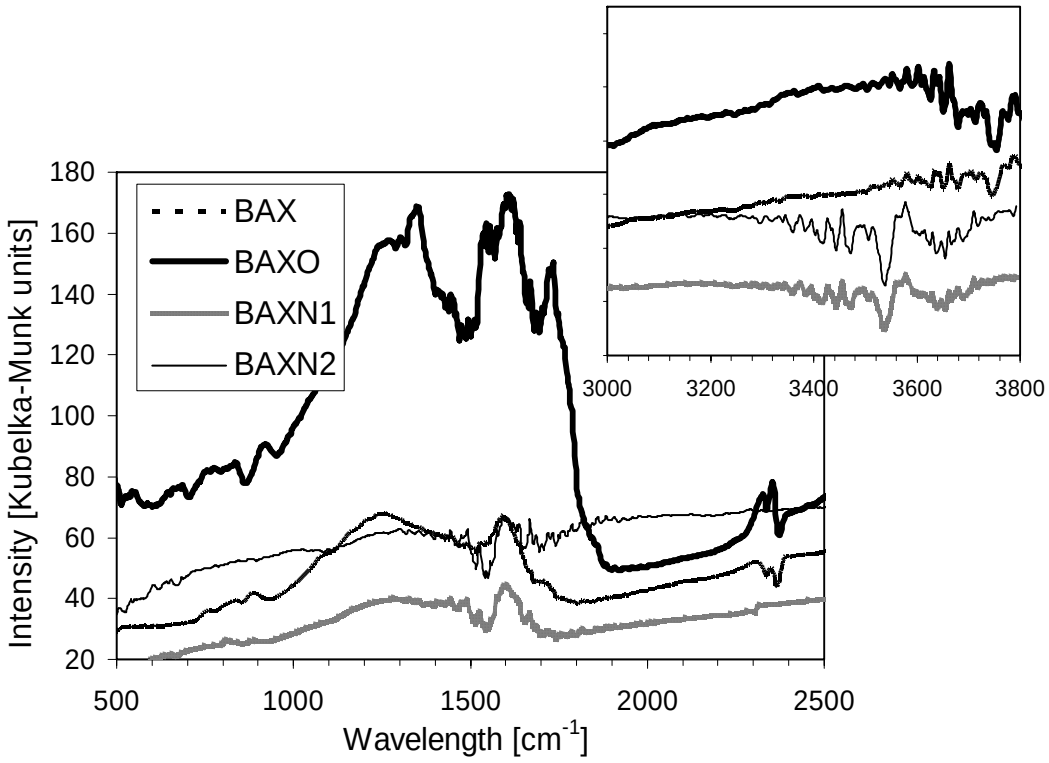

Figure 17: DRIFT spectra for BAX carbon series.

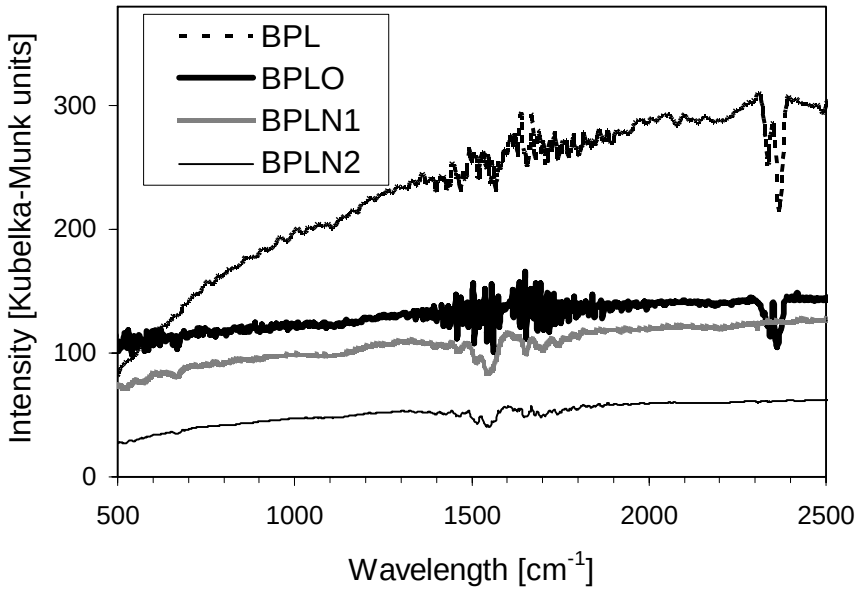

Figure 18: DRIFT spectra for BPL carbon series.

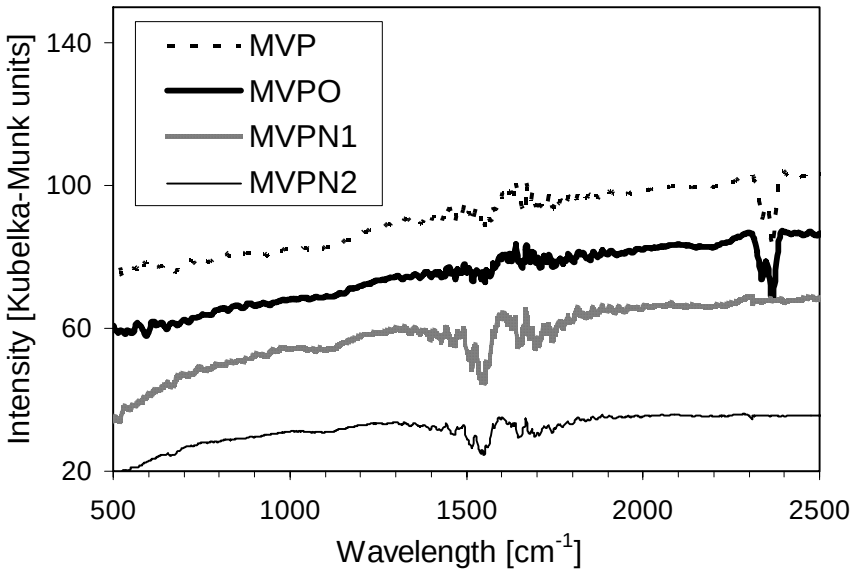

Figure 19: DRIFT spectra for MVP carbon series.

Elemental Analysis Results

The results obtained from elemental analysis of BAX and BPL carbon series are presented in Table 5. They show a significant increase in the nitrogen content after oxidation and modification with urea. The unexpected increase in the content of nitrogen for both samples after oxidation is apparently the result of the incorporation of nitro groups into the matrix of the carbonized material [116]. After modification with urea and heat treatment the amount of nitrogen significantly increased. The effect of urea modification is more significant for the samples treated at 723 K, which have three times more nitrogen than those treated at 1223 K. At 723 K nitrogen is expected to be in the form of -NH and -NH_2, amides or NH_4^+ species [117]. These surface groups decompose at around 873K and some nitrogen is likely converted to aromatic nitrogen species built into the carbon matrix [117]. Although after heating at 1223K, the amount of incorporated nitrogen decreased about threefold compared to those treated at 723 K, the nitrogen content is still significantly higher than that in the initial samples. At 1223 K, the majority of nitrogen incorporated into the carbon matrix is expected to be a component of an aromatic ring in a pyridine – like configurations [75]. It was described in the literature

that carbons with about 1% of nitrogen in the form of pyridine-like groups are catalytically active in the various adsorption processes [28, 81].

Table 5: Elemental analysis of carbon samples

Sample	% C	% H	% N
BAX	73.80	3.64	0.19
BAXO	-----	-----	2.69
BAXN1	75.02	2.46	9.30
BAXN2	73.44	2.31	3.05
BPL	91.23	0.47	0.44
BPLO	-----	-----	0.91
BPLN1	86.36	0.73	3.65
BPLN2	86.61	0.75	1.14

4.1.3 *Adsorption of Acetaldehyde*

All of the previously-described differences in the carbons studied, and changes after oxidation and urea modification should affect the adsorption of acetaldehyde. Acetaldehyde is a small molecule with a van der Waals diameter around 3.8 Å [118]. Due to the presence of the aldehyde group it is able to interact with oxygen- and nitrogen-containing groups on the surface via hydrogen bonding. Moreover, acetaldehyde should also interact in a dispersive way via its hydrocarbon moiety with basal plane of carbons (pore walls) [34]. The types and strength of interactions between acetaldehyde molecules and activated carbons were studied by inverse gas chromatography at infinite dilution. These interactions should be reflected in the values of isosteric heats of adsorption calculated from IGC data from the slope of the dependence of free energy of adsorption on temperature (Figure 20) [51, 84, 119]. The calculated heats are collected in Table 6. The heat of acetaldehyde adsorption on graphitized carbon black was measured to be 25.8 kJ/mol, suggesting that on microporous activated carbons the isosteric heat should be around 52 kJ/mol.

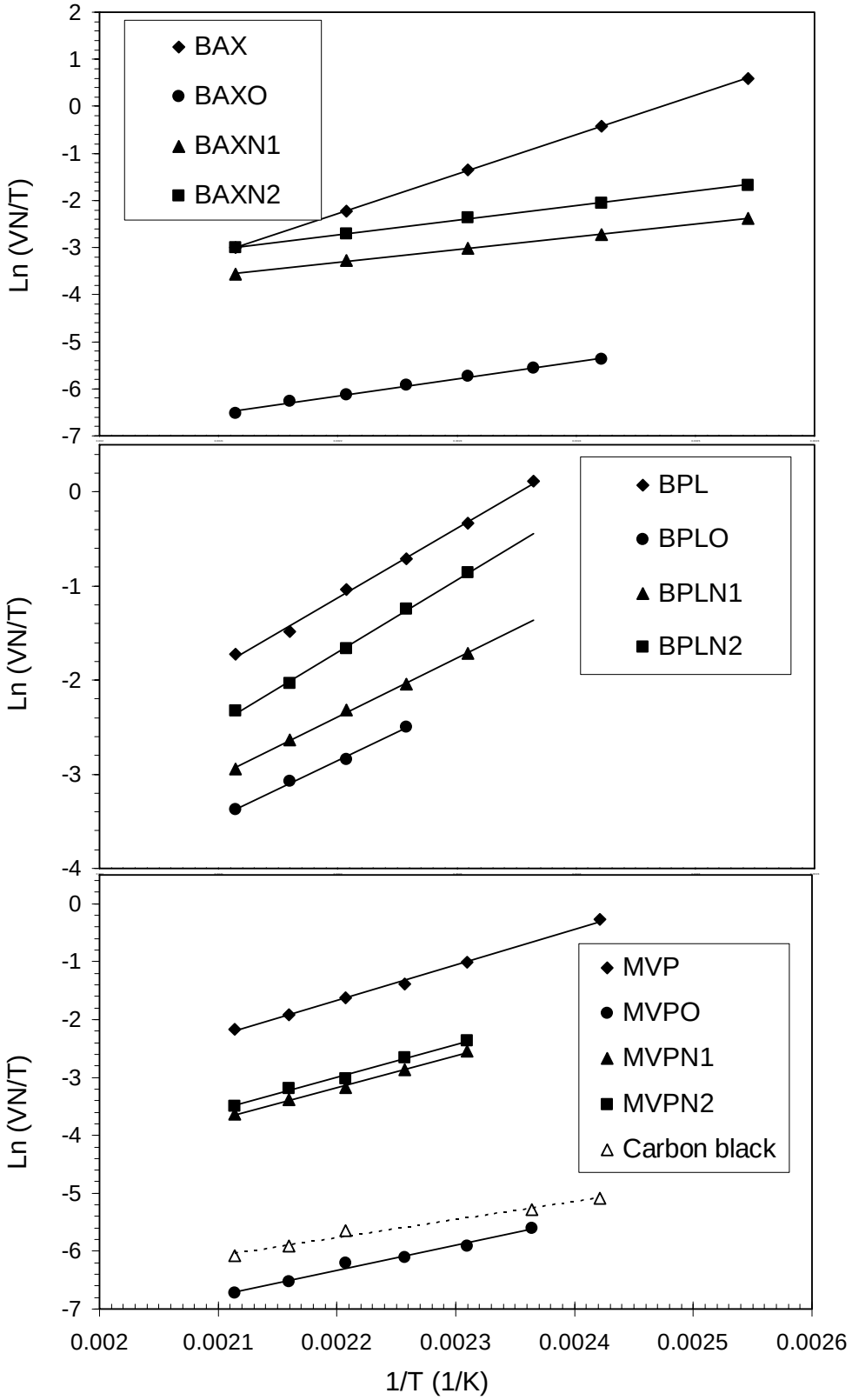

Figure 20: Dependence of $\ln(V_N/T)$ on 1/T for the carbon studied**.**

Comparison of two significantly different samples, BPL and BAX, indicate the differences in the mechanism of adsorption. The heat of acetaldehyde adsorption on BAX is about 8 kJ greater than that for BPL. In fact the comparison of PSDs indicates that the smaller pores, and in a higher volume, are present in the BPL carbon, which should lead to the higher heat of adsorption than that for BAX. The reverse results suggest that in the case of the wood-based carbon the oxygen-containing groups present on the surface contribute to the energetics of the process. To our best knowledge the heat of acetaldehyde adsorption on activated carbon has not been reported. As explained in Chapter 2, the heat of acetaldehyde obtained on microporous carbons should be in the range of 33-51 kJ/mol [34, 51]. Indeed, the values reported in Table 6 are in the expected range. Where hydrogen bonding between the aldehyde group and the carbon surface exists, the heat should be even greater by about 10 kJ/mol [34].

Table 6: Isosteric heats of acetaldehyde adsorption on the carbons studied [kJ/mol].

Sample	Q_{st}	Sample	Q_{st}	Sample	Q_{st}
BAX	69.5±0.3	BPL	61.6±1.6	MVP	51.2±1.5
BAXO	32.4±1.7	BPLO	50.3±2.1	MVPO	35.9±2.2
BAXN1	49.9±1.1	BPLN1	51.9±0.3	MVPN1	45.8±1.8
BAXN2	56.4±1.1	BPLN2	63.7±1.7	MVPN2	47.4±2.3

Based on the above discussion, the presence of functional groups in the very small pores of BAX carbon results in the greater heat of adsorption than that obtained on the BPL sample. After oxidation the heats of adsorption decreased for both carbons; however, the decrease is much more pronounced for the BAXO sample. Although in the case of this carbon the number of functional groups significantly increased, the porous structure was affected to the greatest extent. As shown in Table 1, the volume of micropores decreased about 20%. Another factor which may contribute to a decrease in the adsorption strength is the high density of acidic groups. This density increased more than five times after oxidation as reported in Table 3. As a result, the surface became

more hydrophilic leading to the weaker interactions of the hydrocarbon moiety with the sorbent matrix. Moreover, the hydrogen bond energy is weak compared to dispersive forces in small pores.

Another reason for the decrease may be in inaccessibility of very small pores to acetaldehyde molecules. If functional groups are located at the edge of graphene layers their high density results in blocking the smallest pores for adsorpate molecules. This may also happen in the case of BPLO carbon. This is supported by the fact that in the case of this carbon the pore structure is left almost intact after oxidation.

The effect of oxidation reflected in inaccessibility of small pores is seen also for MVP carbon. After oxidation the heat of acetaldehyde adsorption decreased to the value obtained for oxidized BAX carbon. Although the extent of oxidation for MVPO was much smaller than that for BAXO, the homogeneity of pore structure and their small sizes likely contributed to a significant exclusion of available surface area. It is possible that the treatment with nitric acid fixed oxygen chemical functionalities at the entrances of the micropores, blocking these pores and thus hindering the adsorption of acetaldehyde. It has to be emphasized that the adsorption of acetaldehyde was carried out at infinite dilution where only a few acetaldehyde molecules are injected. These molecules are adsorbed in the narrowest pores they can enter. In the case of MVPO carbon the smallest pores are affected to the greatest extent by the oxidation process.

One can see an apparent discrepancy between the explanation of a decrease in the heat of adsorption and the results obtained from adsorption of nitrogen. When N_2 is adsorbed, the amount of adsorbate is much greater than in our IGC experiment. Moreover, nitrogen covers much larger range of pore sizes than acetaldehyde does at infinite dilution. All of these causes the nitrogen adsorption to be affected less by the oxidation process.

After urea modification and heat treatment at 723 K, the heat of adsorption significantly decreases for all samples suggesting blocking of small pores to acetaldehyde molecule. This is also seen from nitrogen adsorption where a decrease in the volume of micropores, mainly those less than 10 Å, was observed. After treatment at 1223 K an increase in the heat of adsorption is found again, however the initial value is reached only

for BPL carbon. As indicated from other analyses, this carbon is most resistant to heat treatment in the presence of urea.

Since the analysis was done at infinite dilution, if only dispersive interactions play a role, the heat of adsorption should depend on the sizes of small pores. This is related to the value of the characteristic energy of adsorption E^o collected in Table 1. The dependence of the heat of adsorption on the average pore size and characteristic energy of adsorption is presented in Figure 21. For all initial and urea modified carbons studied except BAX, a linear decrease in the isosteric heat of acetaldehyde adsorption is found with increasing average pore size (R^2=0.71). The high value of Q_{st} on the BAX initial sample can be related to the enhanced specific interaction due to the presence of significant amount of oxygen- containing groups [113].

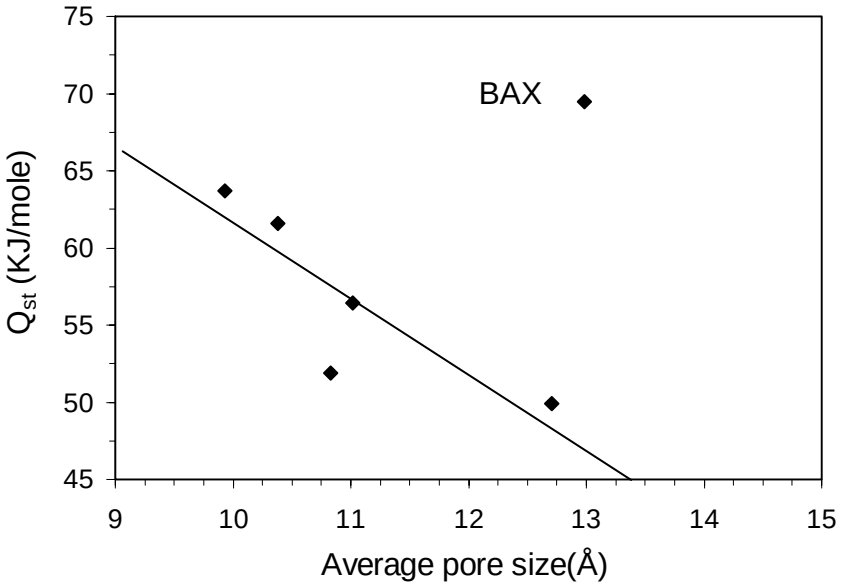

Figure 21: Dependence of Q_{st} on the average pore size of the carbon studied.

The results showed that the heat of adsorption is affected by the presence of large amount of surface groups. The dependence of the heat of adsorption on the amount of various groups on MVP carbon series is shown in Figure 22. The results support our explanation for the variation in the isosteric heat of adsorption. It is clearly seen that for all MVP carbons studied, a linear decrease in the isosteric heat of acetaldehyde adsorption is found with an increase in the total amount of acidic groups and thus total number of groups on the surface. This inverse dependency can be used also to explain the

effect of these surface groups in blocking the pore entrance. Surprisingly, it was found also that the isosteric heat of adsorption increases linearly with the amount of the surface basic groups on these MVP carbon series.

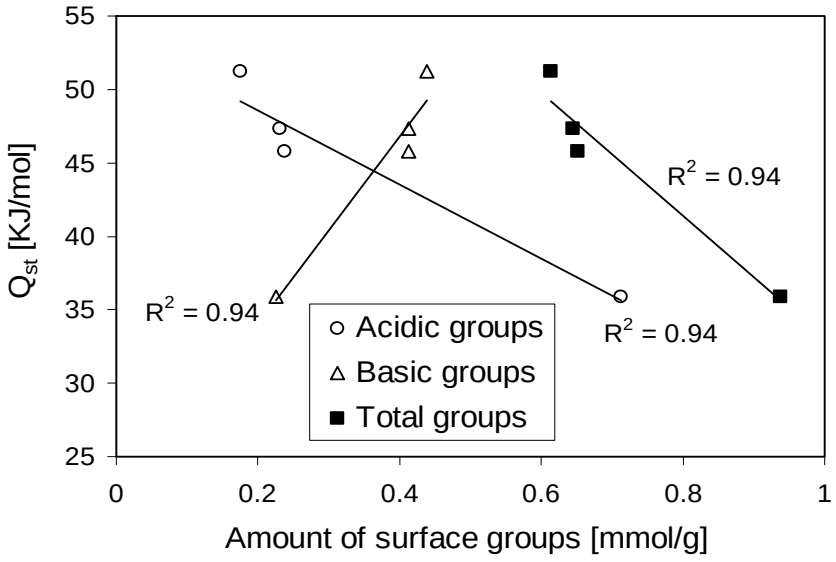

Figure 22: Dependence of Q_{st} on the amount of surface groups on MVP carbon series.

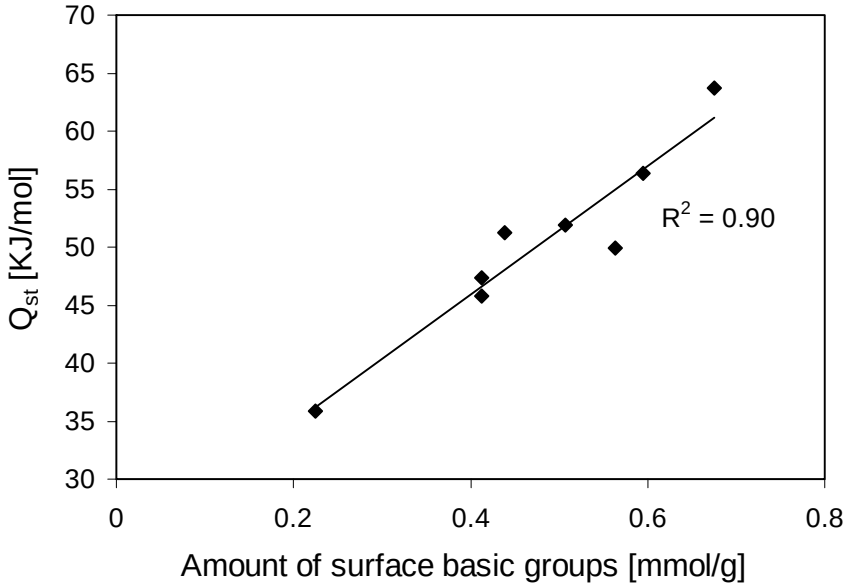

Figure 23: Dependence of Q_{st} on the amount of surface basic groups on MVP carbon series and urea modified carbons.

To examine the effect of surface basic groups on the adsorption process of acetaldehyde, the dependence of isosteric heat of adsorption on the amount of surface basic groups on all carbon samples was also checked. Figure 23 shows that the presence of basic groups enhances the isosteric heat of adsorption not only on MVP but also on all urea-modified carbons.

The capability of carbons to adsorb acetaldehyde was studied under saturation conditions. Figure 24 shows the difference in the DTG for carbons studied before and after acetaldehyde adsorption. For all samples two overlapped peaks are present between 300 K and 600 K. They differ in the intensities indicating almost two-fold greater adsorption on the BAX series of carbons than that on the BPL and MVP series. Taking into account the changes in carbons' structure and surface chemistry, it is likely that the first peak represents weak adsorption of acetaldehyde on chemical groups via specific interactions such as hydrogen bonding. Such adsorption, if occurs, should take place in larger pores where oxygen and nitrogen-containing groups are present and the adsorption potential is weak. The second peak on these curves is related to adsorption of acetaldehyde in small pores via dispersive interactions.

DTG curves shows that oxidation results in an increase in the amount of very weakly adsorbed acetaldehyde which is desorbed around 370 K. The intensity of the second peak decreased for all oxidized carbons. Since the second peak most likely represents desorption of acetaldehyde molecules being adsorbed via dispersive interaction with the pore walls, that decrease can be explained by an increase in the hydrophilic character of the surface resulting in blocking pore entrances.

Incorporation of nitrogen at 723 K results in an increase in the amount of very weakly adsorbed acetaldehyde, which is removed from the surface between 323 and 348 K. The amount of weakly adsorbed species increases, especially for MVPN1 and BAXN2, and it is even greater than that for the initial samples. In the case of BPL series of samples the amount desorbed at this temperature is almost negligible compared to BAX carbons. The fact that for the three series of samples the high temperature parts of the second peak almost overlap (however, differences in the amounts adsorbed exist) indicates similar adsorption strength. This may be related to the adsorption in the small

pores. This overlapping suggests that the removal process is governed only by physical adsorption and in fact we expect it as a predominant force based on the size and chemistry of acetaldehyde molecule.

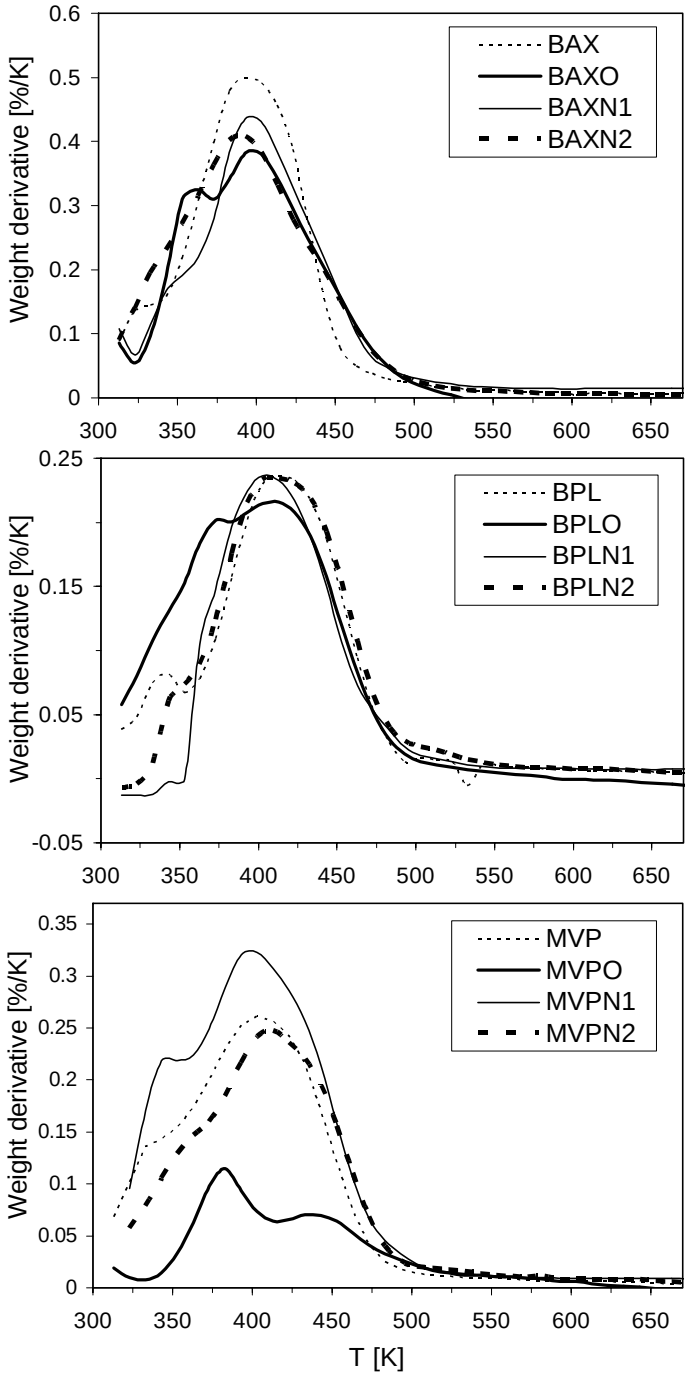

Figure 24: DTG curves in nitrogen for carbons after acetaldehyde adsorption (corrected for the weight loss for the initial samples).

Support for the predominant role of microporosity is presented in Figure 25. When all carbon samples studied are taken into account, the linear trend between the amount adsorbed and the volume of micropores and total pore volume is found with correlation coefficients equal to 0.81 and 0.96, respectively. Assuming that the density of adsorbed acetaldehyde is equal to its liquid density (0.78 g/cm^3) the amount adsorbed in weight percent (Figure 25) was converted to the volume. In the case of BAX, BAXN1 and BAXN2 carbons the volume adsorbed is 0.592; 0.508 and 0.380 cm^3/g, whereas for BPL, BPLN1 and BPLN2 the values are 0.309, 0.249, and 0.303 cm^3/g, respectively. The very good agreement with the volume of micropores (Table 1) indicates that predominantly those pores provide active centers for the adsorption process. Moreover, comparison of these data with the volumes of micropores suggests that in the case of BAX carbons the volume adsorbed is greater than the volume of micropores which supports our hypothesis about contributions of oxygen and nitrogen containing groups located in larger pores to the adsorption process.

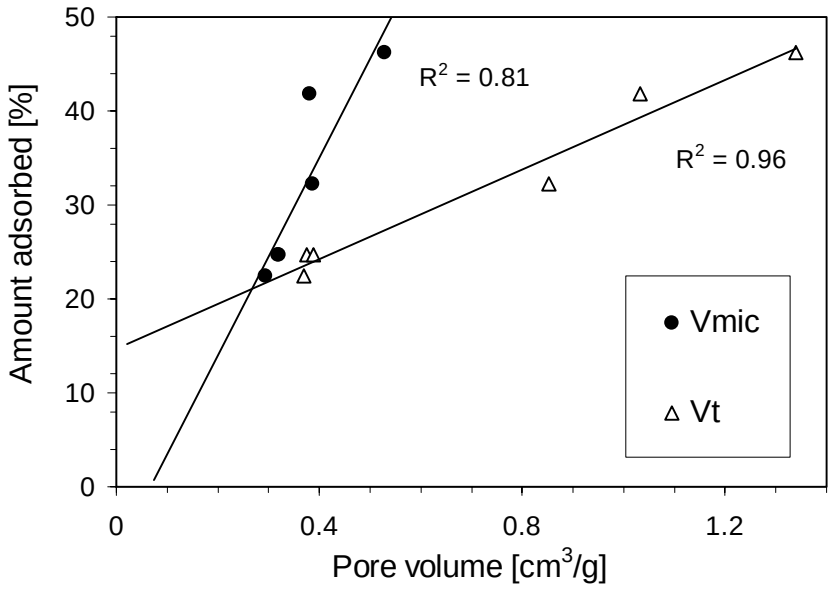

Figure 25: Dependence of the amount of acetaldehyde adsorption on the pore volume (micropores and total pore volume) of carbons.

It is also worth mentioning that the amount of acetaldehyde adsorbed on MVP samples showed similar trends to those observed for the isosteric heat of adsorption with an increase in the amount of surface basic groups (Figure 26). The presence of acidic groups on the surface results in a decrease of the amount adsorbed even though their presence is expected to enhance specific interactions.

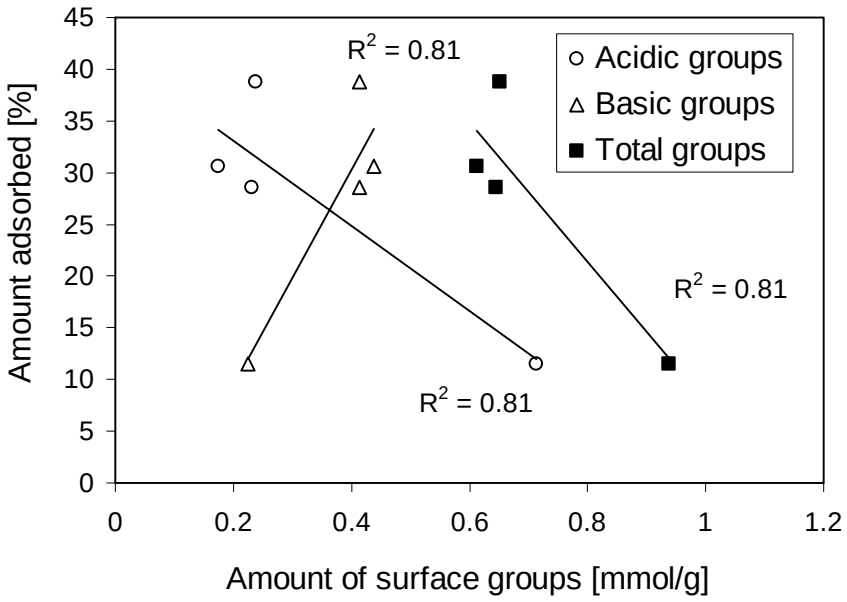

Figure 26: Dependence of the amount of acetaldehyde adsorbed on the amount of surface groups on MVP carbon series.

4.2 Valeric Acid

4.2.1 Surface Characterization

From the literature review (Chapter 2), it is clear that adsorption of small molecule weak organic electrolytes such as valeric acid on activated carbon should be controlled by two major features: its pore structure and surface chemistry [65, 93-95]. The latter factor was indicated to have a significant effect on the uptake [18, 45, 98, 99]. To study both effects, the surface of the carbons chosen for this work was altered by oxidation with nitric acid and urea modification followed by heat treatment at 723 K or 1223 K [13, 28]. New samples of BAX and BPL carbon series (initial, oxidized and urea modified) were used in this study. They are referred to with the same names as those in section 3.2. Another sample of BAX carbon was heated in nitrogen at 1223 K at the same conditions as its urea-modified counterpart. It is referred to as BAXHT.

Although the initial carbons are identical to those used in the acetaldehyde study (section 4.1), very slight variation in the surface structure and chemistry is found for the modified samples. As mentioned in section 3.2, oxidation process was done with a slight difference in the stirring time of the initial carbons with nitric acid (20 hours compared to 24 hours in the acetaldehyde study). Moreover, urea-modified carbons were heated at 723 or 1223 K for one hour in nitrogen atmosphere during urea-modifications compared to 50 minutes in the acetaldehyde study. It has to be pointed out that it is practically impossible to obtain identical results on the same carbon when the modification process is repeated, even if the procedures were done identically. A wood-based carbon such as BAX is less resistant to changes and thus is usually more affected (low temperature carbon, chemical activation). Although it is impossible to obtain the same results, the general trend for variation in porosity and surface chemistry after oxidation and urea modification are the same as those shown in section 4.1 [122-125].

The structural parameters and the results obtained from Boehm titration are presented in Tables 7 and 8, respectively. As expected, the changes in the surface structure and chemistry of activated carbons follow the same trends as those discussed for acetaldehyde adsorption in section 4.1.1. It is worth mentioning that oxidation increased $V_{<10Å}$ for both samples, although that increase is much more pronounced for BAXO

(about 40%) carbon than that for BPLO (around 10 %). Urea treatment at 723 K and 1223 K increased the volumes of micropores (<10 Å) on both carbons except for BPLN1 where a slight decrease is observed. This increase is more pronounced for BAXN2 carbon.

Table 7: Structural Parameters calculated from nitrogen adsorption isotherms.

Sample	S_{BET} [m^2/g]	V_t [cm^3/g)]	$V_{(<20\ A)}$ [cm^3/g]	$V_{(<10\ A)}$ [cm^3/g]	E^o [kJ/mol]
BAX	2266±84	1.339	0.528±0.010	0.123±0.003	15.6
BAXO	1362±50	0.521	0.362±0.007	0.174±0.004	18.4
BAXN1	2317±86	1.358	0.539±0.011	0.125±0.003	15.8
BAXN2	1618±60	0.876	0.378±0.007	0.153±0.004	18.5
BAXHT	1619±60	0.845	0.367±0.007	0.164±0.004	18.9
BPL	901±33	0.376	0.337±0.006	0.186±0.005	21.1
BPLO	938±35	0.404	0.338±0.006	0.201±0.005	20.8
BPLN1	802±30	0.357	0.285±0.005	0.168±0.004	20.9
BPLN2	922±34	0.396	0.318±0.006	0.182±0.005	21.0

Table 8: Results of Boehm Titration (mmol/g).

Sample	pH	Carboxylic	Lactonic	Phenolic	Acidic	Basic	Total
BAX	6.55	0.255	0.140	0.367	0.763±0.033	0.363±0.020	1.126
BAXO	3.76	1.117	0.921	0.671	2.709±0.119	0.094±0.005	2.813
BAXN1	7.1	---	---	---	0.526±0.023	0.340±0.018	0.866
BAXN2	6.92	---	---	---	0.402±0.017	0.400±0.022	0.802
BAXHT	7.42	0.000	0.100	0.250	0.350±0.015	0.400±0.022	0.750
BPL	7.54	0.000	0.025	0.163	0.188±0.008	0.450±0.024	0.638
BPLO	5.57	0.135	0.542	0.125	0.802±0.035	0.488±0.027	1.290
BPLN1	6.99	---	---	---	0.110±0.005	0.500±0.028	0.610
BPLN2	6.78	---	---	---	0.136±0.006	0.520±0.029	0.674

4.2.2 *Adsorption of Valeric Acid*

Adsorption from Aqueous Solution

Our current understanding of adsorption of lower aliphatic acids from aqueous solution by activated carbons [18, 55, 59, 60, 63] indicates that the adsorption is governed by two major interactions, physical and chemical. The former are mainly both dispersive interactions including the microporosity effect, and specific hydrogen bonding, whereas the latter includes surface chemistry effects such as acid-base reactions. To find which features are the most important in the case of valeric acid, the adsorption isotherms from aqueous solution were measured at 333 K. The effect of temperature on adsorption was also studied by comparing the amounts adsorbed at 333K and 303 K. The isotherms are presented in Figure 27 and Figure 28 along with the fit to the Freundlich equation [45, 54, 126]. The fitting parameters are collected in Table 9. As shown, good fits with correlation coefficients better than 0.9 for all samples was obtained. This is typical for surfaces with heterogeneous adsorption sites [54]. Figure 29 shows the low concentration range in the log scale. The fit is also good in this range.

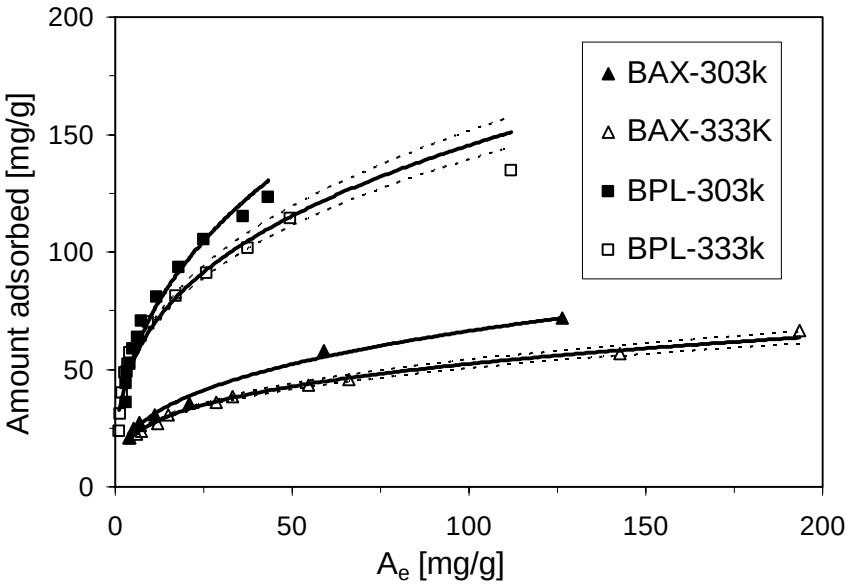

Figure 27: Valeric acid adsorption isotherms from aqueous solution on the initial carbons at 303 K and 333 K. Dashed lines represent the error range.

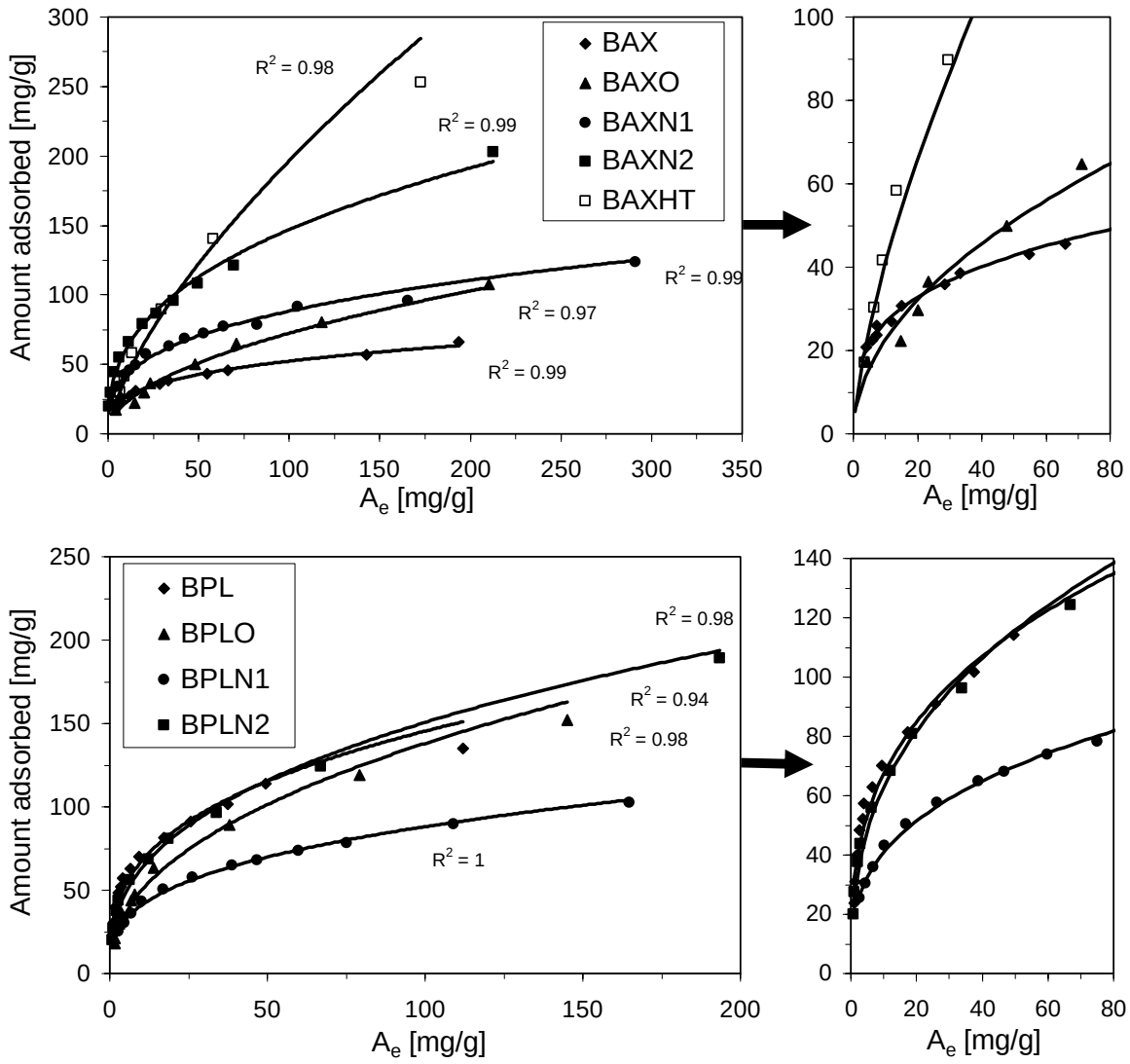

Figure 28: Valeric acid adsorption isotherms from aqueous solution at 333 K (left). Solid lines indicate the fit to Freundlich equation.

The temperatures of adsorption (333 K and 303 K) were chosen to investigate the performance of activated carbon for the removal of valeric acid under conditions close to ambient. It is clearly seen that an increase in temperature decreased the uptake on both carbons (Figure 27). This is expected since the adsorption process is exothermic [18, 66]. An increase in temperature drives the adsorption isotherm towards a lower surface coverage for a given equilibrium concentration. The same behavior was observed on the modified carbon materials where higher uptake was observed at 303 K. The precision of

the experiment is revealed by the gray lines in Figure 27 which represent the error range measurement. They indicate satisfactory reproducibility of the adsorption isotherms.

Table 9: Fitting parameters to the Freundlich equation.

Sample	n	K_F
BAX	0.29	13.62
BAXO	0.50	7.080
BAXN1	0.33	19.81
BAXN2	0.38	25.45
BAXHT	0.33	26.39
BPL	0.33	31.12
BPLO	0.45	17.74
BPLN1	0.34	18.88
BPLN2	0.38	26.16

The higher uptake on BPL carbon than that for BAX (Figures 27 and 28) suggests the importance of microporosity and hydrophobicity of the surface. This is supported by a noticeable decrease in the amount adsorbed after oxidation. It is interesting that the valeric acid uptake decreased for BPL carbon after oxidation while for the BAX carbon, after an initial decrease, a significant increase is observed. As described in Chapter 2, Nekrassow [59] attributed the decrease in the uptake of the lower aliphatic acids after oxidation of activated carbons to an increase in the polar nature of the carbon surface resulting in an increased effective competition by water for the sites on the surface. Bruns [60] related this decrease to the change in the surface porosity after oxidation. Since the surface porosity for BPL carbon did not change significantly after oxidation, this decrease can be linked to an increase in the number of surface oxygen groups introduced into the surface. An increase in acidity is related to an increase in the polarity of the surface which is in an agreement with Nekrassow hypothesis [59].

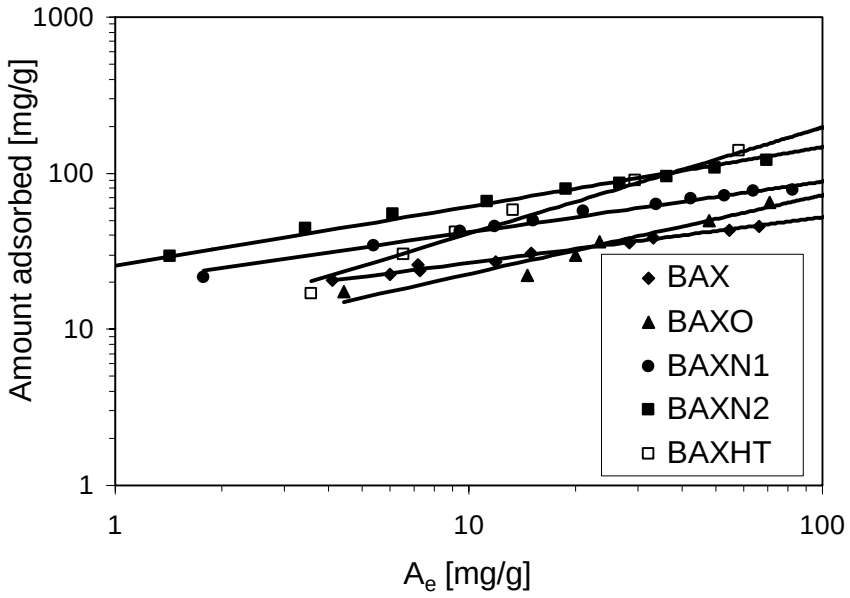

Figure 29: Low concentration range in the log scale for valeric acid adsorption isotherms from aqueous solution at 333 K on BAX carbon series.

Carbon basicity can also have an effect of adsorption of valeric acid due to its acidic character. As shown in Table 7 the number of basic groups is much higher on BPL carbons than on BAX. Another factor which can explain the observed trend is the possible repulsive forces between the carboxylic group of the valeric acid molecule and the surface of activated carbon, which became more negatively charged with increasing surface acidity [45, 127-129]. This factor, however important, cannot be discussed in detail here since the experiments were performed without controlled pH of the suspension. As a result of this, the apparent isotherms were measured where two forms of valeric acid (molecule or ion) contribute to adsorption.

Similar factors as given above seem to be true in explaining a decrease in valeric acid uptake on BAXO at low concentration. The density of acidic groups and carboxylic groups increased significantly on this carbon which may contribute both to a decrease in an available surface of graphene planes where hydrocarbon moiety can accommodate and to an increase in repulsive interactions due to the low pH of this carbon surface [45].

It is expected here that hydrogen bonding of carboxylic acid groups with oxygen on the surface is not a predominant force for valeric acid adsorption from solution due to

adsorption and clustering of water on those primary adsorption centers [45, 130-135]. On the other hand, the volume of pores smaller than 10Å increased for BAXO, which could explain an increase in the uptake at high concentrations. As the equilibrium concentration of solute in solution increases, there will be more valeric acid molecules available for interactions via the carbon moiety, mainly in pores smaller than 10Å in width where adsorption potential is the highest (the critical size of valeric acid is about 4Å) [33]. The number of valeric acid molecules adsorbed by unit weight of BAXO increases, hence decreasing the surface area available to the water molecules. Supporting for this is a very low energy of water interactions with graphene planes of activated carbons [130].

It is interesting that the valeric acid uptake increased noticeably for BAX carbon after urea modification at both temperatures while it decreased on BPL carbon after modification at 723 K and showed no significant change on BPLN2. This variation in the uptake is related to the changes in surface chemistry and porosity addressed above. The number of acidic groups decreased significantly for BAX carbon after urea modification at both temperatures while the number of basic groups and the volume of pores smaller than 10 Å increased. The effect of modification was more noticeable on BAXN2. This results in an increase in an available surface of graphene planes where hydrocarbon moiety can accommodate and in a decrease in repulsive interactions due to the low pH of this carbon surface [45]. This trend is also observed for BAXHT for which both the basicity and the volume of small pores increased. A smaller increase in the uptake on BAXHT compared to BAXN2 is likely the result of the weaker nature of basic groups, which are only oxygen- based. A similar explanation can be used to describe the decrease in the uptake on BPLN1. Although the number of acidic groups decreased on this carbon resulting in a less hydrophilic carbon, the volume of pores smaller than 10 Å also decreased significantly. Since in the case of BPLN2, urea modification changed the surface chemistry only slightly with the preserved porosity, the unchanged uptake on BPL carbons shows the predominant effect of microporosity and hydrophobicity of the surface.

If surface chemistry is involved in the adsorption mechanism, we expect different interaction behavior between valeric acid and various types of groups on the surface. In order to understand the mechanism involved, the adsorption isotherms of valeric acid on

the oxidized and urea modified carbons should be analyzed separately. Figure 30 shows the correlation between unit capacity parameter K_f and the density of basic groups on the initial and oxidized carbons. Higher density of those groups results in the higher unit capacity parameter, which seems to be consistent with the possibility of chemical interactions of valeric acid with electron donor centers. If we assume that basic groups are not only the oxygen-containing pyrene type organic structures but also free valences at the edges of the carbon crystallite [23] the correlation found seems to be logical from the point of view of an increase in the adsorption capacity due to the specific interactions.

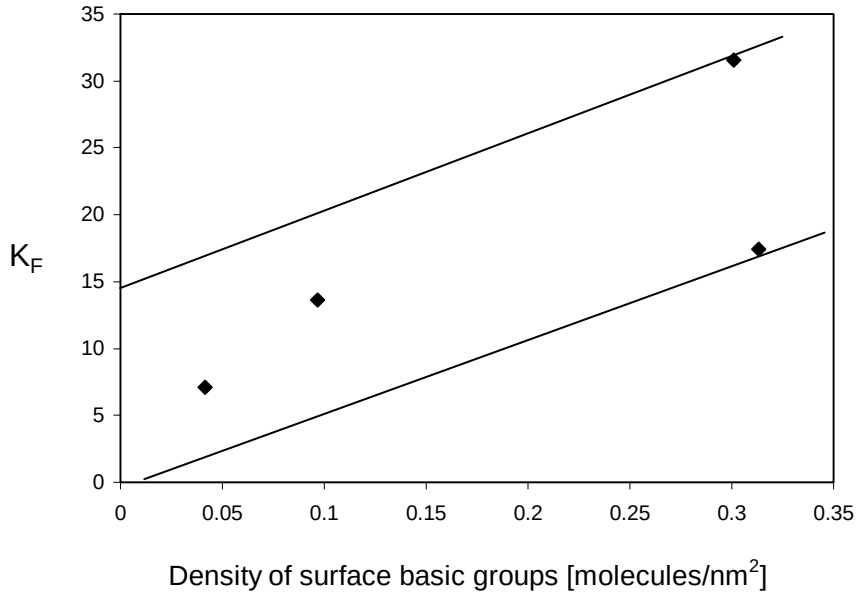

Figure 30: Dependence of the unit capacity parameter K_F on the density of basic groups on the initial and oxidized carbons. The area between solid lines shows the trend.

Figures 31 and 32 show the correlation between unit capacity parameter K_F and either the amount of total groups or the volume of pores smaller than 10 Å, respectively. The dependence is found only for the initial carbons and those modified at 1223 K. It is clearly seen that the capacity factor increases with an increase in the $V_{<10\ Å}$ (Figure 31) while a decrease is noticed with an increase in the total number of groups (Figure 32), indicating that these two parameters have opposite effects, attractive and repulsive respectively, toward valeric acid molecules. Although K_F showed a good correlation with

the total amount of surface groups, it didn't show a direct correlation with either acidic or basic groups. As mentioned in section 2.1, pyridine-like configuration is expected to be the main basic groups on the urea-modified carbons at 1223K. It is worth mentioning that urea-modified carbons at 723K were excluded from those correlations. The exclusion was done since the experiments were run without controlling pH. Both valeric acid in the solution and the surface groups on carbon are likely to have molecular and ionized forms, depending on the pH. These correlations with the surface chemistry indicate that the presence of different types of groups on the surface exerts different interaction behavior with the valeric acid molecules while the net interaction depends on the total number of groups. It is interesting that no correlation was found between the heterogeneity parameter and particular surface features. This suggests that adsorption sites are complex and consist of both, surface groups and pore size.

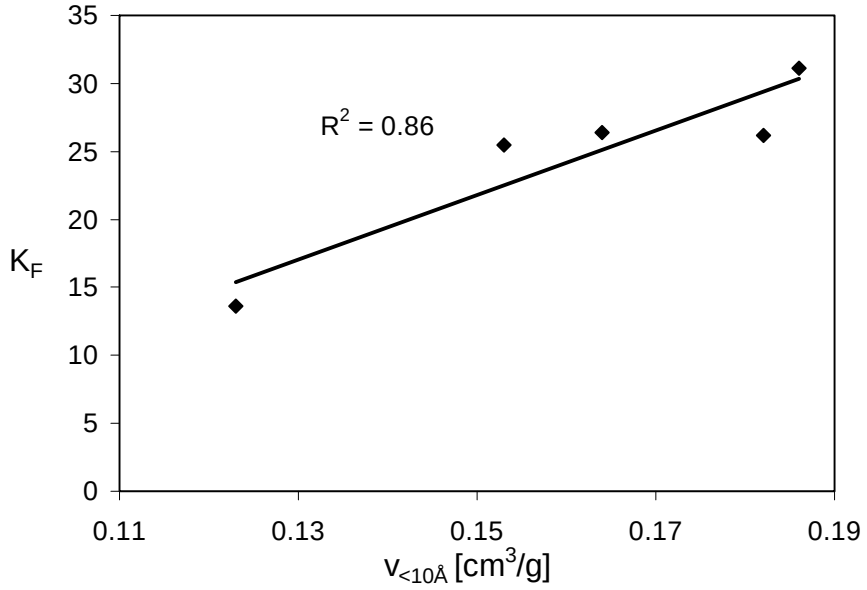

Figure 31: Dependence of the unit capacity parameter K_F on $V_{<10\ Å}$ of the initial and modified (1223K) carbons.

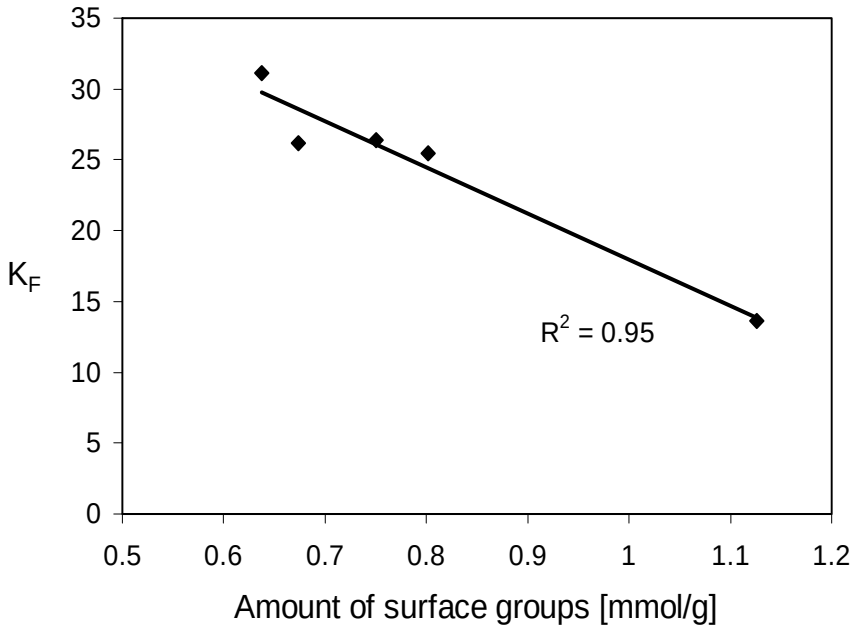

Figure 32: Dependence of the unit capacity parameter K_F on the total amount of groups on the initial and modified (1223K) carbons.

Since the unit capacity factor of the Freundlich equation showed some dependence on the surface chemistry of the carbons studied, the amount of valeric acid adsorbed on the surface (molecules/nm^2) at low equilibrium amount of valeric acid (5 mg of acid/ per g of carbon, calculated from the fitted isotherms) was plotted versus the amount of surface groups. From the results presented in Figure 33 it is seen that adsorption at low surface coverage increases with an increase in the density of basic groups. This finding indicates the importance of surface chemistry and specific interactions as the most energetically favorable at low concentration of valeric acid. As mentioned in Chapter 2, the surface groups introduced into the carbon surface as a result of oxidation and urea modification are of different chemical nature and thus are expected to interact differently with the valeric acid molecules being adsorbed. Based on this, the oxidized and urea-modified carbons will be considered separately while analyzing the amount of valeric acid adsorbed at low and high equilibrium amounts.

With an increase in the concentration of valeric acid, the adsorbate should occupy the volume of small pores, similar in size to the molecule. Taking this mechanism into consideration, the volume adsorbed at the equilibrium amounts of 200 and 500mg of

acid/g of carbon (calculated from the fitted isotherms) was plotted versus the volume of pores smaller than 10 Å for the initial and oxidized carbons.

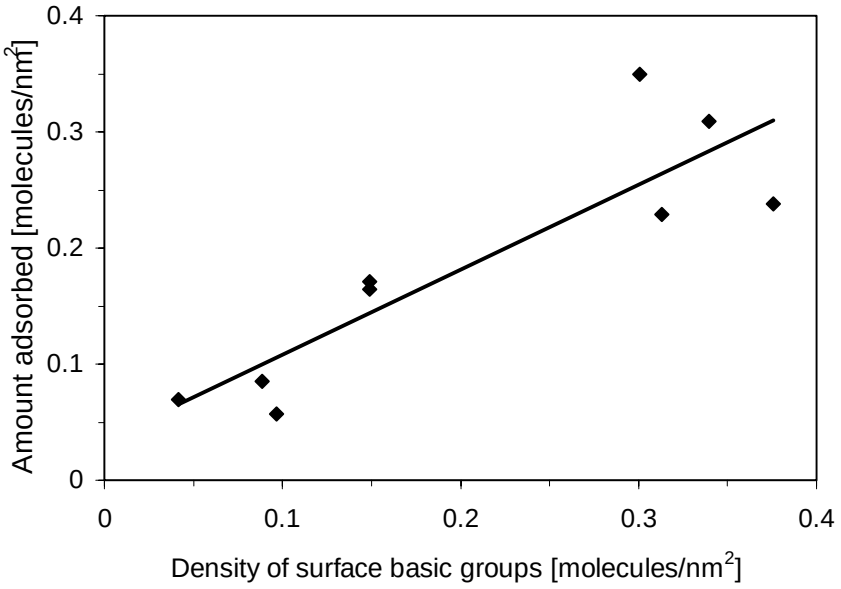

Figure 33: Dependence of the amount adsorbed at low equilibrium amount (5 mg of valeric acid/g of carbon) on the density of surface basic groups.

As seen from Figure 34A, a direct correlation between these two quantities exists. The fit becomes even better when we extrapolate the equilibrium amount to 500 mg of acid/g of carbon (Figure 34B). In such a case the volume adsorbed is only slightly greater than $V_{< 10\ Å}$. This suggests that some volume of larger micropores is also occupied by valeric acid at the high equilibrium amount of 500 mg of valeric acid per gram of carbon. It is likely that adsorption on basic centers located in larger pores than 10Å takes place.

The dependence of the amount of valeric acid adsorbed (calculated from the fitted isotherms) at low (5 mg of acid/g of carbon) and high concentration (500 mg of acid/g of carbon) on the surface chemistry and porosity of the carbons (before and after modification with and without urea at 1223 K) was also evaluated. Figures 35 and 36 shows the dependence of the amount adsorbed at A_e=5 (mg acid/g of carbon) on the total number of groups, and on $V_{<10\ Å}$, respectively. The amount adsorbed on the urea modified carbons at 723 K was excluded again from these correlations. It is clearly seen

that the adsorption at low surface coverage increases with an increase in the $V_{<10\ Å}$, while it decreases with an increase in the amount of all surface groups including acidic and basic groups.

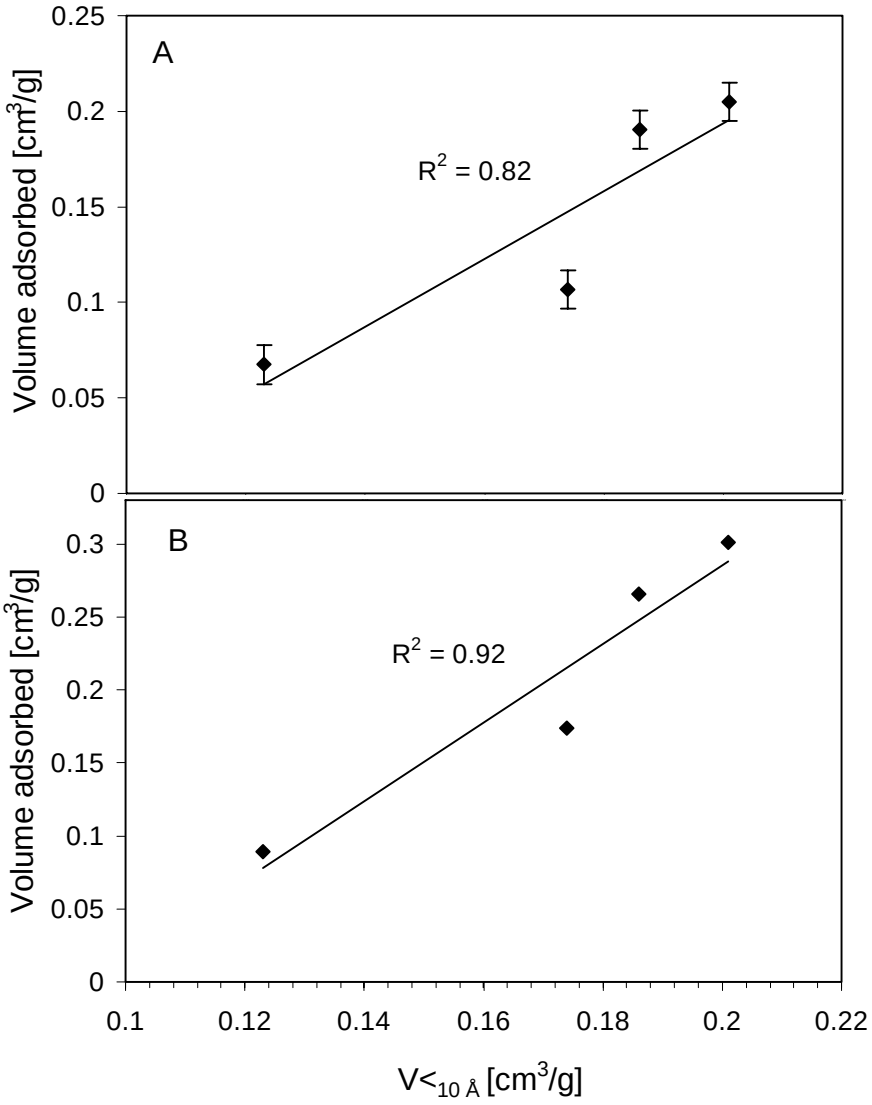

Figure 34: Dependence of the volume adsorbed at high equilibrium amount ((A) 200 mg of valeric acid/g of carbon and (B) 500 mg of valeric acid/g of carbon) on the volume of micropores smaller than 10 Å of the initial and oxidized carbons.

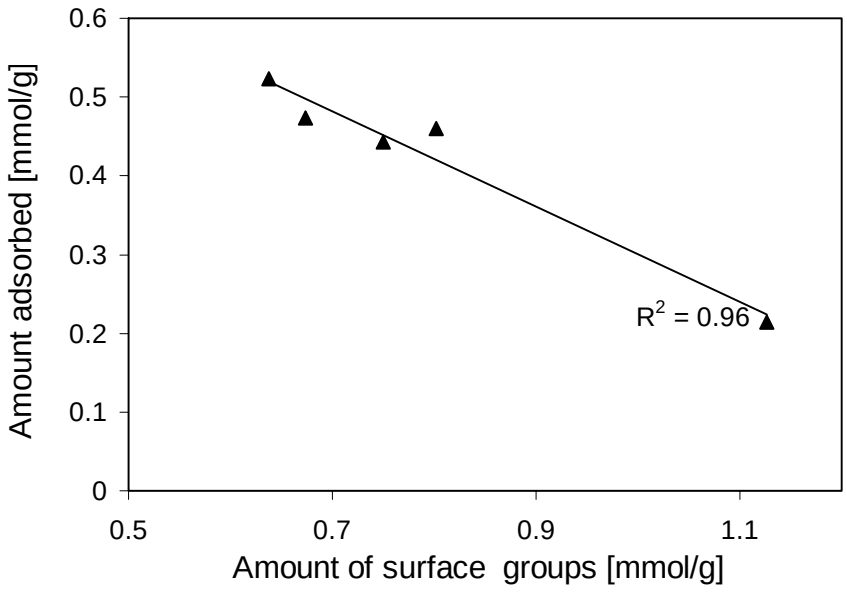

Figure 35: Dependence of the amount adsorbed at low equilibrium concentration (5 mg/g) on the total amount of groups on the initial and modified carbons at 1223 K.

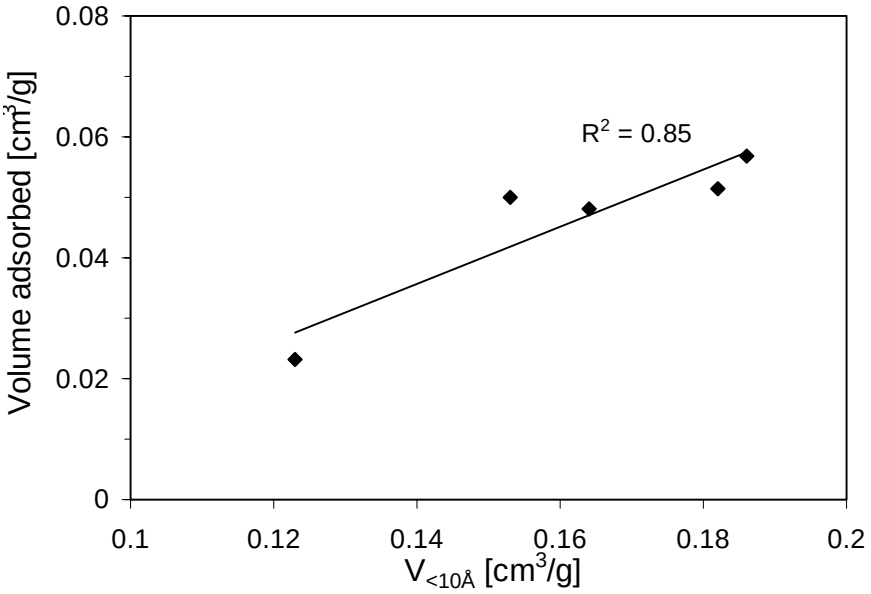

Figure 36: Dependence of the volume adsorbed at low equilibrium concentration (5 mg/g) on $V_{<10\,Å}$ of the initial and modified carbons at 1223K.

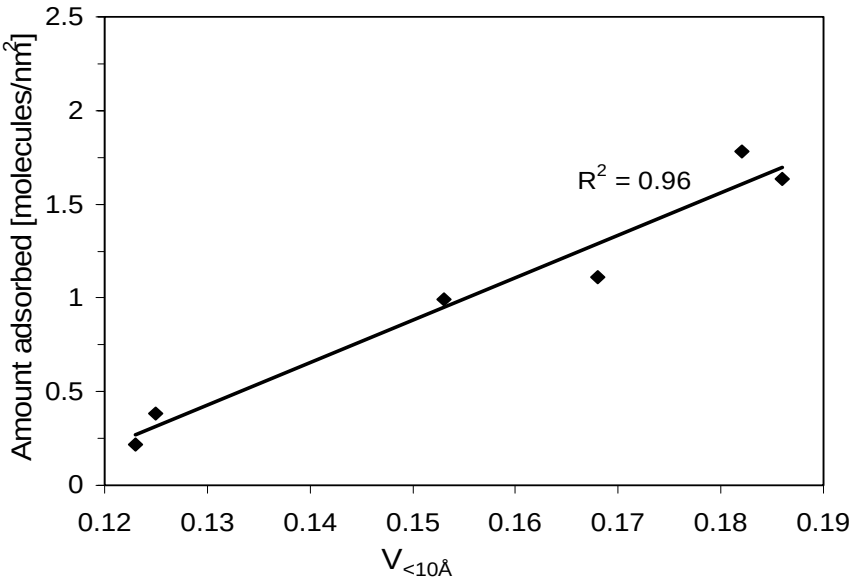

Figure 37: Dependence of the amount adsorbed at the high equilibrium amount (500 mg of valeric acid/g of carbon) on $V_{<10\,Å}$ (the initial and urea modified carbons).

At higher concentration (A_e = 500 mg/g), although a similar correlation exists with the number of surface groups, the dependence on $V_{<10\,Å}$ is much weaker. This was expected since the pores smaller than 10 Å should be filled at low surface coverage as the most energetically favorable sites. The presence of the groups containing heteroatoms increases the polarity of the surface and results in the valeric acid molecules being in competition with the water molecules for occupying those sites (acidic and basic groups).

Moreover, the acidic surface groups make the surface negatively charged resulting in a repulsion of the valeric acid molecules [45]. This explains the low adsorption on BAX carbon. At this high concentration (A_e = 500 mg/g), the presence of the basic groups on all urea-modified carbons (723K and 1223K) results in enhancing the valeric acid uptake on the carbons studied(Figure 37).

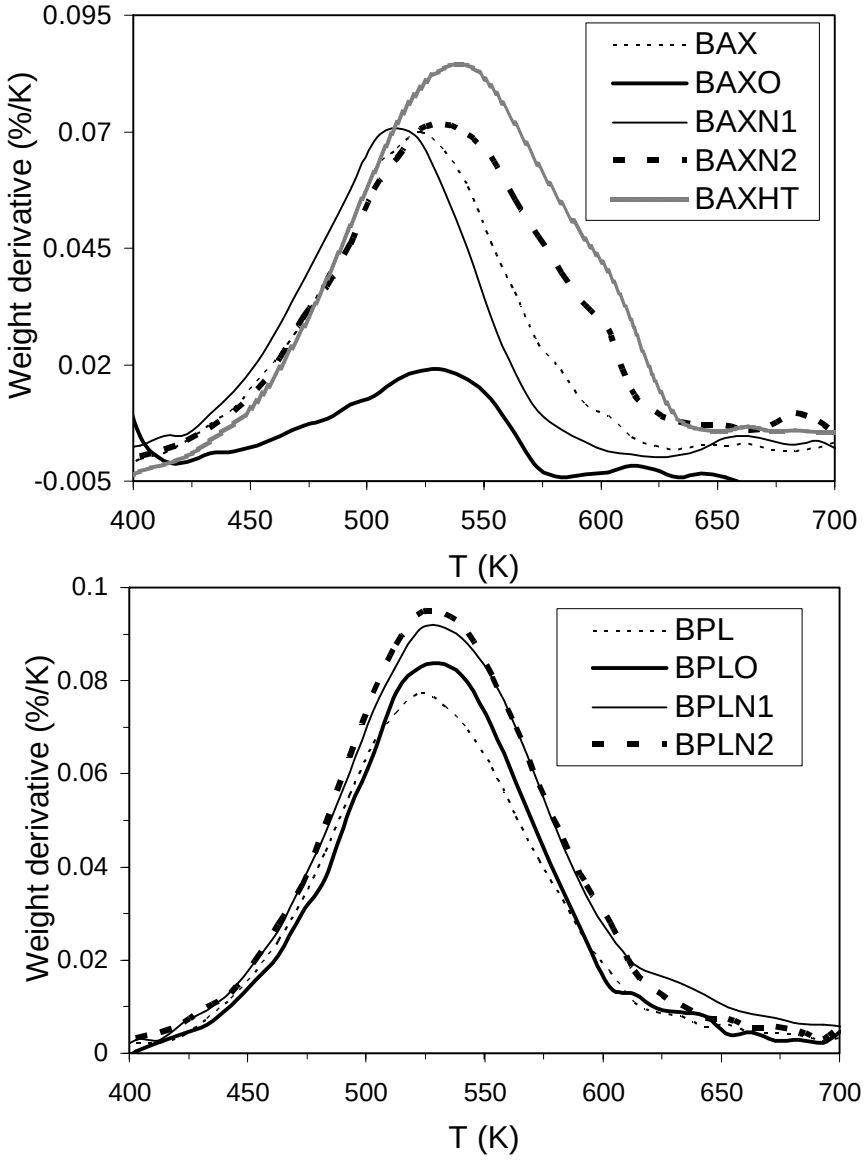

Figure 38: Difference in the DTG curves for carbons before and after valeric acid adsorption from solution (adsorption on 0.1 g from 500 mg/g of valeric acid, after drying at 400 K for 1 h).

A specific pattern of valeric acid desorption is expected when thermal analysis is done on the samples previously exposed to adsorption from solution. The position and broadness of the peak should depend on the strength of valeric acid interactions with the carbon surface. Valeric acid can be weakly adsorbed in large pores where oxygen and nitrogen containing groups are present and where hydrogen bonding is possible. For

adsorption from an aqueous solution, this type of interaction is excluded due to the presence of water molecules, which are more favorably adsorbed on these groups. To study the strongest interactions at high equilibrium concentration, 0.1g samples of carbons after valeric acid adsorption from solution (500 mg/g of carbon) were dried at 400 K for 1 hour in order to remove weakly adsorbed (via nonspecific interactions) acid (the boiling point of valeric acid is 458 K) and water. Differences in DTG curves between those carbons and the initial counterparts are shown in Figure 38. For all samples a broad peak is present between 400 and 600 K. The width and intensity of these peaks differ from one carbon to another. It is clear that the amount of strongly adsorbed valeric acid increased on all carbons after modifications except for BAXO where a noticeable decrease is observed. The largest amount adsorbed (biggest weight loss) is found for carbons modified at 1223 K. After modification with urea the peaks became broader indicating stronger adsorption (high temperature expansion) which is likely the result of interactions of valeric acid with nitrogen groups introduced onto the surface and /or more adsorption sites formed in small micropores. Those micropores seem to play a predominant role in the case of BAXHT where a well pronounced high temperature shoulder is revealed. The large decrease of adsorption on BAXO is the result of a significant decrease in the volume of micropores and also in the number of basic groups. Moreover, it is important to mention that the amount of acidic groups increased significantly on the surface of this carbon. These groups, as found before, exert a repulsion effect on valeric acid adsorption.

By linking the amount of valeric acid adsorbed to the structural and chemical features of the carbon studied, good correlations were found between the amounts of valeric acid adsorbed per unit surface area with the densities of basic groups on the surface (Figure 39). The amount adsorbed seems to increase linearly with an increase in the amount of those groups on the surface. Moreover, the amount of valeric acid adsorbed appears to decrease as the overall amount of groups on the surface increases. Due to the differences in the nature of surface groups on the initial and oxidized carbons (mainly oxygen–type) and on the urea modified carbons (nitrogen origin), different interaction behavior of valeric acid with the surface is expected.

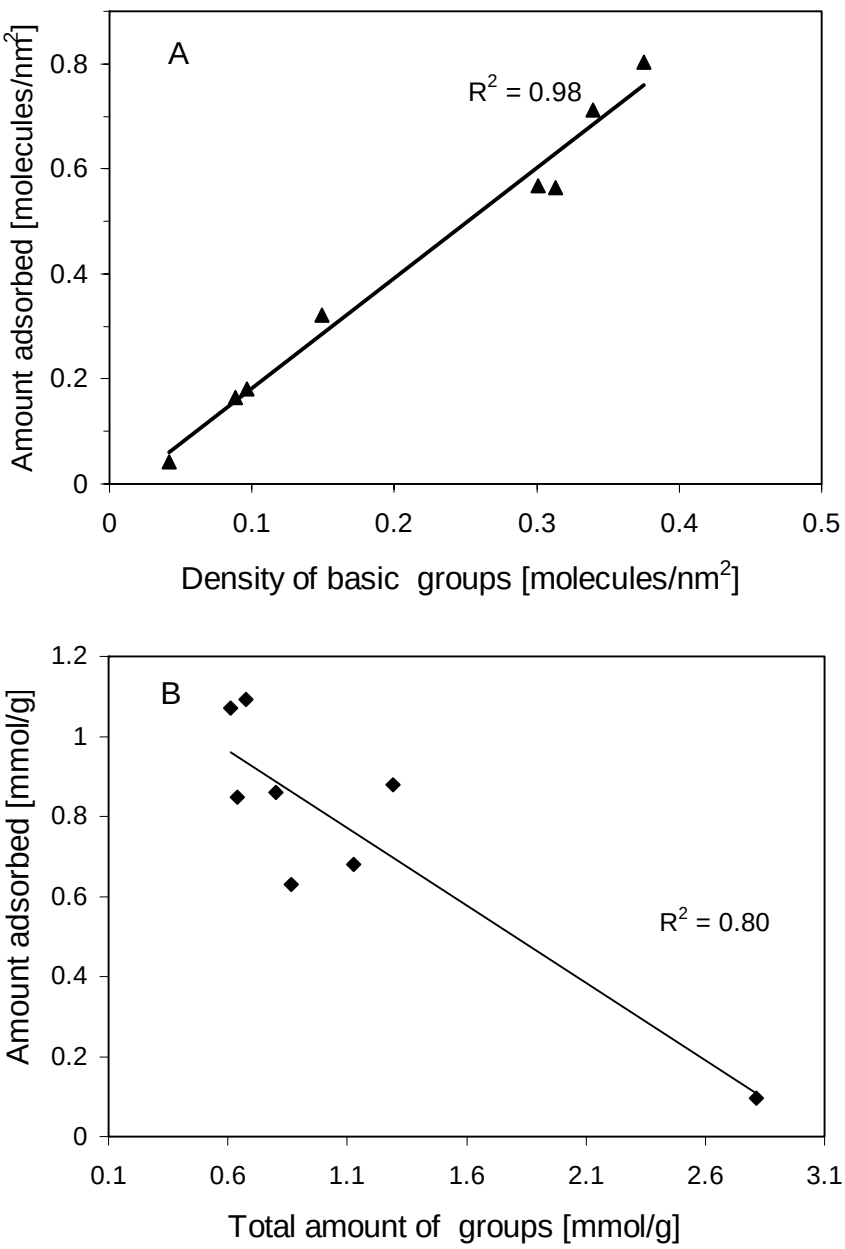

Figure 39: Dependence of the amount of valeric acid strongly adsorbed: on the density of surface basic groups (A) and on the total amount of surface groups (B).

The amounts of valeric acid strongly adsorbed were linked to the structural and chemical features of the surface of the initial and oxidized carbons (Figure 40) or the urea-modified carbons (Figure 41) separately. It is seen from Figure 40 that the amount of valeric acid adsorbed is governed by carbon basicity since the dependence of the amount adsorbed on the amount of surface basic groups on the initial and oxidized carbons showed a very good correlation coefficient. The slope suggests that, on the average, two molecules of valeric acid are attached to one basic center. The presence of acidic groups decreased the amount adsorbed. As mentioned before, these acidic groups can decrease the adsorption by exerting repulsive interactions or by providing sites for competitive adsorption of water molecules. Similar results of an increased adsorption of valeric acid with an increase in the surface basic groups are obtained on the urea modified carbons (Figure 41). On the other hand, the amount of valeric acid adsorbed decreased when the amount of acidic groups increased. It is interesting that the absolute value of the slope is similar to those in Figure 40 (around 2) indicating similar strength of attractive/repulsive forces.

Besides the influence of surface chemistry on the amount of valeric acid strongly adsorbed on the surface of urea-modified carbons, the pores of small sizes should also affect the amount adsorbed by enhancing the adsorption potential. Figure 42 presents the dependence of the volume of valeric acid strongly adsorbed on the volume of pores smaller than 10 Å. In the case of oxidized carbon, no correlation was found for the strongly adsorbed amount and the volume of pores smaller than 10 Å.

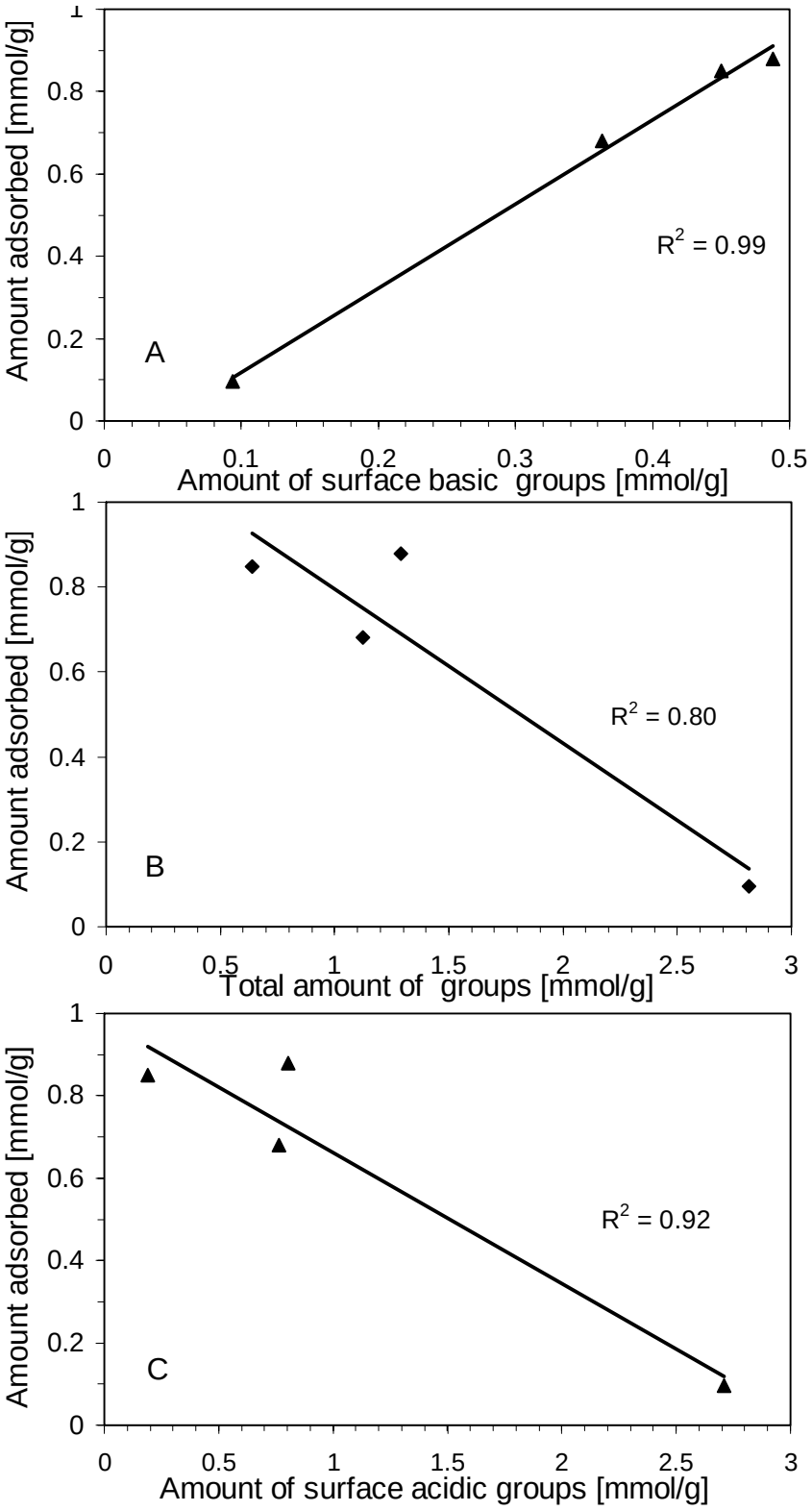

Figure 40: Dependence of the amount of valeric acid strongly adsorbed on the initial and oxidized carbons on: the amount of surface basic groups (mmol/g) (A); total amount of surface groups (mmol/g) (B); and amount of surface acidic groups (mmol/g) (C).

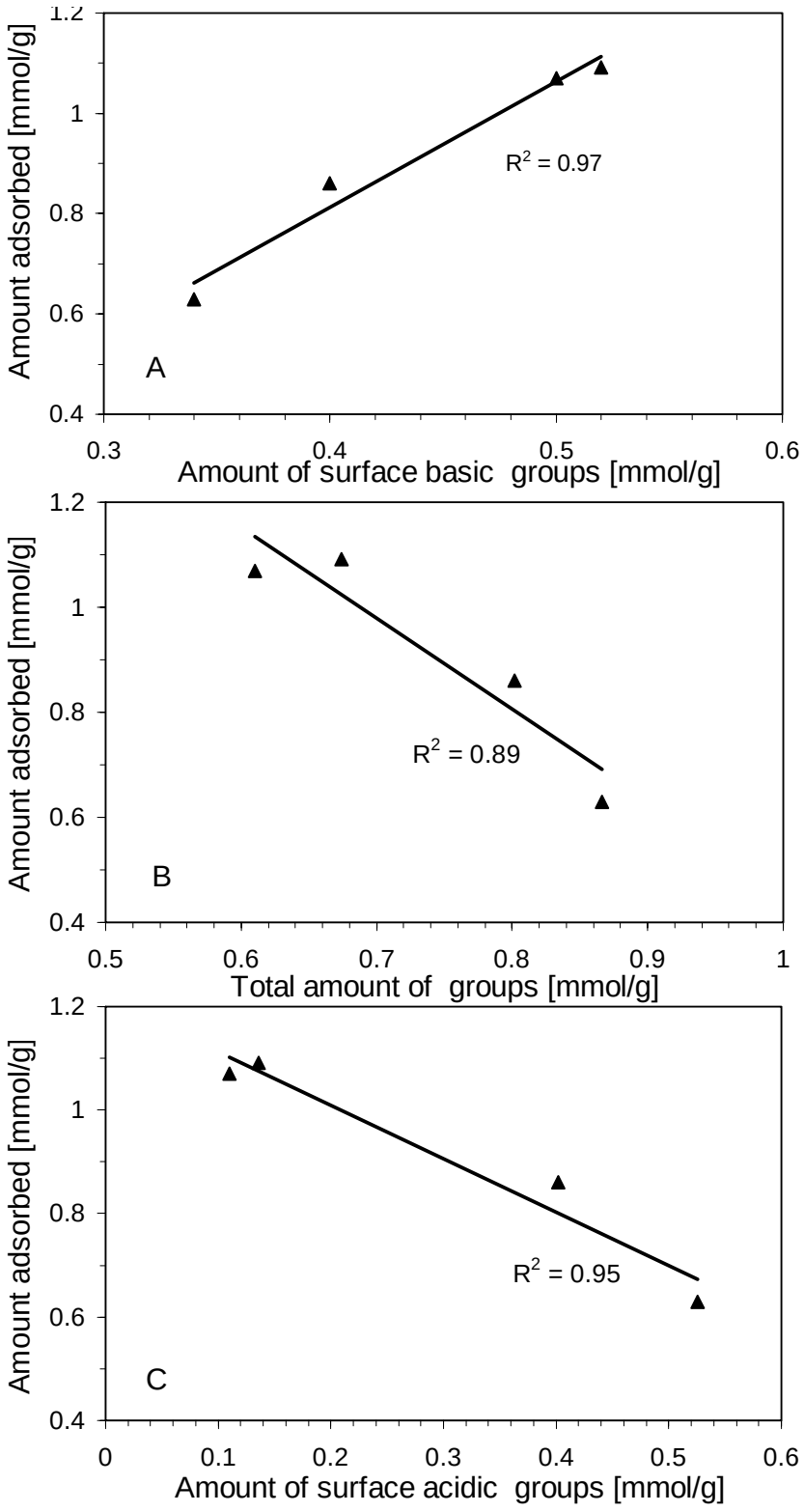

Figure 41: Dependence of the amount of valeric acid strongly adsorbed on the urea modified carbons on: the amount of surface basic groups (mmol/g) (A); total amount of surface groups (mmol/g) (B); and amount of surface acidic groups (mmol/g) (C).

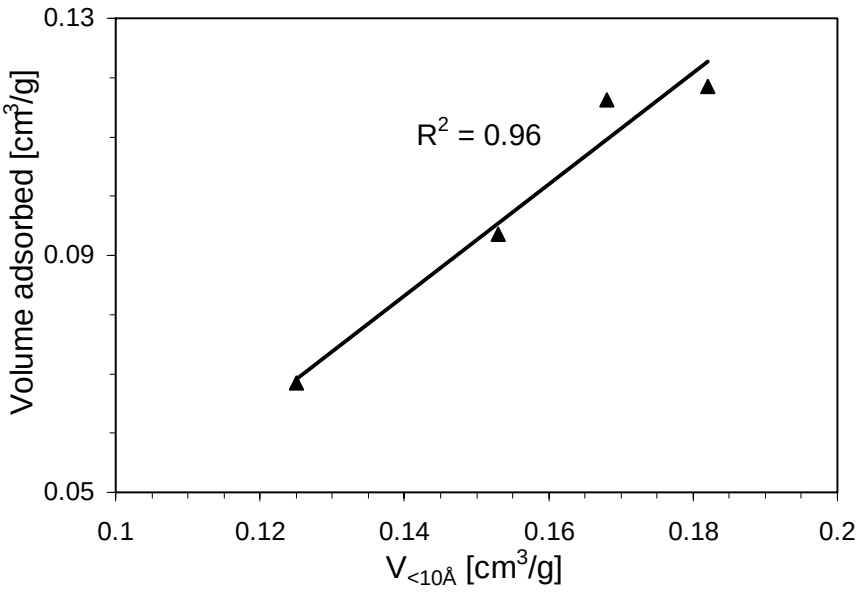

Figure 42: Dependence of the amount of valeric acid strongly adsorbed on $V_{<10\,Å}$ of the urea modified carbons.

Adsorption from Vapor Phase

The presence of water and its interactions with surface functional groups should affect the adsorption of valeric acid. To eliminate the influence of water, valeric acid vapors were adsorbed on the initial and oxidized activated carbons and then thermal analysis was done to estimate the amount adsorbed and the strength of the adsorption forces [124, 125]. The DTG curves and the difference in the DTG curves for carbons before and after valeric acid adsorption are presented in Figure 43. On DTG curves two main peaks are present. The first peak is at the same position as that observed for desorption of water. Since the experiments were done in the containers where the influence of the outside atmosphere was eliminated, that peak likely represents desorption of valeric acid weakly adsorbed in large pores where oxygen containing groups are present and where hydrogen bonding is possible despite of the bonding of residual water. Support for this is the observed increase in the intensity of this peak for carbons after oxidation. In the interpretation of isotherms measured from an aqueous solution we excluded the presence of valeric acid interactions with the surface oxygen-containing

groups due to the competitive water adsorption on those groups. For all carbons broad peaks are present between 400 and 600 K their spread and intensity differ.

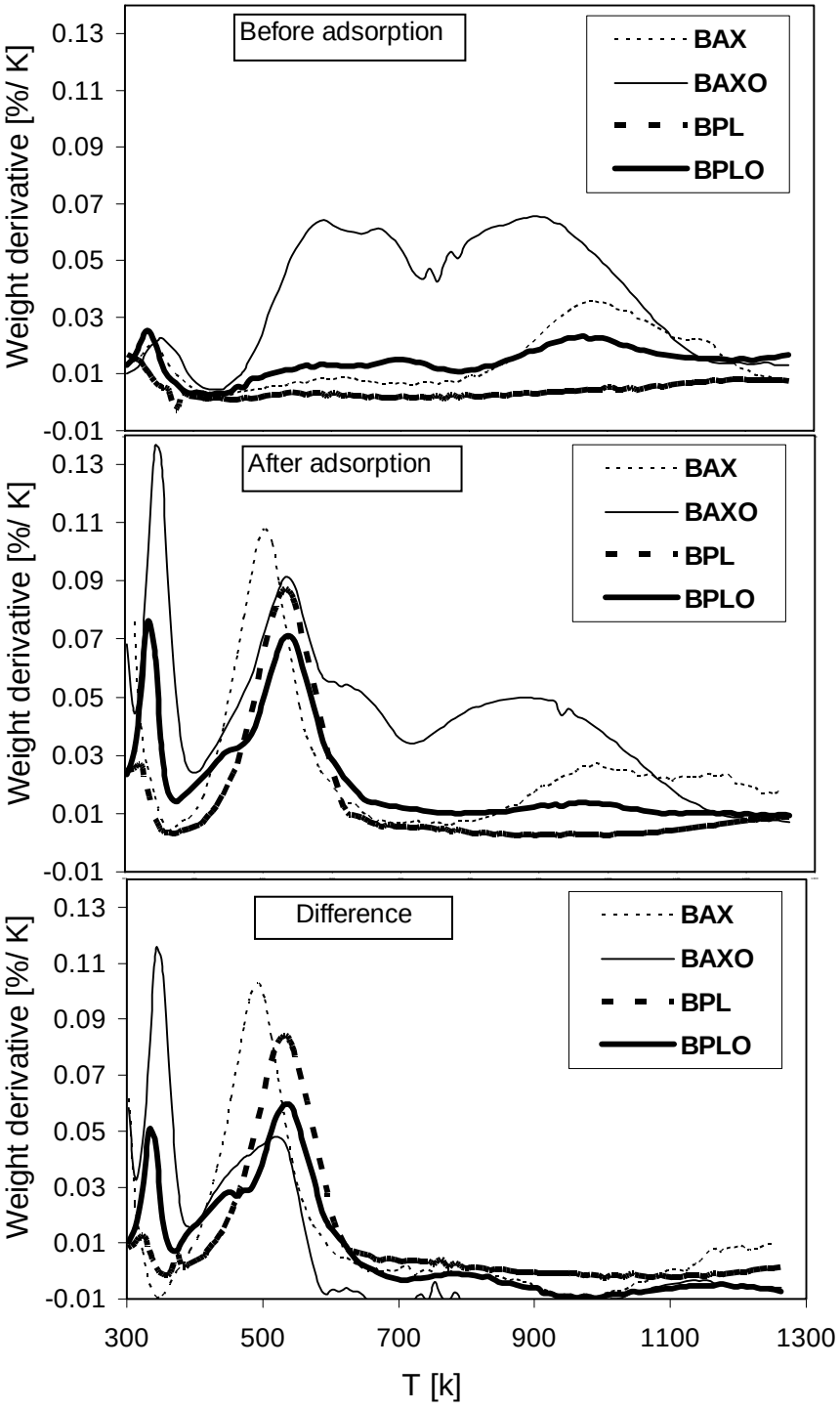

Figure 43: DTG curves for carbons before and after valeric acid adsorption from vapor phase.

In the temperature range between 400-600 K, we also expect the removal of valeric acid from the bulk phase in larger pores since its boiling point is close to 450 K [118]. The biggest amount adsorbed is found on BAX carbon and the smallest is on BAXO. Moreover, the species present on BAX desorb at the lowest temperature indicating weakest adsorption forces. Linking that behavior to the structural and chemical features of the carbon studied suggests that the high volume of micropores in the BAX is responsible for enhanced adsorption. After oxidation, the intensity of the main peak decreases for BAXO as a result of a significant decrease in the volume of micropores. In the case of BPLO the amount adsorbed does not change, however the peak becomes more complex with a low temperature shoulder representing weaker adsorption. Supporting for this interpretation are correlations presented in Figures 44 and 45. The importance of microporosity is shown in Figure 44 where the amount of valeric acid adsorbed revealed increasing linear trend with an increase in the volume of micropores smaller than 10Å. The presence of oxygen containing groups and acidic groups enhances hydrogen bonding between valeric acid and these groups. The importance of hydrogen bonding is seen in Figure 45 where the amount of valeric acid desorbed at temperature less than 410 K (first peak) shows very good correlation with the surface oxygen groups, particularly the acidic ones.

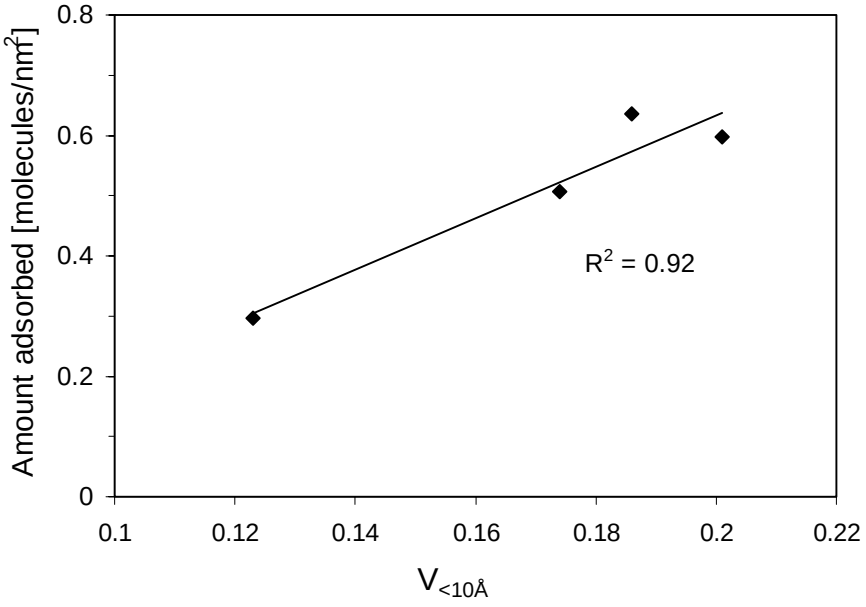

Figure 44: Dependence of the amount of valeric acid adsorbed from vapor phase on $V_{<10\,Å}$.

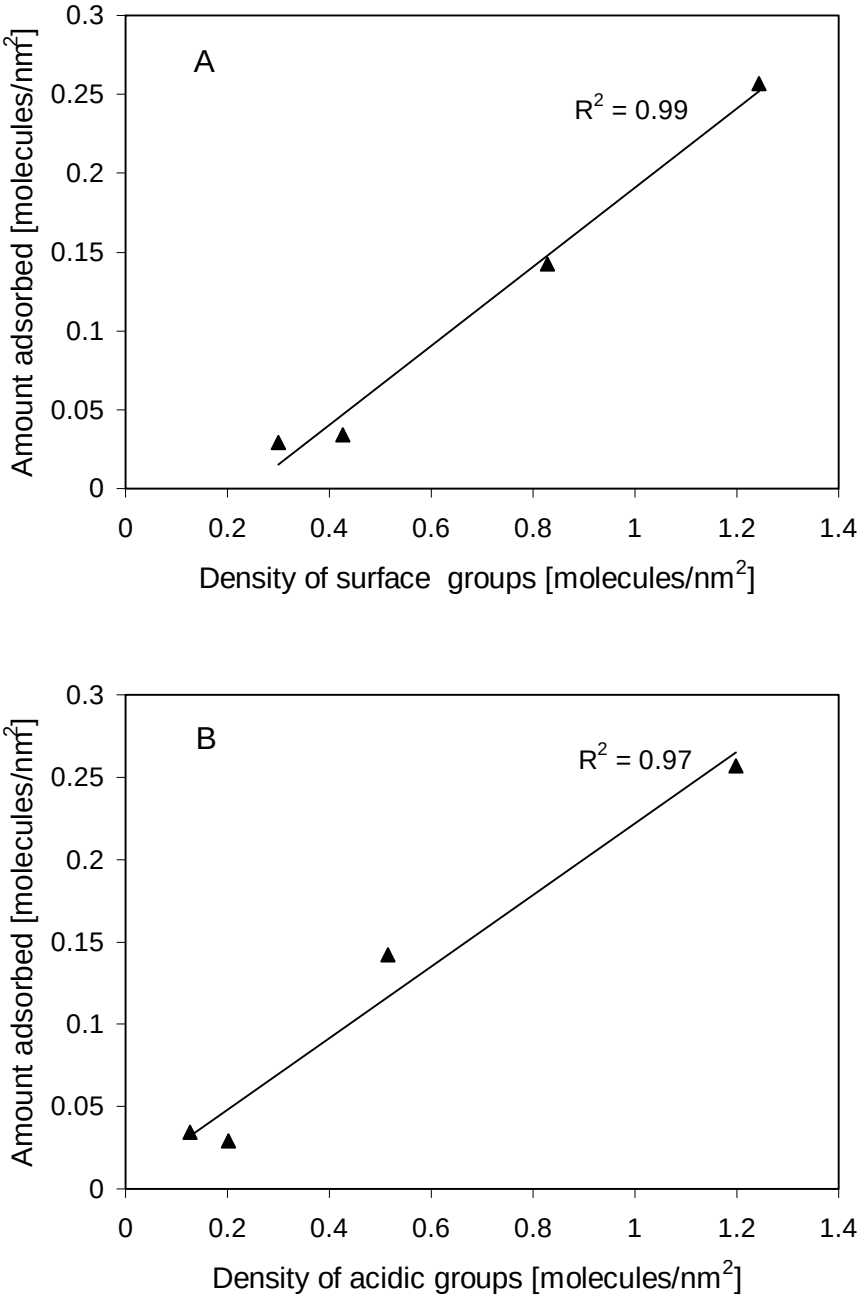

Figure 45: Dependence of the amount of valeric acid desorbed at T< 410 K on: density of total surface groups (A) and density of surface acidic groups (B).

IGC Studies at Finite Concentration

Adsorption of valeric acid on activated carbon was also studied using IGC at finite concentration. The isotherms were measured on BPL carbon series at several temperatures. In order to obtain a good fitting for the isotherms at low and high surface coverage, each isotherm was divided into several subsets of data points. Each subset contains a certain number of data points selected which has a different fit than the other subsets. By considering a sequence of overlapping subsets, the whole range of data can be covered. The subsets were fitted into a polynomial equation of the third-order.

The isotherms are shown in Figures 46, 47, 48 and 49. Very good fitting with correlation coefficients greater than 0.99, were obtained for all carbons. It is clearly seen that the amount of valeric acid adsorbed decreased on all carbons as the temperature increased. It is important to mention that the difference in the amount adsorbed at low surface coverage at the temperatures used in this study is not significant, which may lead to interpretation errors. However, the same trend of variation is observed on all carbons.

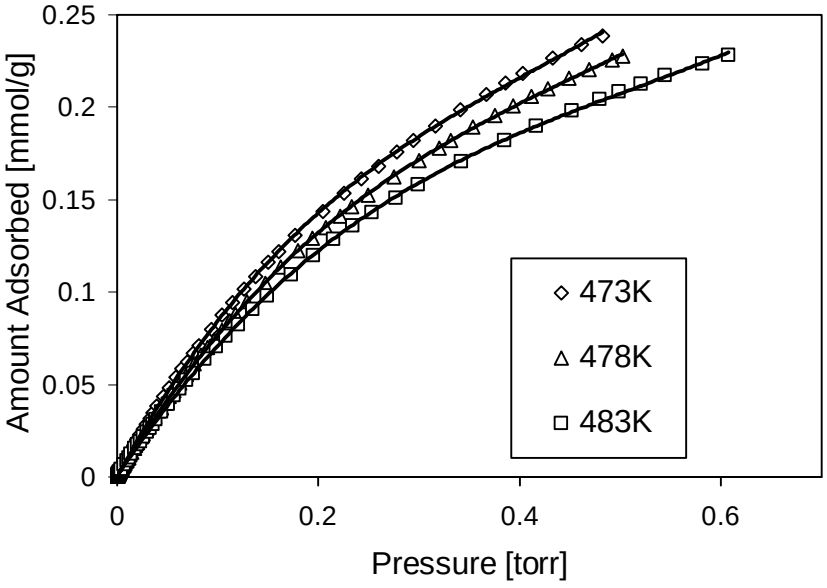

Figure 46: Valeric acid adsorption on sample BPL (solid lines indicate the goodness of the fit).

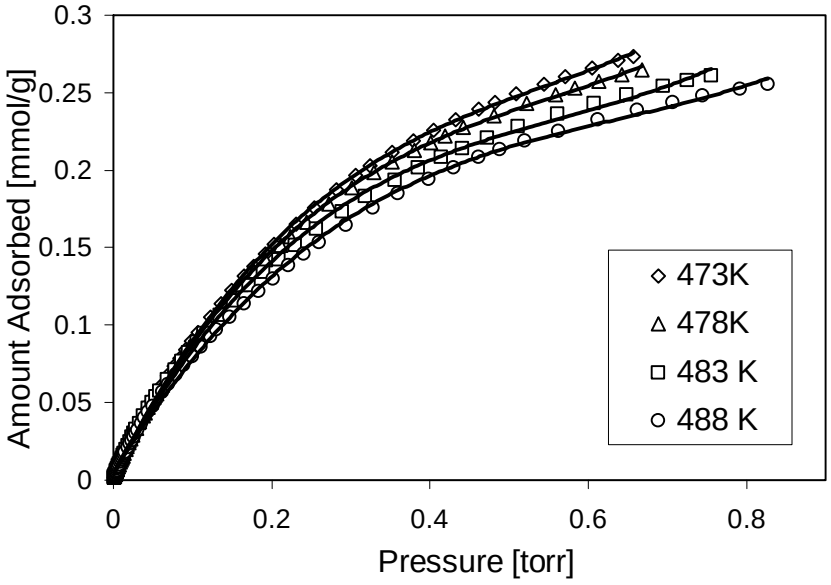

Figure 47: Valeric acid adsorption on sample BPLO (solid lines indicate the goodness of the fit).

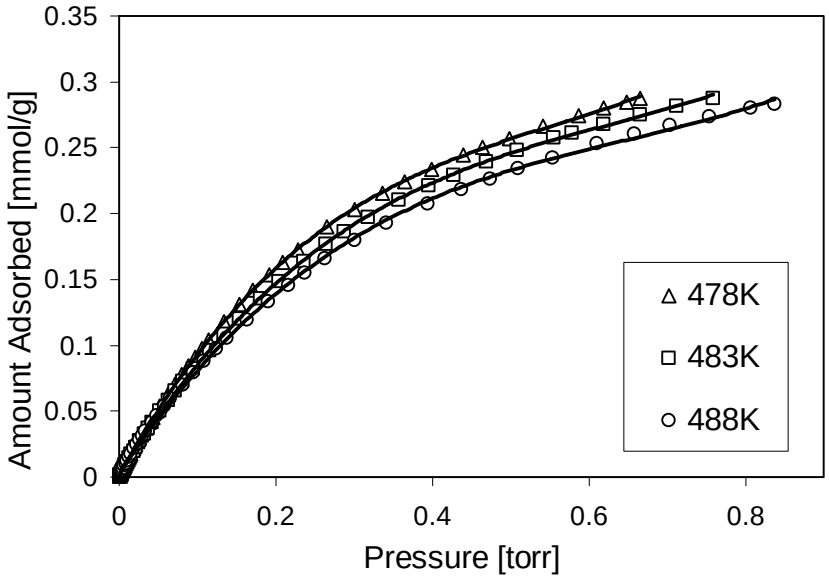

Figure 48: Valeric acid adsorption on sample BPLN1 (solid lines indicate the goodness of the fit).

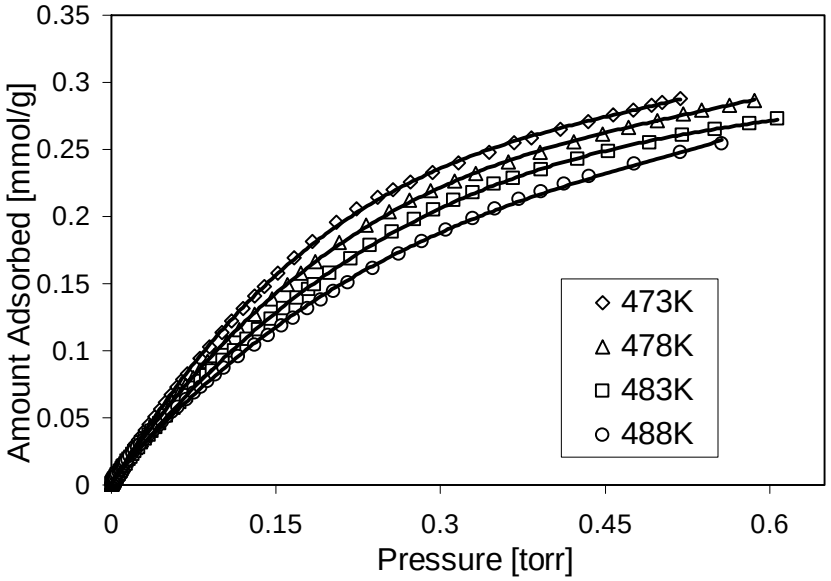

Figure 49: Valeric acid adsorption on sample BPLN2 (solid lines indicate the goodness of the fit).

In order to study the effect of oxidation and urea modification on valeric acid uptake, the isotherms measured at the same temperature should be compared. Figures 50 and 51 show the comparison of the isotherms for the initial and modified carbon series obtained at common temperatures of 478 K and 483 K.

It is interesting that the amount of adsorbed valeric acid increased on BPL carbons after oxidation and urea modification with the highest uptake on BPLN2. At low pressure, the error in calculating the amount of valeric acid adsorbed increases owing to the long tailing of the back profile of the peaks at the temperatures of measurements. In order to analyze these isotherms, both surface chemistry and pore structure of activated carbons should be taken into consideration. It is worth mentioning that the amount of surface basic groups increased on BPL carbons not only after urea modification but also after oxidation. The direct dependence between the amount of valeric acid strongly adsorbed and the amount of surface basic groups is clearly seen. These groups can play a role in the adsorption process via specific interaction in the form of acid-base type.

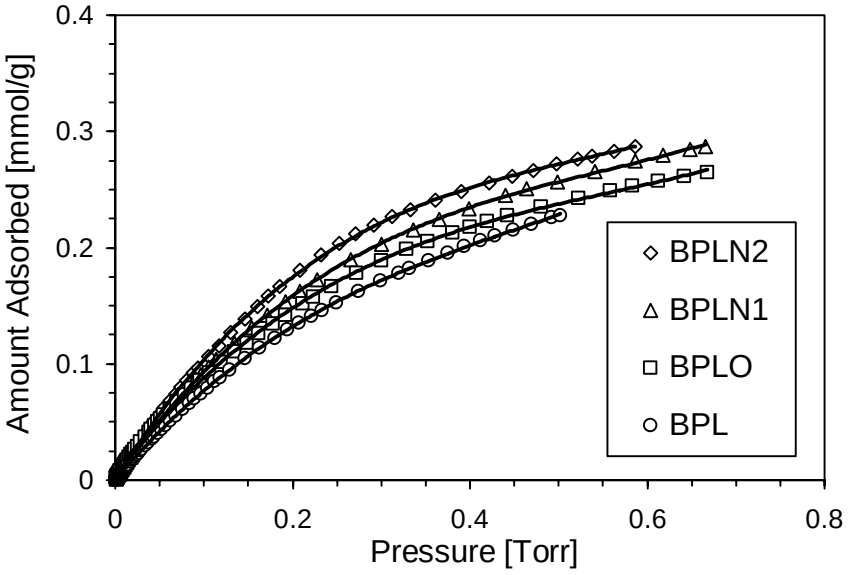

Figure 50: Comparison of valeric acid adsorption isotherms at 478 K on BPL carbons.

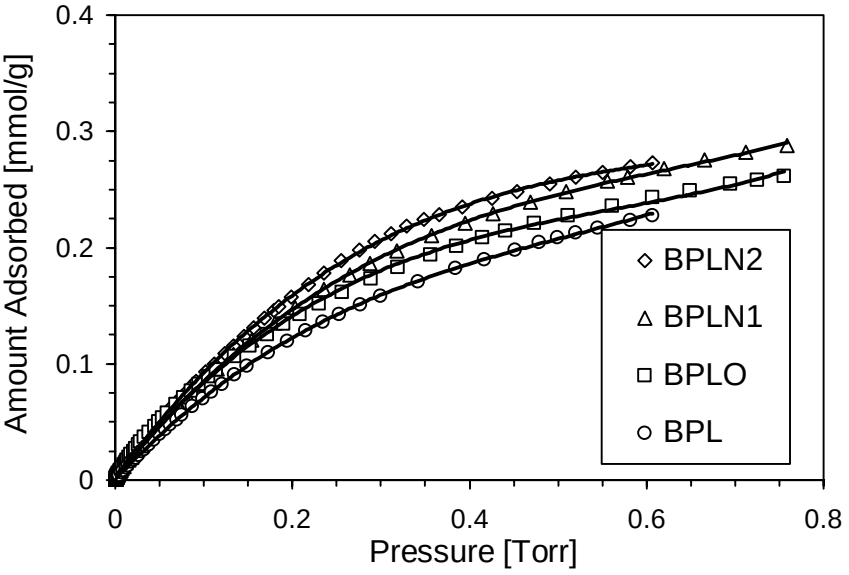

Figure 51: Comparison of valeric acid adsorption isotherms at 483 K on BPL carbons.

At very low surface coverage, if only dispersive interactions play a role, the amount adsorbed should depend on the size and volume of small pores. Although the amount adsorbed at low surface coverage (0.005 torr) showed some dependence on the presence of small pores, they cannot be considered for any correlations because of the low precision of the method in this range.

Figure 52 shows the dependence of the amount adsorbed at 0.2 torr on the amount of surface basic groups of carbons. Good correlation coefficients were obtained (R^2= 0.91). It is interesting that the amount adsorbed does not show any correlation with the volume of micropores or pores smaller than 10 Å. These results suggest that at a pressure of 0.2 torr, the surface chemistry and mainly the presence of basic groups plays a predominant role in the adsorption of valeric acid. At higher surface coverage (P= 0.4 torr), the amount of valeric acid adsorbed showed higher correlation coefficient with the surface basic groups (R^2= 0.93).

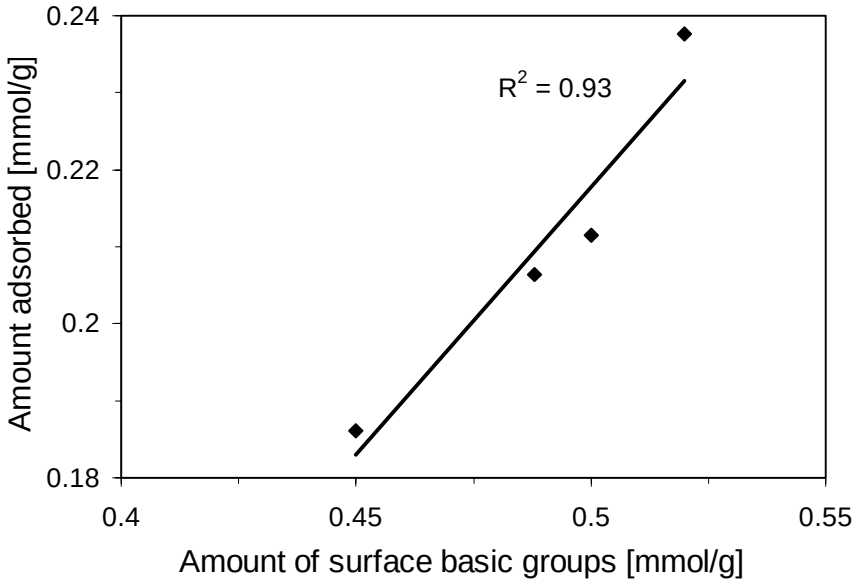

Figure 52: Dependence of the amount adsorbed at 483 K and p = 0.2 torr on the amount of surface basic groups of the carbons studied.

Based on the analysis of valeric acid uptake, we can conclude that the mechanism of adsorption is different at low and at high surface coverage. It is expected that valeric acid adsorption is controlled by both dispersive and specific interactions. The latter is of the direct acid-base type.

4.3 EthylMethylAmine (EMA)

The initial carbons used in this study are BAX and BPL. These two carbons were modified by the oxidation and urea modification methods described in section 3.2. The modified carbons are referred to as before: BAXO and BPLO for the oxidized carbons and as BAXN1, BPLN1, BAXN2, BPLN2 for the urea modified ones. N1 and N2 stand for heating temperatures of 723 K and 1223 K, respectively.

4.3.1 Adsorption of EMA from Aqueous Solution and Vapor Phase

The surface structure and chemistry of the carbons used in this study after modification showed similar trends to those presented in sections 4.1.1 and 4.2.1. A description of the structural parameters and surface chemistry is presented in Table 10.

Table 10: Results of Boehm Titration (mmol/g) and Structural Parameters Calculated from Nitrogen Adsorption at 77 K.

Sample	S_{BET} [m^2/g]	V_t [cm^3/g)]	$V_{(<20\ A)}$ [cm^3/g]	$V_{(<10\ A)}$ [cm^3/g]	Acidic	Basic	Total
BAX	2260±84	1.334	0.528± 0.010	0.123± 0.003	0.763± 0.033	0.363± 0.020	1.126
BAXO	1107±41	0.511	0.336± 0.006	0.142± 0.004	2.15± 0.094	0.075± 0.004	2.225
BAXN1	2352±87	1.380	0.549± 0.011	0.136± 0.003	0.625± 0.027	0.525± 0.028	1.150
BAXN2	1613±60	0.873	0.386± 0.007	0.169± 0.004	0.325± 0.014	0.325± 0.018	0.650
BPL	901±33	0.376	0.319± 0.006	0.186± 0.004	0.188± 0.008	0.450± 0.025	0.638
BPLO	842±31	0.395	0.308± 0.006	0.204± 0.005	0.850± 0.037	0.300± 0.017	1.150
BPLN1	895±33	0.409	0.333± 0.006	0.200± 0.005	0.150± 0.006	0.625± 0.034	0.775
BPLN2	976±36	0.439	0.348± 0.007	0.201± 0.005	0.175± 0.007	0.450± 0.025	0.625

Based on the literature review in Chapter 2 and the results obtained for acetaldehyde and valeric acid, the EMA adsorption should also depend on both porosity and surface chemistry of the carboneous adsorbents. Due to the polar nature of the EMA molecule and its small size, its adsorption is expected to be dependent on microporosity, which is responsible for the dispersive interactions, and on surface chemistry, which controls acid-base, hydrogen bonding and dipole-dipole interactions. In order to analyze the magnitude of these effects, the adsorption isotherms from aqueous solutions were measured at 299 K. The isotherms are presented in Figure 53 along with the fit to the modified Freundlich equation [9, 30, 45].

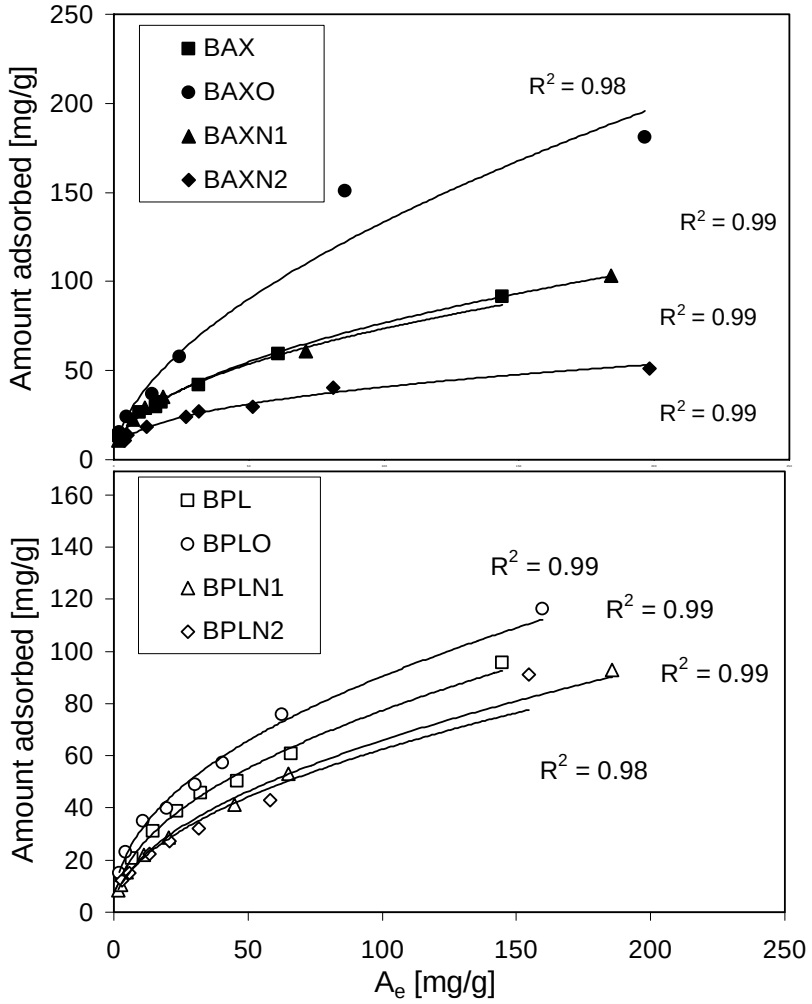

Figure 53: Ethylmethylamine adsorption isotherms from aqueous solution at 299 K. Solid lines indicate the fit to Freundlich equation.

The isotherms showed good fits with correlation coefficients greater than 0.98 for all samples. The fitting parameters are collected in Table 11. It is clearly seen that the values of the capacity factor for both carbons increased after oxidation, while a decrease is noticed for samples after thermal urea treatment. That decrease is more pronounced for carbons treated at 1223 K.

Table 11: Freundlich Fitting Parameters for isotherms measured at 299K.

Sample	n	K_F	Sample	n	K_F
BAX	0.457	8.99	BPL	0.489	8.15
BAXO	0.565	9.88	BPLO	0.461	10.83
BAXN1	0.484	8.27	BPLN1	0.508	6.34
BAXN2	0.389	6.82	BPLN2	0.500	6.24

The amount of EMA adsorbed increases on both carbons after oxidation whereas the urea modification followed by thermal treatment decreases the adsorbate uptake. In order to analyze the isotherms, the differences in surface chemistry and porosity between all carbons must be taken into consideration along with the physical and chemical properties of the adsorbate itself. It was shown in section 4.2 that the uptake of valeric acid depends not only on surface chemistry and porosity but also acid-base interactions play an important role in the adsorption process at low surface coverage [124, 125]. Based on these results, we expect to explain the behavior of EMA using a similar approach. For instance, much larger uptake on BAXO than that on BAXN2 in spite of the higher volume of pore smaller than 10 Å in the latter sample can be attributed to the surface chemistry effect since the amount of acidic groups greatly increased on BAX carbon after oxidation while a decrease is noticed for BAXN2. Moreover, since EMA can strongly bond to surface oxygen using hydrogen bonding it may be able to compete with water for high-energy sites more effectively resulting in an increase in the amount adsorbed on oxidized carbons. Since oxidation makes the surface of activated carbons more acidic and EMA is basic in nature, it can be adsorbed on the surface via acid- basic neutralization reactions.

To explain the variations in the amount adsorbed, differences in the porosity also have to be taken into account. In the presence of pores smaller than 10 Å EMA can be adsorbed strongly via dispersive forces. This, besides the above mentioned increase in the number of acidic groups, can contribute to the dramatic increase in the amount adsorbed on BAX after oxidation. On the other hand, the effect of small pores cannot be seen in the case of urea-modified carbons, where, in spite of a significant increase in $V_{<10Å}$ the amount adsorbed is not affected. In fact, the increase in $V_{<10Å}$ is expected to increase the amount of EMA adsorbed via dispersive interactions but at the same time the decrease in the number of acidic oxygen groups on the surface results in a decrease in the EMA amount adsorbed via specific interactions. The observed decrease in the number of oxygen groups explains the decrease in the uptake of EMA on the urea-modified carbons. Support for this is the similarity in the uptake between BAX and BAXN1 where the numbers of acidic groups on those two carbons are close to each other.

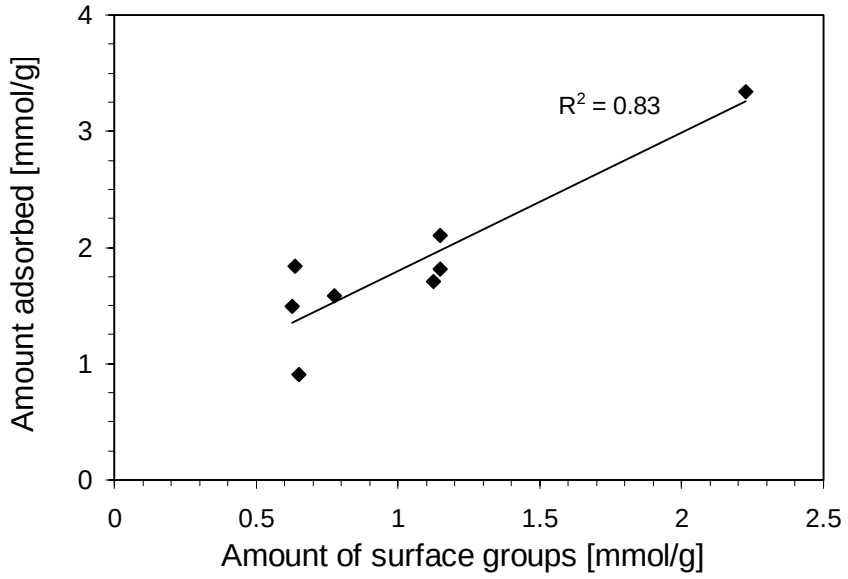

Figure 54: Dependence of the uptake at high equilibrium amount of EMA (200 mg of EMA/g of carbon) on the total amount of surface groups.

In order to better understand the adsorption process, the uptake at two equilibrium amounts, 5 mg and 200 mg of ethylmethylamine per gram of carbon, were correlated with the surface features, which are expected to have an influence on the adsorption

process. For 200 mg of ethylmethylamine per gram of carbon the amount adsorbed shows an increasing trend (Figure 54) with an increase in the amount of surface groups indicating an importance of surface chemistry in the adsorption process. Due to the fact that oxygen and nitrogen functionalities likely differ in acidic/basic properties and thus in the strength of interactions with EMA, the uptake at low equilibrium amounts of EMA (5 mg/g of carbon) was analyzed separately for carbons containing oxygen groups (initial and oxidized) (Figure 55) and nitrogen functionalities (Figure 56). In both cases a relatively good linear correlation was found indicating the importance of acid-base interactions at low surface coverage. Those interactions include either a direct acid-base reaction or hydrogen bonding, and dipole-dipole interactions. The fact that the slope is few times greater when oxygen groups are taken into account than that for groups containing nitrogen suggests the predominant role of oxygen functionalities in EMA adsorption.

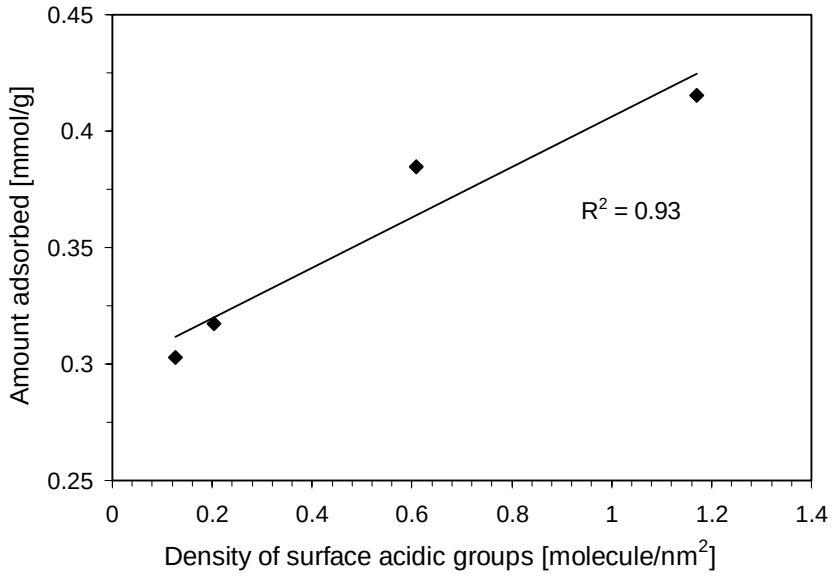

Figure 55: Dependence of the EMA uptake on the initial and oxidized carbons at low equilibrium amount (5 mg EMA/g of carbon) on the density of surface acidic groups.

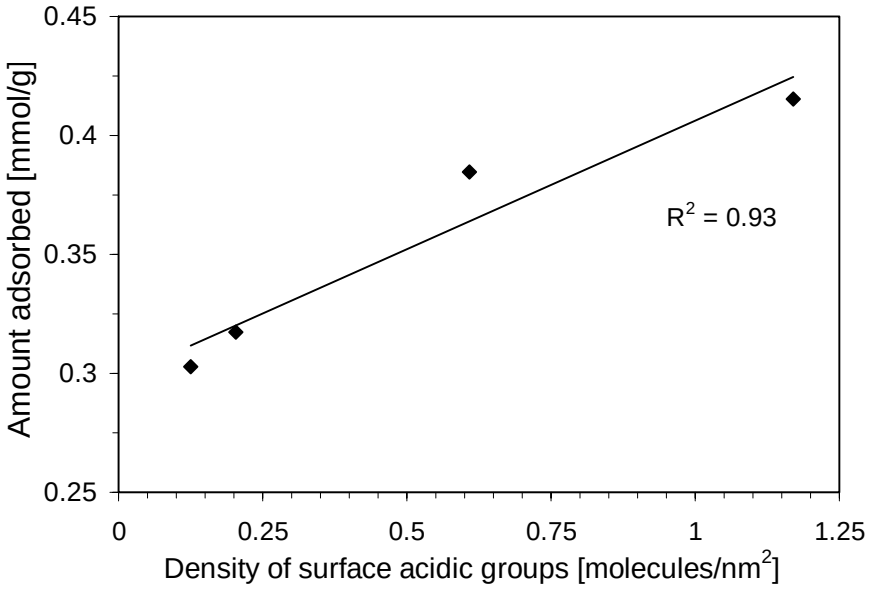

Figure 56: Dependence of EMA uptake on urea modified carbons at low equilibrium concentration (5 mg/g) on the density of surface acidic groups.

EMA is a stronger base than ammonia with a hydrogen atom and a lone pair of electrons attached to the nitrogen atom. As mentioned above, it can interact via weak dipole-dipole interactions as well as it can donate or accept hydrogen bonds. The latter is a relatively strong interaction, which requires high energy to be broken. Moreover, due to the presence of acidic centers on the carbon surface, especially carboxylic groups, acid-base neutralization reaction is expected. Although acidic and polar centers on the activated carbons surface are found to play a major role in the adsorption process of EMA, the extent and strength of those interactions is yet to be estimated. To do this, adsorption of EMA vapors on activated carbons surfaces was carried out and the amounts desorbed were studied using thermal analysis. The differences in TG curves for carbons before and after EMA adsorption are presented in Figure 57. The weight losses at different temperature ranges can be linked to various types of interactions of EMA with the carbon surface [137]. On the TG curves several step-downs representing the different types of interactions can be seen. An important and quite unusual feature is an increase in the weight for all carbons at elevated temperatures. This increase, especially well-defined for BAX and oxidized carbons indicates the incorporation of nitrogen into the carbon

matrix. Oxidation of the surface seems to create favorable preconditions for this kind of surface modification and the process deserves further investigation.

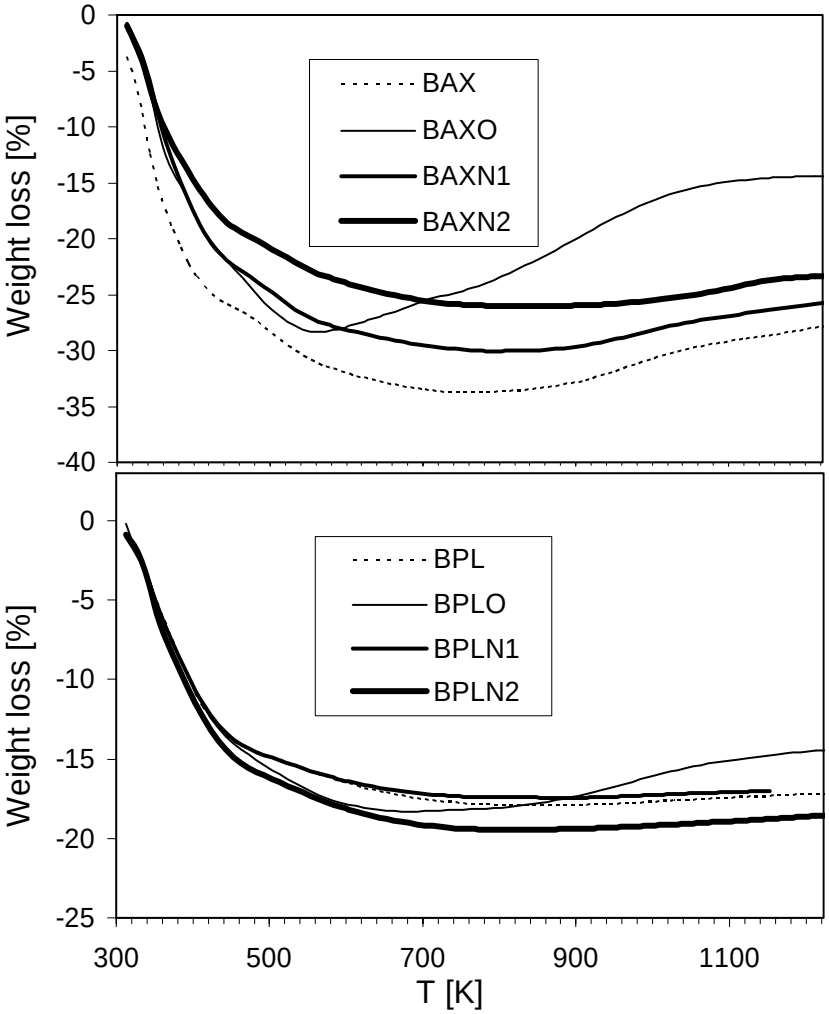

Figure 57: The difference in the TG curves for carbons before and after ethylmethylamine adsorption from vapor phase.

More details are derived from TA analysis when DTG curves are analyzed (Figure 58). As weight is lost, the shapes and positions of the peaks can be linked the type and strength of EMA interactions with the carbon surface. In order to explore this path, the chemistries of both, the EMA molecule and the carbon surface have to be analyzed [68]. The difference in electronegativity between nitrogen, carbon, and hydrogen atoms and the presence of a lone pair of electrons on nitrogen atom produce a dipolar moment for EMA. The negative charge is close to nitrogen atom and the positive

charge is close to the carbon and hydrogen atoms. The presence of polar oxygen and nitrogen groups on the carbon surfaces with positive and negative charges on their atoms give rise to specific dipole-dipole interactions between the surface groups and the EMA molecules. The various configurations related to those interactions are presented in Figure 59. As presented, adsorption can take place by the interaction of the positive charge on the methyl or ethyl carbon of the EMA molecule with the negative charge on the oxygen atoms of the carboxylic, lactonic, or phenolic groups. The interactions between the nitrogen atom of EMA and the carbon atoms of the carboxylic and lactonic groups can happen but they are less favorable due to steric effects. When nitrogen-containing groups are present on the surface, the negative charge is located near nitrogen atom and the positive charge close to the carbon and hydrogen atoms. The dipole-dipole interactions take place with the opposite charge located on the EMA atoms.

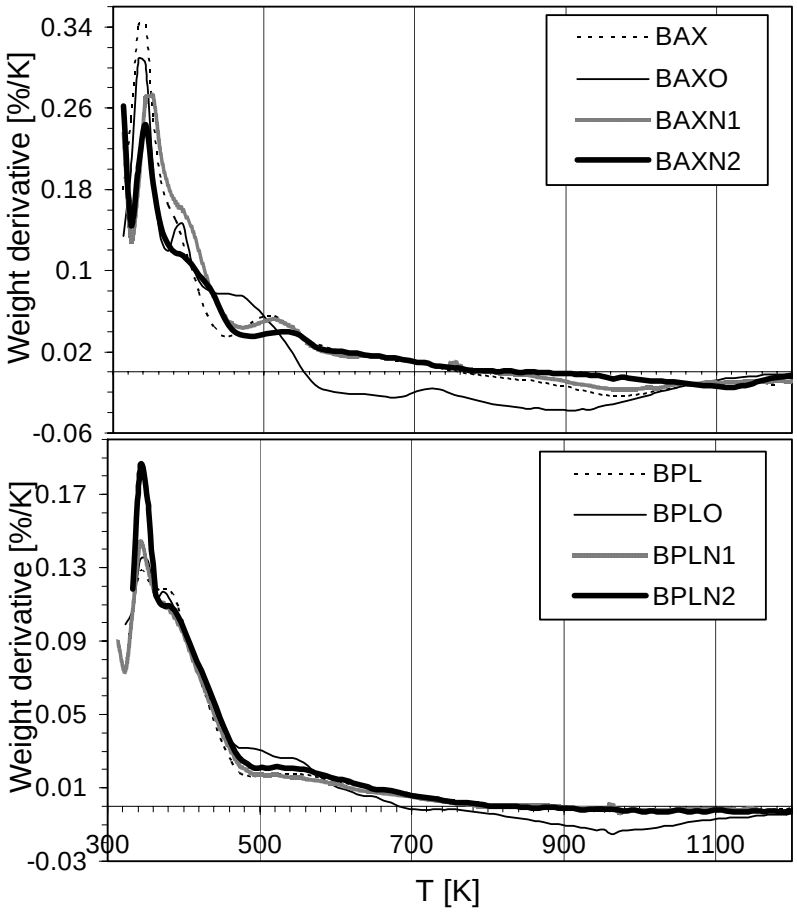

Figure 58: The difference in the DTG curves for carbons before and after ethylmethylamine adsorption from vapor phase.

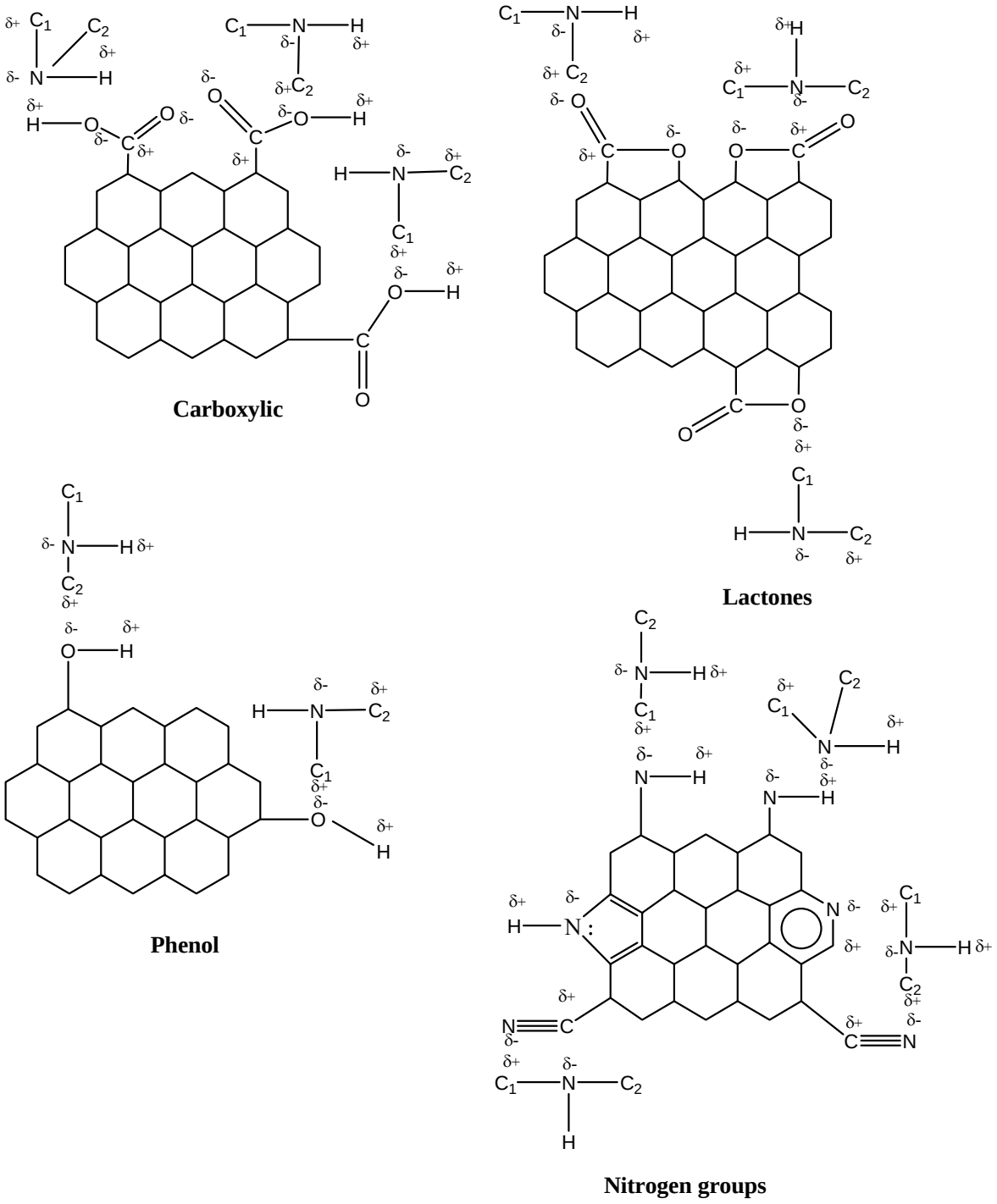

Note: C_1 and C_2 represent methyl and ethyl groups respectively

Figure 59: Examples of dipole-dipole interactions between EMA molecules and various surface groups.

Hydrogen bonding is another possible type of specific interaction (variation of dipole-dipole interactions) that occurs between either the hydrogen atom of the EMA molecules and the lone pair of electrons on the oxygen and nitrogen atoms of the surface groups of all carbon samples, or the hydrogen atoms of the surface acidic groups and the lone pair of electrons on the nitrogen atom of the EMA molecule. Figure 60 shows several examples of the hydrogen bonding interactions between the EMA molecules and the carbon surfaces.

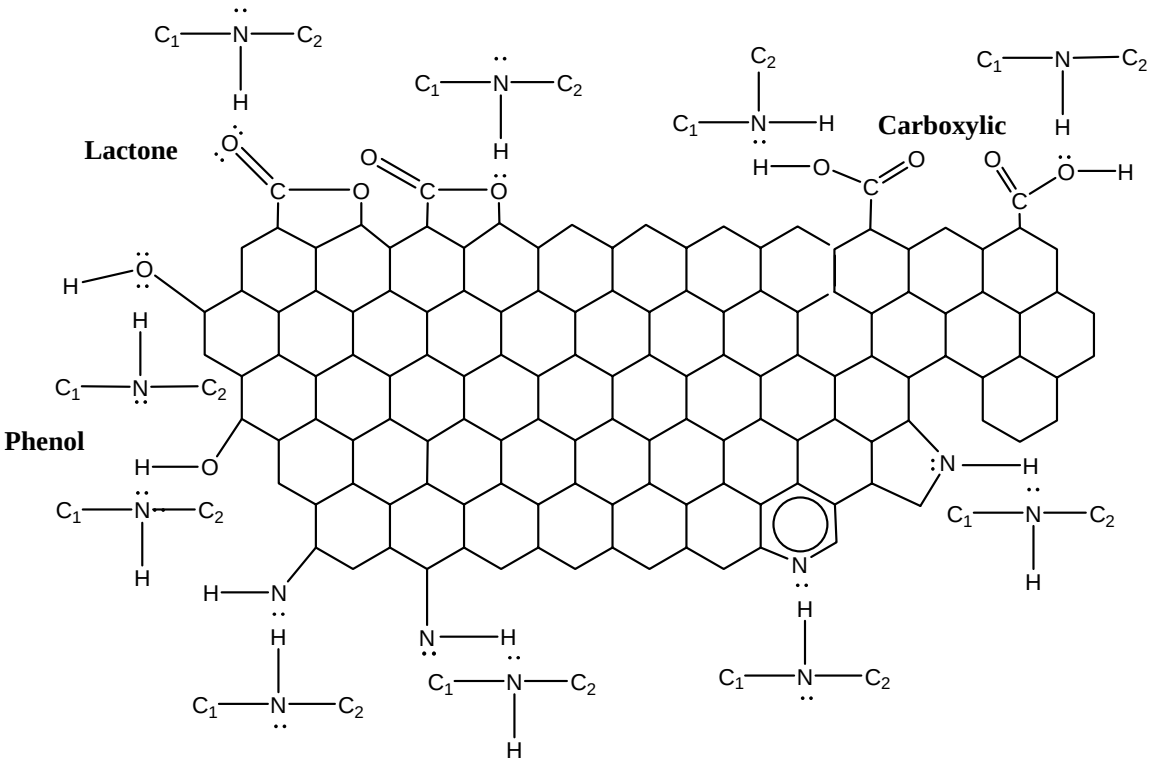

Hydrogen bonding

Note: C_1 and C_2 represent methyl and ethyl groups respectively

Figure 60: Examples of hydrogen bonding interactions between the EMA molecules and various surface groups.

It is important to mention that in the case of adsorption from solution, the high pK_a of EMA (10.7) along with the acidic or close to neutral pH of the carbon surface ensures the presence of either EMA or surface acidic groups in the ionic forms. Although our experiments were done without the pH control, the pH of the solution is smaller than the pK_a of EMA and greater than the pK_a of the surface groups. EMA will be present in the protonated form while the strong acids on the surface will be dissociated. As a result, EMA will be bound to the latter groups via simple neutralization reaction:

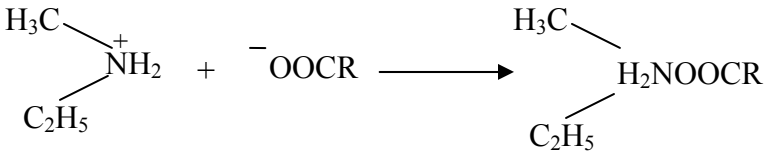

(20)

Moreover, ethylmethylammonium ions present in the solution (protonated EMA [138-140]) can be adsorbed on the surface via dispersive interactions.

In the case of adsorption from the vapor phase the EMA molecule can be protonated in the following reaction with the formation of ethylmethylammonium ions adsorbed on the surface:

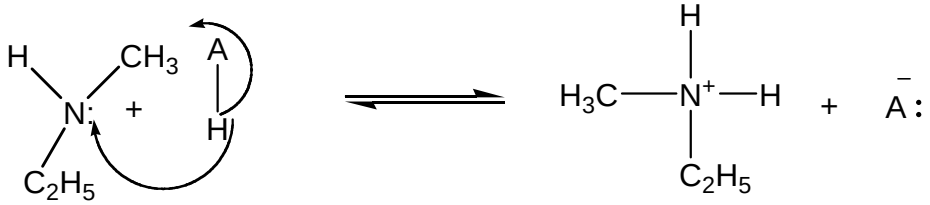

(21)

Those ethylmethylammonium ions are thermally unstable and decompose to alkylamine and ethylene at elevated temperatures (around 573K) following the path similar to Hofmann-elimination reaction [138-140]:

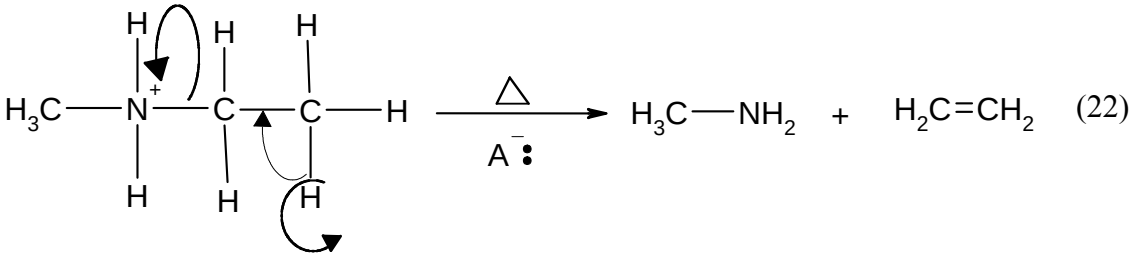

(22)

Based on the description of the possible chemical mechanisms taking place between the EMA molecules and the surface groups, the interpretation of the DTG curves presented in Figure 58 can be attempted. The peaks at temperature lower than 350 K can be linked both to desorption of the traces of water molecules and desorption of EMA weakly adsorbed (dispersive forces) in the pore system (boiling point of EMA is 309.6 K [118]) and via dipole-dipole interactions. Due to the expected decomposition of ethylmethylammonium ions at about 573 K [137], only peaks which appear at temperature lower than 463 K (steep weight loss on the TG curves) are taken into account for the interpretation of the specific adsorption, described here as interactions of EMA molecules with different types of surface groups via hydrogen bonding with the oxygen and nitrogen centers and Lewis type acid-base interactions. If this interpretation is feasible one could expect the correlation between the amounts adsorbed (desorbed) and the amounts of surface acidic groups present on carbon. Indeed, data presented in Figure 61 show a relatively well-defined trend of an increase in the amount adsorbed with an increase in acidity for all carbons but the oxidized ones.

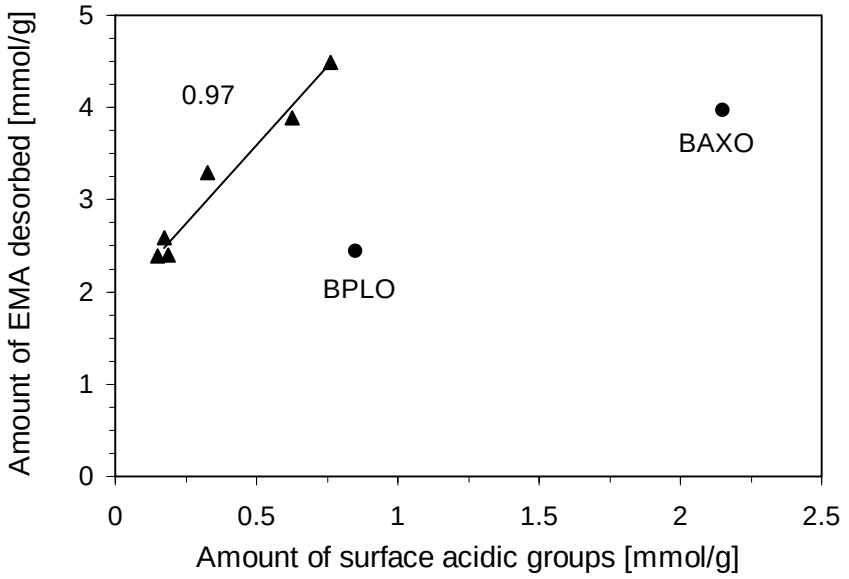

Figure 61: The dependence of the amount desorbed at T< 463 K on the amount of acidic groups. (Solid circles represent the oxidized samples not taken into account for the correlation).

The justification for exclusion of the oxidized samples from the correlation is in their strongly acidic character. As mentioned above, the high density of carboxylic groups promotes the acid base reaction, which results in the formation of ethylmethylammonium ions. Those ions adsorbed on the surface start to decompose at a temperature above 463 K and ethylene and methylamine are formed. After decomposition, ethylene desorbs from the surface which is seen as DTG peaks at about 500 K. Alkylamines, on the other hand, have the tendency to interact further with the surface and via a not yet known mechanism, it is incorporated in the form of nitrogen groups into the carbon matrix at T > 573 K. This is seen in the TG curves as an increase in the weight. The presence of oxygen-containing groups, especially carboxylic, makes the acid-base reaction easier to occur and thus more alkylamine is retained on the surface in a quasi-stable state before its incorporation into the carbon matrix. Also, the high intensity of the peak at about 500 K for the oxidized samples supports the mechanism proposed.

Table 12: Nitrogen content.

Sample	Nitrogen [%]	Sample (after heating)	Nitrogen [%]	Sample (after EMA adsorption and heating)	Nitrogen [%]
BAX	0.14	BAX	0.77	BAX	1.19
BAXO	2.69	BAXO	1.50	BAXO	3.01
BAXN1	2.46	BAXN1	1.56	BAXN1	1.91
BAXN2	0.86	BAXN2	0.95	BAXN2	1.23
BPL	0.44	BPL	0.48	BPL	0.71
BPLO	0.91	BPLO	0.81	BPLO	1.25

To check the extent of nitrogen incorporation after adsorption of EMA, a portion of each carbon sample was heated to 1273 K in a nitrogen atmosphere under the same conditions as thermal analysis was done and the content of nitrogen was evaluated. The content of nitrogen for the non-heated samples, heated samples at 1273K and samples

after EMA adsorption and heating are reported in Table 12. Apparently unusual increase in the content of nitrogen for the initial BAXO sample is the result of the incorporation of nitro groups into the matrix of low the temperature carbonized material [123]. After heat treatment of the initial samples the amount of nitrogen decreased for BAXO and BAXN1 as a result of decomposition of thermally unstable either nitro or amine groups. For other carbons a slight increase is found, likely due to an increase in the degree of carbonization and removal of volatile hydrocarbons. After adsorption of EMA followed by heat treatment, the content of nitrogen noticeably increased compared to the sample not exposed to EMA adsorption. The most significant increase is noticed for the oxidized samples following the mechanism proposed above. The differences in the amount of incorporated nitrogen into the carbon matrices support our hypothesis about the importance of the acid-base reaction for this kind of carbon modification.

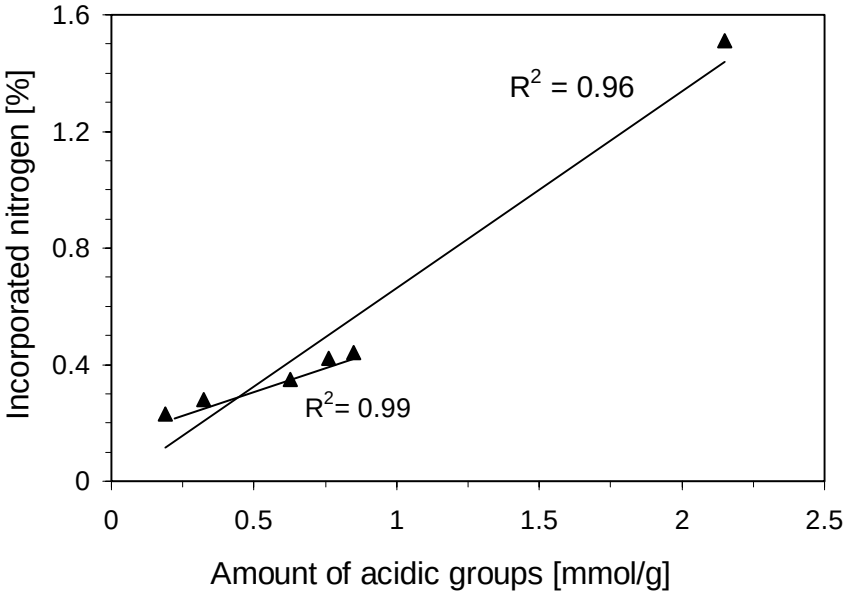

Figure 62: The relationship between the nitrogen incorporated into the carbon matrix and the amount of surface acidic groups (long line correlates all points).

Since the amount and the strength of EMA adsorption on activated carbons shows dependence on the surface oxygen-containing acidic sites, the amount of nitrogen incorporated into the carbon matrix, following the acid-base neutralization reaction (Eq. 21) is also expected to show similar trend. In Figure 62, the dependence of the amount of

nitrogen incorporated into the surface calculated by subtracting the content in the initial heated samples from those after EMA adsorption and heat treatment on the number of surface acidic groups is plotted. A linear increase in the nitrogen content with an increase in number of acidic groups on the surface is clearly seen indicating the importance of the acid-base interactions in the process of nitrogen incorporation using basic compounds as a source of nitrogen.

4.3.2 Adsorption of EMA Vapor on Activated Carbon Filters: Dynamic Adsorption

Although the mechanism of EMA adsorption from vapor phase was studied and the process showed that the interactions with the surface acidic groups are energetically more favorable than adsorption in the porous structure, unfortunately the kinetics of the process was not evaluated. In this section, the effect of porosity and surface chemistry on the adsorption of high concentrations of EMA from a humid air stream is analyzed. The discussion focuses on both adsorption capacity and adsorption kinetics. The analysis is based on the obtained breakthrough capacities under different experimental conditions. To identify the role of surface chemistry and structural features, new samples of BAX and BPL carbons were used. The two carbon surfaces were further modified using the same methods described in section 3.2.

Table 13: Results of Boehm Titration and Structural Parameters Calculated from Nitrogen Adsorption.

Sample	Acidic (mmol/g)	Basic (mmol/g)	$V_{<10Å}$ (cm^3/g)	$V_{<20Å}$ (cm^3/g)	S_{BET} (m^2/g)
BPL	0.200±0.009	0.450±0.025	0.193±0.005	0.328±0.006	950±35
BPLO	0.775±0.034	0.200±0.011	0.177±0.004	0.325±0.006	1034±38
BPLN1	0.150±0.006	0.500±0.028	0.202±0.005	0.341±0.007	958±35
BPLN2	0.225±0.009	0.475±0.026	0.182±0.oo4	0.308±0.006	905±33
BAX	0.825±0.036	0.275±0.015	0.121±0.003	0.481±0.009	2169±80
BAXO	2.400±0.105	0.025±0.001	0.164±0.004	0.351±0.007	1140±42
BAXN1	0.425±0.018	0.250±0.013	0.120±0.003	0.478±0.009	2140±79

Although surface modifications showed similar effects as in section 4.3.1, the exact surface characterization is required since it is very important for the interpretation of the results on adsorption of EMA. The structural features and surface chemistry of the new samples of activated carbons were determined and a summary of the results obtained is presented in Table 13. The only exception is a decrease in the volume of pores smaller than 10 Å found for both carbons after modification except for BPLN1 where it slightly increased.

The dynamic adsorption of EMA was carried out in wet air (70% humid). The variation in the breakthrough times with the carbon bed weights was measured and the results are shown in Figure 63. As expected, straight lines with various slopes and intercepts were obtained. The breakthrough times linearly increased with an increase in bed weight indicating an increase in the adsorption capacity, showing the applicability of Eq.17.

The parameters of Wheeler–Jonas equation (Eq.17), W_e and k_v , were calculated from the slope and the intercept of the lines presented in Figure 63 and are collected in Table 14. Both parameters decreased after surface modifications of the initial carbons. If adsorption of EMA on the carbon was taking place via dispersive interactions with the microporous structure, an increase in W_e with increasing W_o would be expected. The contribution of these interactions explains the higher W_e value (capacity) on BAX carbon compared to that on BPL ($W_{e(BAX)} = 2 \times W_{e(BPL)}$). The volume of micropores for the latter carbon is 0.33cm^3/g compared to 0.48 cm^3/g for BAX.

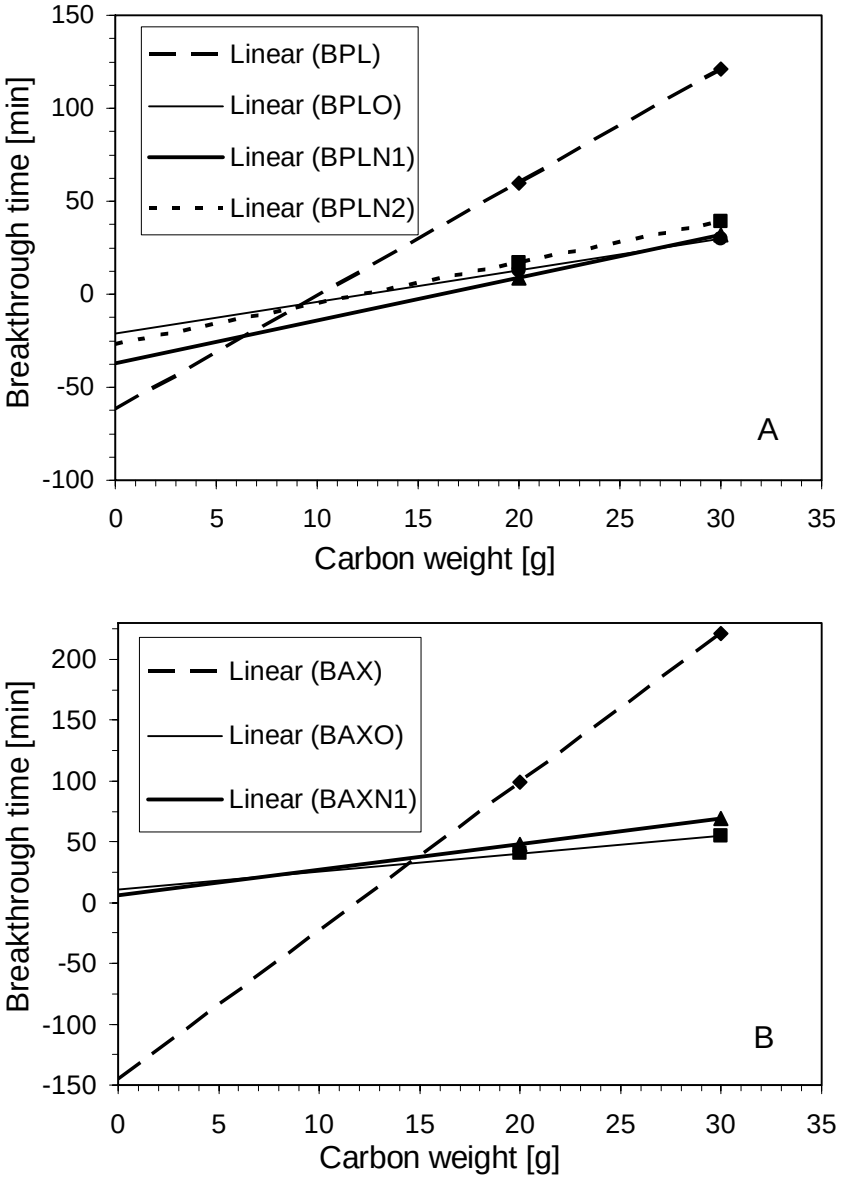

Figure 63: Breakthrough time vs. weight for BPL (A); and BAX (B) carbons for a test with inlet concentration 1000 ppm EMA, and humid air: 70% RH.

The trend in W_e values for the other modified carbons suggests a different mechanism of adsorption. This is based on the fact that in spite of the similarities in the micropore volumes between BPL and BPLO carbons, the static adsorption capacity, W_e, for BPLO decreased significantly in comparison with the unmodified sample. Similar results were observed between BAX and BAXN1. The experimental error on the values obtained for k_v is quite high: as it is derived from the intercept with the y-axis, a small

variation of the slope (e.g. on the value of W_e) will lead to a big change in k_v. But the general trend is very clear. The treated carbons do not only suffer from a drop in capacity but the adsorption kinetics also become much slower (Table 14).

In order to explain the observed variations in W_e and k_v, several factors affecting the adsorption process have to be considered. These include the effect of humidity, the weight of the carbon beds, the type and density of the surface groups and finally any experimental errors.

Table 14: W_e and k_v obtained from the Wheeler-Jonas equation.

Carbon	Capacity W_e (g/g)	k_v min^{-1}
BPL	0.15	2500
BPLO	0.05	2350
BPLN1	0.06	1700
BPLN2	0.06	2250
BAX	0.30	1300
BAXO	0.04	≈ 0
BAXN1	0.05	≈ 0

The results obtained in section 4.3.1 on adsorption of EMA from aqueous solution [141] revealed a strong, linear dependence of the amount of EMA adsorbed on the quantity of acidic surface groups. The uptake of EMA on the oxidized carbons was greater than that on the initial counterparts. The apparent discrepancy in the data presented here may be related to different experimental conditions, which probably lead to different mechanisms of adsorption. Under the prior assigned experimental conditions, both EMA and the surface acidic groups existed in their ionic forms since the pH of the solution was below the pK_a of EMA (pK_a~10.7) and above the pK_a of the carboxylic acid groups on the surface. Thus adsorption of EMA was the result of the direct acid-base reaction between EMA molecules and the surface acidic groups identical to that presented in eqn.20. This type of interaction is stronger and energetically more favorable

than hydrogen bonding and dispersive interactions. The condition of the experiments described here result in a quite different mechanism of adsorption. Being in vapor phase, EMA is likely to exist in the molecular form and the specific interactions can take place only via hydrogen bonding with surface functional groups. On the other hand, these groups are known to strongly adsorb water molecules present in the system [102, 105]. Under the experimental conditions (70% humidity), competition for the polar adsorption sites exists. The results obtained indicate that water is preferably adsorbed. Those water molecules adsorbed on the modified samples in the forms of clusters [142, 143] block the pore entrances and thus limit the accessibility of EMA to small pores. These pores, similar in size to EMA, are the high-energy adsorption centers for our adsorbate. In the case of unmodified carbons, the density of acidic groups is not high enough to promote large water clusters and to create physical obstacles for pore accessibility. Modification with nitrogen, and introduction of basicity, besides resulting in repulsion forces for EMA adsorption, also results in attraction of water via hydrogen bonding. This, as in the case of the oxidized carbons, limits the amount of EMA adsorbed. When carbons become more hydrophilic, the enhanced water uptake will severely shorten breakthrough times, even for soluble compounds and the available adsorption space will become less accessible: the EMA will have to pass a water barrier to enter the available micropores (see Table 14).

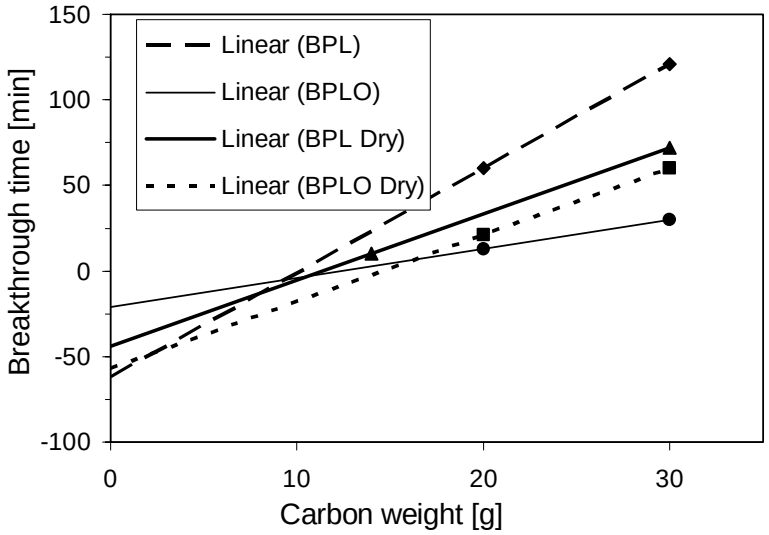

Figure 64: Comparison of breakthrough time vs. weight of carbon for a test with inlet concentration 1000 ppm EMA, and humid air: 0% and 70% RH.

To confirm the mechanism proposed, the EMA breakthrough experiments were carried out in the absence of water vapor. The dependence of the breakthrough times for BPL and BPLO on the carbon weights are presented in Figure 64. It is clearly seen that the presence of humidity increased the breakthrough time of EMA on BPL while it had an opposite effect on BPLO carbon. According to Lodewyckx and Vansant [102], the decrease in the capacity in the presence of water vapor is related to a decrease in an accessibility of adsorption centers due to the competition for the available micropore volume between the preadsorbed water, the water in the air stream and the organic vapor. This, along with an increase in the number of oxygen containing groups after oxidation explains the lower breakthrough times on BPLO carbon under humid conditions. On the other hand, in the case of BPL carbon, which is prepared at high temperature thus lacking strong acidic groups, EMA has a tendency to replace the adsorbed water molecules. This happens owing to the presence of hydrocarbon moiety in the EMA molecule, which accounts for its high affinity toward the hydrophobic surface of a carbon pore. Moreover, when adsorption occurs at dry conditions, the presence of a significant amount of basic groups on BPL surface exerts a repulsion effect on EMA molecules leading to a decrease in the capacity.

Table 15: Water uptake at 70% RH (g/g).

Sample	Water uptake (g/g)
BPL	0.339
BPLO	0.342
BAX	0.733
BAXO	0.352

To support our hypothesis, the water uptakes at 70% RH were measured on the initial and oxidized carbons. These uptakes are collected in Table 15. The similar water uptake on the initial and oxidized BPL carbons reveals the importance of microporosity.

In fact W_o didn't change significantly on this carbon. The slightly higher value on the oxidized BPL carbon can be attributed to the acidic groups present on the surface with preserved porosity. For BAX carbon after oxidation, the water uptake at 70 % humidity decreased significantly in comparison with the initial carbon. This is the result of a significant decrease in the microporosity. At high humidity the volume of micropores governs the water adsorption process [102, 143, 144]. The dependence of water uptake on the volume of micropores is shown in Figure 65. Although only four points were obtained, the linear trend is apparent.

The above described differences in mechanisms in dry and wet conditions are supported by similar values of W_e, calculated through Eq. 18, for EMA adsorption on BPL (0.09688) and BPLO (0.0975) in dry air. Since the micropore volumes are similar for these two carbons, similar W_e were expected. A slight difference in W_e values lies well within the experimental error.

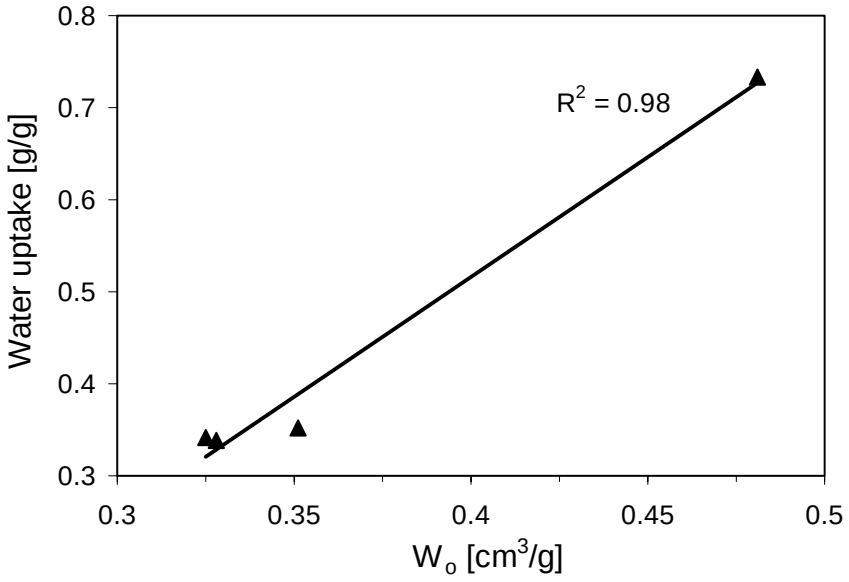

Figure 65: Dependence of the of water uptake at 70 % RH on the volume of micropores.

CHAPTER 5
SUMMARY AND CONCLUSIONS

Activated carbons have been used for a long time to effectively treat drinking water, waste water and industrial gas stream. In spite of their extensive industrial applications as adsorbents, little research has been performed to evaluate application of activated carbon to remove low concentrations of odoriferous compounds of human sweat. In this research, activated carbons of different origins were altered by oxidation and urea modification for best performance toward adsorption of human sweat odorous compounds. Acetaldehyde, valeric acid and ethylmethylamine were chosen as representative probe molecules because of their major contribution to human sweat. It is expected that they interact with the carbon surface via different mechanisms.

The effect of oxidation and urea modification on the wood origin and coal origin activated carbons is different. The surface chemistry and pore size distributions of activated carbons of wood origin are more susceptible to these treatments than those of coal origin. Oxidation introduces significant amounts of surface oxygen groups, which are mainly acidic in nature, to the surface of all the carbons. The changes in the volume of micropores and mesopores are mainly noticed for the wood-based carbons. The

amount of basic groups increases noticeably as a result of urea modification on the surface of all carbons. Exact reproducibility of the results for the surface chemistry and structural features of activated carbons in case of repeated oxidation and urea modifications is practically impossible, but the general trend of changes is preserved.

The results presented in this work show that the adsorption of acetaldehyde, valeric acid and ethylmethylamine on activated carbons depends, in general, on two factors: the pore size distributions and surface chemistry. The importance and thus the weight/contribution of each factor varies depending on the chemical nature and size of the adsorbate, the presence of compatible pore sizes along with the type and amount of surface groups on the adsorbent. In case of acetaldehyde adsorption, the presence of very small pores, close to the size of acetaldehyde molecules, and oxygen containing groups (to certain extent) increase the heat of adsorption to its maximum value. This is due to the contribution of hydrogen bonding to dispersive interactions of hydrocarbon moiety with the activated carbon pore walls. Small density of surface oxygen groups and nitrogen basic groups can enhance the heat of adsorption. Extensive oxidation leads to a decrease in the strength of adsorption forces. This happens due to the blocking of the pore entrances with functional groups and a decrease in the accessibility of hydrophobic surface where the dispersive interactions of hydrocarbon moiety with small pore walls can be enhanced. On the other hand, the amount of acetaldehyde adsorbed via hydrogen bonding at equilibrium conditions can be enhanced when functional groups containing oxygen or nitrogen are present. These groups can provide additional adsorption centers when all high energy centers, small pores are filled with acetaldehyde molecules. The results presented in this study show significant capacity of activated carbons, either initial or modified for adsorption of acetaldehyde.

The adsorption of valeric acid from aqueous solution on activated carbons shows the dependence on both, pore structure and surface chemistry. The later governs the adsorption at low concentrations. The presence of acidic groups on the surface of activated carbons, mainly carboxylic groups, decrease the uptake at low equilibrium concentrations by exerting repulsive interactions or by changing the polarity of the surface thus increasing its affinity toward water. In contrast, basic groups are a positive factor at low concentrations; they enhance the amount adsorbed due to the acid-base

interactions. At higher concentrations of acid (but still in the low range), the volume of small micropores (< 10 Å) is a predominant factor determining the capacity of carbons toward valeric acid removal from an aqueous solution. Although our research showed that the amount of surface basic groups and the volume of small micropores (< 10 Å) both enhance the uptake of valeric acid, the amount of strongly adsorbed valeric acid depends on the basic groups for all carbons.

This work also demonstrated how water and its interactions with surface functional groups affect the adsorption of valeric acid. Removal of valeric acid from vapor phase shows different mechanism of adsorption than that from aqueous solution. From vapor phase, both specific interactions, mainly hydrogen bonding and dispersive interactions control the adsorption process, simultaneously. Hydrogen bonding is a weaker adsorption force and the amount of valeric acid adsorbed is controlled by the total number of surface groups. The amount adsorbed via dispersive interactions depends on the presence of the very small pores. The amount adsorbed via specific interactions increases noticeably after oxidation as a result of introduction of oxygen groups.

Adsorption of EMA from an aqueous solution depends mainly on the surface chemistry of activated carbons. Porosity plays an important but not predominant role in the strength and the extent of the adsorption process. The uptake of EMA appeared to increase after oxidation as a result of acid-base interactions of adsorbate molecules with the incorporated oxygen groups. Thermal urea modification result in a decrease in the uptake especially for carbons modified at 1223 K as a result of the repulsive forces. The amount of EMA adsorbed on all carbons at high concentration depends on the total number of surface groups indicating the importance of hydrogen bonding. At low concentrations, the amount of EMA adsorbed depends on the type of surface groups, mainly the density of acidic groups. Acid-base interactions and hydrogen bonding govern the adsorption process at low concentrations. When adsorption of EMA from a vapor phase under equilibrium conditions is considered, interactions with the surface acidic groups are energetically more favorable than adsorption in the porous structure. This acid-base interactions of EMA were found exclusively for initial and oxidized carbons where strong acidic groups as carboxylic are present. They not only increase the amount adsorbed but also promote the incorporation of nitrogen when carbon is exposed to heat

treatment. This is the result of thermal decomposition of ethylmethylamine cations and formation of amines, which react with the carbon surface at elevated temperatures.

The adsorption of high concentrations of ethylmethylamine vapor from a humid air stream by an activated carbon bed has been also studied and the adsorption capacity and kinetics were evaluated. The adsorption behavior is quite different from the adsorption of trace quantities from an aqueous solution. The introduction of surface groups has no direct effect on EMA adsorption. On the other hand, these surface groups enhance water adsorption from the air stream, and hinder organic vapor adsorption. Thus the modified carbons exhibit a lower apparent capacity and slower adsorption kinetics for EMA than the untreated ones. Carbons developed for liquid adsorption of EMA are not necessarily good for vapor phase applications.

As a general conclusion, activated carbons used in this study are effective adsorbents for the removal of the human sweat odoriferous compounds: acetaldehyde, valeric acid and ethylmethylamine (EMA). Surface chemical heterogeneity along with the presence of pores smaller than 10Å can enhance the adsorption of these odorous adsorbates that are of different chemical nature. Different mechanisms of adsorption from liquid phase and vapor phase are found. The oxygen and nitrogen groups introduced into the surface as a result of oxidation and urea modification usually have varying effect for the adsorption based on the type of the compound and the phase from which adsorption takes place. In the case of adsorption from a vapor phase at dry conditions, both porosity and surface chemistry contribute to the process by exerting dispersive and specific interactions, respectively. The latter can be in form of dipole-dipole, hydrogen bonding or acid-base interactions. In adsorption from vapor phase under humid conditions, the presence of surface groups enhances water adsorption via hydrogen bonding and hence decreases the uptake of the probe compounds on the carbon surface. Although both dispersive and specific interactions seem to play a role in the adsorption process of valeric acid and EMA from aqueous solution, the amount of strongly adsorbed molecules depend mainly on the surface chemistry. Surface basic groups enhance the adsorption of valeric acid from aqueous solution while the presence of acidic groups increase the amount of EMA adsorbed. EMA adsorbed via acid-base interactions can be incorporated into the surface of activated carbon in the form of nitrogen groups by thermal treatment.

Finally, it is important to mention that in systems like human sweat when acetaldehyde, valeric acid and EMA molecules are all present, the adsorption process is much more complex. Different surface groups exert opposite effects on the adsorption process of each compound based on its chemical nature. Based on the results found in this work, the activated carbons used showed different performance with each of the probe compounds. For efficient removal of a mixture of acetaldehyde, valeric acid and EMA molecules, the activated carbons used should be featured by the presence of large volume of micropores smaller than 10Å. Moreover, the presence of acidic and basic groups, to a certain extent, on the surface of activated carbons is very important. Activated carbons with surface chemistry and porosity as those for initial BAX carbon is expected to show good performance toward such mixtures. Urea modified carbons at 723 K also showed a good adsorption capacity toward all of the probe compounds used in this study.

CHAPTER 6
CONTRIBUTIONS

This research provides the fundamentals of adsorption of body odor components on activated carbons. The work is expected to expand the application of activated carbons as human odor adsorbent from vapor phase (indoor filters) and liquid phase (carbon pads and deodorants). Adsorption of acetaldehyde, valeric acid and ethylmethylamine (EMA) on activated carbon depends on surface chemistry and the presence of pores smaller than 10Å. Owing to the differences in the chemical nature and size of the above odorous compounds, different mechanisms govern their adsorption.

5.1 Acetaldehyde Adsorption

A. Acetaldehyde adsorption depends on both surface chemistry and porosity of the carbon.

B. Hydrogen bonding and dispersive interactions contribute to the heat of acetaldehyde adsorption.

C. The presence of very small pores (<10Å) and small amount of oxygen containing groups (~0.3 mmol/g) increase the heat of adsorption to reach its maximum value.

D. Extensive oxidation results in a hydrophilic surface. Oxygen-containing groups block the pore entrances which results in a decrease in the strength of adsorption forces.

E. After urea modification, surface basic groups enhance the isosteric heats of adsorption while surface acidic groups have a negative effect on the heat.

F. At very low surface coverage acetaldehyde tends to adsorb in the small pores whereas with increasing surface coverage, acetaldehyde gradually adsorbs in larger pores where interaction with functional groups start to contribute to the adsorption process.

G. Oxidation and urea modifications increase the amount adsorbed via hydrogen bonding owing to the increase in the amount of surface polar groups.

H. Oxidation and urea modifications decrease the amount adsorbed via dispersive interactions due to a decrease in the volume of micropores and an increase in the hydrophilic character of the surface.

5.2 Valeric Acid Adsorption

A. The presence of basic groups on the surface of activated carbons enhances the uptake of valeric acid at low concentrations where the adsorption process is governed by acid-base interactions. The presence of acidic groups, mainly carboxylic groups, exerts repulsive interactions and increases the affinity of the adsorbent toward water by changing the polarity of the surface.

B. At higher concentrations of valeric acid, the volume of small micropores (< 10 Å) determines the capacity of carbons toward the valeric acid removal.

C. Urea modifications at both temperatures enhance the amount of valeric acid strongly adsorbed due to the introduction of basic groups which enhance the acid-base interactions.

D. The amount of valeric acid strongly adsorbed (molecules/nm^2) from aqueous solution on activated carbon greatly depends on the density of surface basic groups rather than the volume of pores smaller than 10 Å.

E. Dispersive interactions and hydrogen bondings, rather than acid-base interactions, control the adsorption process of valeric acid from a vapor phase at dry conditions.

F. The amount of valeric acid adsorbed from a vapor phase via hydrogen bonding increases after oxidation as a result of introduction of surface oxygen groups while the amount adsorbed via dispersive interactions decreases owing to a decrease in the volume of the very small pores.

G. Both oxidation and urea modifications enhance the removal of valeric acid from vapor phase at dry conditions.

5.3 EMA Adsorption

A. EMA adsorption from a liquid phase and vapor phase (dry and humid conditions) on activated carbons is governed by quite different mechanisms.

B. Adsorption of EMA from aqueous solution at low and at high equilibrium concentrations depends mainly on the surface chemistry of activated carbons rather than porosity which does not play a predominant role in the strength and the extent of the adsorption process.

C. At low equilibrium concentrations, specific acid-base interactions control the adsorption process. The presence of acidic groups, mainly carboxylic, enhances the adsorption of EMA while basic groups exert repulsive forces.

D. Oxidation increases the uptake of EMA as a result of incorporation of oxygen acidic groups while thermal urea modification results in a decrease in the uptake especially for carbons modified at 1223 K. This happens due to the repulsive forces.

E. Dipole-dipole, hydrogen bonding or specific acid-base interactions govern the mechanism for EMA adsorption from a vapor phase at dry conditions. The interactions with the surface acidic groups are energetically more favorable than adsorption in the porous structure. Acid-base interactions are predominant mainly in case of initial and oxidized carbons where strong acidic groups such as carboxylic are present.

F. The importance of acidic groups on the surface for EMA adsorption is not only in their enhancing effect on the amount adsorbed but on promotion the incorporation of nitrogen into the surface by heat treatment. This is the result of thermal decomposition of ethylmethylamine cations and formation of amines, which react with the carbon surface at elevated temperatures. After EMA adsorption, the spent carbons can be thermally treated so they can have new application in catalytical processes such as hydrogen sulfide adsorption.

G. Oxidation and urea modifications decrease the amount adsorbed at high concentrations of EMA vapor from a humid air stream. This is because water competes with EMA molecules for the surface groups. Water adsorbs preferably via hydrogen bonding and thus hinders EMA adsorption.

REFERENCES

1. Abassi, W. A., Streat, M., Adsorption of Uranium from Aqueous Solutions Using Activated Carbon. *Separ. Sci. Technol.* **29**, 1217 (1994).
2. Bansal, R. C., Donnet, J. B., Stoeckli, F., *Active Carbon*; Marcel Dekker, NewYork, 1988.
3. Gregg, S. J., Sing K. S. W., *Adsorption, Surface Area and Porosity*; Academic Press, NewYork, 1982.
4. Puri, B. R., In *Chemistry and Physics of Carbon*; Walker P. J., Ed., Marcel Dekker, New York, 1970, Vol. 6.
5. Boehm, H. P., *In Advances in Catalysis*; Academic Press, New York, 1966, Vol. 16.
6. Bandosz, T. J., Jagiello, J., Contescu, C., Schwarz, J. A., Characterization of the Surfaces of Activated Carbons in Terms of Their Acidity Constant Distributions. *Carbon* **31**, 1193 (1993).
7. Jagiello, J., Bandosz, T. J., Schwarz, J. A., Carbon Surface Characterization in Terms of Acidity Constant Distribution. *Carbon* **32**, 1026 (1994).
8. Contescu, A., Contescu, C., Putyera, K., Schwarz, J. A., Surface Acidity of Carbons Characterized by Their Continuous pK_a Distribution and Boehm Titration. *Carbon* **35**, 83 (1997).
9. Zawadzki, J., *In Chemistry and Physics of Carbon*; Thrower, P. A., Ed., Marcel Dekker, New York, 1989, Vol. 21.
10. Fanning, P. E, Vennice, M. A., A DRIFTS Study of the Formation of Surface Groups on Carbon by Oxidation. *Carbon* **31**, 721 (1993).
11. Donnet, J. B., Guilpain, G., Surface Treatments and Properties of Carbon Fibers. *Carbon* **27**, 749 (1989).
12. Kozlowski, C., Sherwood, P. M., X-Ray Photoelectron Spectroscopic Studies of Carbon Fibre Surfaces VII-Electrochemical Treatment in Ammonium Salt Electrolytes. *Carbon* **24**, 357 (1986).
13. Adib, F., Bagreev, A., Bandosz, T. J., Effect of the pH and Surface Chemistry on the Mechanism of H_2S Removal by Activated Carbons. *J. Colloid Interface Sci.* **216**, 360 (1999).

14. Papirer, E., Bantzer, J., Sheng, L., Donnet, J. B., Surface Groups on Nitric Acid Oxidized Carbon Black Samples Determined by Chemical and Thermodesorption Analysis. *Carbon* **29**, 69 (1991).
15. Otake,Y., Jenkins, R. G., Characterization of Oxygen-Containing Surface Complexes Created on a Microporous Carbon by Air and Nitric Acid Treatment. *Carbon* **31**, 109 (1993).
16. http://www.wipn.com
17. Duong, D. Do., *Adsorption Analysis: Equilibria and Kinetics*; Imperial College Press, London, 1998.
18. Mattson, J. S., Mark, H. B., *Activated Carbon, Surface Chemistry and Adsorption from Solution*; Marcel Dekker, New York (1971).
19. Smisek, M., Cerny, S., *Active Carbon*; Elsevier: Amsterdam, 1970.
20. Stoeckli, H. F., Microporous Carbons and Their Characterization: The Present State of the ART. *Carbon* **28**, 1 (1990).
21. Donnet, J. B., Papirer, E., Wang, W., Stoeckli, H. F., The Observation of Activated Carbons by Scanning Microscopy. *Carbon* **32,** 183 (1994).
22. Marsh, H., Heintz, E. A., Rodriguez-Reinoso, F. Eds., *Introduction to Carbon Technologies*; University of Alicante, Alicante, Spain, 1997.
23. Leon y Leon, C. A., Radovic, L. R., *In Chemistry and Physics of Carbon*; P.A. Thrower, Ed., Marcel Dekker, New York, 1992, Vol. 24.
24. Bandosz T. J., Inverse Gas Chromatography at Infinite Dilution as a Method to Determine the Structural and Chemical Features of Activated Carbon Surfaces, *Encyclopedia of Colloid and Interface Science*; A. Hubbard Ed., M. Decker, 2002.
25. Vidic R. D., Siler, D. P., Vapor-Phase Elemental Mercury Adsorption by Activated Carbon Impregnated with Chloride and Chelating Agents. *Carbon*, **39**, 3 (2001).
26. Hayden, R. A., U.S. Patent 5,444,031, 1995.
27. Matviya T. M., Hayden, R. A., U.S. Patent 5,356,849, 1994.
28. Adib, F., Bagreev, A., Bandosz, T. J., Adsorption/Oxidation of Hydrogen Sulfide on Nitrogen-Containing Activated Carbons *Langmuir* **16,** 1980 (2000).
29. Brunauer, S., *The Adsorption of Gases and Vapors*; Princeton: London, 1943 vol. 1.

30. Newcombe, G., Drikas, M., Hayes, R., Influence of Characterised Natural Organic Material on Activated Carbon Adsorption: II. Effect on Pore Volume Distribution and Adsorption of 2-Methylisoborneol. *Water Res.* **31**, 1065 (1997).
31. Dubinin, M. M., Water Vapor Adsorption and the Microporous Structures of Carbonaceous Adsorbents. *Carbon* **18**, 355 (1980).
32. Branton, P. J., Hall, P. G., Sing, K. S. W., Reichert, H., Schüth, F., Unger K., Physisorption of Argon, Nitrogen, and Oxygen by MCM-41, a Model Mesoporous Adsorbent. *J. Chem. Soc. Faraday Trans.* **90**, 2965 (1994).
33. Everett, D. H., Powl, J. C., Adsorption in Slit-Like and Cylindrical Micropores in the Henry's Law Region. *J. Chem. Soc. Faraday Trans. 1* **72**, 619 (1976).
34. Avgul, N. N., Kiselev, A. V., *In Chemistry and Physics of Carbon*; Walker P. J. Jr. Ed., Marcel Dekker, New York, 1970, Vol. 6.
35. Bandosz, T. J., Jagiello, J., Schwarz, J. A., Effect of Surface Chemical Groups on Energetic Heterogeneity of Activated Carbons. *Langmuir* **9**, 2528 (1993).
36. Adamson, A. W., *Physical Chemistry of Surfaces*; 2nd edition, Academic Press, New York, 1967.
37. Trapnell, B. M. W., *Chemisorption*, Academic Press, New York, 1955.
38. Dubinin, M. M., *In Chemistry and Physics of Carbon*; P.L. Walker, Jr., Ed., M. Dekker: New York, 1966; *Vol. 2*.
39. Mangun, C. L., Benak, K. R., Daley, M.A., Economy, J., Oxidation of Activated Carbon Fibers: Effect on Pore Size, Surface Chemistry, and Adsorption Properties. *Chem. Mater*. **11**, 3476 (1999).
40. Dimotakis, E., Cal, M. P., Economy, J., Rood, M.; Larson, S. M., Chemically Treated Activated Carbon Cloths for Removal of Volatile Organic Carbons from Gas Streams: Evidence for Enhanced Physical Adsorption. *Environ. Sci. Technol.* **29**, 1876 (1995).
41. Kaneko, Y., Abe, M., Ogino, K., Adsorption Characteristics of Organic Compounds Dissolved in Water on Surface-Improved Activated Carbon Fibres. *Colloids Surfaces* **37**, 211 (1989).

42. Pendleton, P., Wong, S. H., Schumann, R., Levay, G., Denoyel, R., Rouquerol, J., Properties of Activated Carbon Controlling 2-Methylisoborneol Adsorption. *Carbon* **35**, 1141 (1997).
43. Franz, M., Arafat, H. A., Pinto, N. G., Effect of Chemical Surface Heterogeneity on the Adsorption Mechanism of Dissolved Aromatics on Activated Carbon. *Carbon* **38**, 1807 (2000).
44. Considine, R., Denoyel, R., Pendleton, P., Schumann, R., Wong, S. H., The Influence of Surface Chemistry on Activated Carbon Adsorption of 2-Methylisoborneol from Aqueous Solution. *Colloids Surfaces A: Physicochem. Eng. Aspects* **179**, 271 (2001).
45. Karanfil, T., Kitis, M., Kilduff, J., Wigton, A., Role of Granular Activated Carbon Surface Chemistry on the Adsorption of Organic Compounds. 2. Natural Organic Matter. *Environ. Sci. Technol.* **33**, 3225 (1999).
46. Jelski, W., Chrostek, L., Szmitkowski, M., Metabolism of Ethyl Alcohol in the Human Body. *Postepy Hig. Med. Dosw.* **53**, 871 (1999).
47. Cal, M. P., Rood, M. J., Larson, S. M., Gas Phase Adsorption of Volatile Organic Compounds and Water Vapor on Activated Carbon Cloth. *Energy & Fuels* **11**, 311 (1997).
48. Dubinin, M. M., The Potential Theory of Adsorption of Gases and Vapors for Adsorbents with Energetically Nonuniform Surfaces. *Chem. Rev.* **60**, 235 (1960).
49. Cal, M. P., *Doctoral Dissertation*: Characterization of Gas Phase Adsorption Capacity of Untreated and Chemically Treated Activated Carbon Cloths, University of Illinois at Urbana-Champaign; University of Michigan Press: Ann Arbor, MI, 1995.
50. Rong, H., Ryu, Z., Zheng, J., Zhang, Y., Influence of Heat Treatment of Rayon-Based Activated Carbon Fibers on the Adsorption of Formaldehyde. *J. Colloid Interface Sci.* **261**, 207 (2003).
51. Domingo-Garcia, M., Fernandez-Morales, F. J., Lopez-Garzon, F. J., Moreno-Castilla, C., Perez-Mendoza, M., On the Adsorption of Formaldehyde at High Temperatures and Zero Surface Coverage. *Langmuir* **15**, 3226 (1999).

52. Hayashi, T., Kumita, M., Otani, Y., Removal of Acetaldehyde Vapor with Impregnated Activated Carbons: Effects of Steric Structure on Impregnant and Acidity. *Environ. Sci. Technol.* **39**, 5436 (2005).
53. Traube, J., Ueber die Capillaritatsconstanten Organischer Stoffe in Wassriger Losung, *Annalen* **265**, 27 (1891).
54. Freundlich, H., On Adsorption from Solution. *Physik. Chemie*, **57**, 385 (1907).
55. Landt, E., Knop, W., Adsorption Displacement and Molecular Orientation on Activated Ash-Free Charcoal. *Z. Phys. Chem*. **A162**, 331 (1932).
56. Parkash, S., Adsorption of Weak and Non-electrolytes by Activated Carbon. *Carbon* **12,** 37 (1974).
57. Wang, S. W., Hines, A. L., Farrier, D. S., Adsorption of Aliphatic Acids from Aqueous Solutions onto Activated Carbon, *J. Chem. Eng. Data* **24,** 345, 1979.
58. Holmes, H. N., McKelvey, J. B., The Reversal of Traube's Rule of Adsorption. *J. Phys. Chem*. **32**, 1522 (1928).
59. Nekrassow, B., Adsorption in Solutions. XVI. Reversal of Traube's Adsorption Law. *Z. Physik. Chem*. **136**, 379 (1928).
60. Bruns, B., The Effect of Disintegration of Charcoal on the Adsorption of Fatty Acids. *Kolloid-Z.*, **54**, 33 (1931).
61. Hansen, R. S., Fu, *Y.*, Bartell, F. E., Multimolecular Adsorption from Binary Liquid Solutions. *J. Phys. Chem.* **53**, 769,(1949)
62. Hansen, R. S., R. P. Craig, The Adsorption of Aliphatic Alcohols and Acids from Aqueous Solutions by Non-porous Carbons. *J. Phys. Chem.* **58**, 211(1954).
63. Weatherburn, A. S., Rose, G. R. F., Bayley, C. H., Adsorption of Soap by Carbon Black. *Can. J. Research* **27F**, 179 (1949).
64. Reade, M. A., Weatherburn, A. S., Bayley, C. H., The Adsorption of Sodium Myristate by Carbon Black. *Can. J. Research* **27F**, 426 (1949).
65. Kipling, J. I., Adsorption from Solutions of Non-electrolytes, Academic Press: New York, 1965.
66. Mattson, J. A., Mark, H. B., Malbin, M. D., Weber, W. J., Crittenden, J. C., Surface Chemistry of Active Carbon: Specific Adsorption of Phenols. *J. Colloid Interface Sci.* **31,** 116 (1969).

67. Ellison, M. D., Crotty, M. J., Koh, D., Spray, R. L., Tate, K. E., Adsorption of NH_3 and NO_2 on Single-Walled Carbon Nanotubes. *J. Phys. Chem. B* **108**, 7938 (2004).
68. Pérez-Mendoza, M., Domingo-Garcı´a, M., Lo´pez-Garzo´n, F. J., Adsorption of Methylamines on Carbon Materials at Zero Surface Coverage. *Langmuir* **16**, 7012 (2000).
69. Donnet, J. B., Park, S. J., Surface Characteristics of Pitch-Based Carbon Fibers by Inverse Gas Chromatography Method. *Carbon* **29**, 955 (1991).
70. Derouanne, E. G., Zeolites as Solid Solvents. *J. Mol. Catal. A: Chem.* **134**, 29 (1998).
71. Jagtoyen, M., Derbyshire, F., Activated Carbons from Yellow Poplar and White Oak by H_3PO_4 Activation. *Carbon* **36**, 1085 (1998).
72. Boehm, H. P., Some Aspects of the Surface Chemistry of Carbon Blacks and Other Carbons. *Carbon* **32,** 759 (1994).
73. Henkin, R.I., Body Odor. *JAMA* **273**, 1171 (1995).
74. Bandosz, T. J., Jagiello, J., Schwarz, J. A., Comparison of Methods to Assess Surface Acidic Groups on Activated Carbons. *Anal. Chem*. **64**, 891 (1992).
75. Bagreev, A., Lahaye, J., Nanse, G., Strelko, V., Porous Structure and Surface Chemistry of Nitrogen Containing Carbons from Polymers. *Carbon* **37**, 585 (1999).
76. Kortum, G., Vogel. W., Andrussow, K., *Dissociation Constants of Organic Acids in Aqueous Solutions*; Butterworth, London, 1961.
77. Bandosz, T. J., Buczek, B., Grzybek, T., Jagiello, J., The Determination of Surface Changes in Active Carbons by Potentiometric Titration and Water Vapour Adsorption. *Fuel* **76**, 1409 (1997)
78. Jagiello, J., Stable Numerical Solution of the Adsorption Integral Equation Using Splines. *Langmuir* **10**, 2778 (1994).
79. Burg, P., Fydrych, P., Cagniant, D., Nanse, G., Bimer, J., Jankowska, A., The Characterization of Nitrogen-Enriched Activated Carbons by IR, XPS and LSER Methods. *Carbon* **40**, 1521 (2002).
80. Blazso, M., Thermal Decomposition of Oligomeric and Polymeric Hindered Amine Light Stabilizers. *J. Anal. & Applied Pyrolysis* **58**, 29 (2001).

81. Villar-Rodil, S., Martinez-Alonso, A., Tascon, J. M. D., Studies on Pyrolysis of Nomex Polyaramid Fibers. *J. Anal. &Applied Pyrolysis* **58**, 105 (2001).
82. Olivier, J. P., Conklin, W. B., *Presented at the 7th Int. Conf. On Surf. & Coll. Sci*.; Compiegne, France, 1991.
83. Lastokie, C. M., Gubbins, K. E., Quirke, N., Pore Size Distribution Analysis of Microporous Carbons: A Density Functional Theory Approach. *J. Phys. Chem.* **97**, 4786 (1993).
84. Conder J. R., Young C. L., *Physicochemical Measurement by Gas Chromatography*; Wiley: NewYork, 1979.
85. Voelkel, A., Inverse Gas Chromatography: Characterization of Polymers, Fibers. *Crit. Rev. Anal. Chem.* **22**, 411 (1991).
86. Tijburg, I., Jagiello, J., Vidal, A., Papirer, E., Inverse Gas Chromatographic Studies on Silica: Infinite Dilution and Finite Concentration Measurements. *Langmuir* **7**, 2243 (1991).
87. Paryjczak, T., *Gas Chromatography and Catalysis*; Polish Scientific Publisher, Warszawa, 1986.
88. Glueckauf, E., Theory of Chromatography. Part II. Chromatograms of a Single Solute. *J. Chem. Soc. London*, 1302 (1947).
89. Habgood, H. W., Flood, E. A., Ed., *The Solid-Gas Interface*; Marcel Dekker: New York, 1967.
90. Karger, B. L., Sewell, P. A., Castells, R. C., Hartkoft, A., Gas Chromatographic Study of the Adsorption of Insoluble Vapors on Water. *J. Colloid Interface Sci*. **35**, 328 (1971).
91. Hartkoft, A.; Karger, B. L., Study of the Interfacial Properties of Water by Gas Chromatography. *Acc. Chem. Res*. **6**, 209 (1973).
92. Salame, I. I, Bandosz, T. J., Study of Diethyl Ether Adsorption on Activated Carbons Using IGC at Finite Concentration. *Langmuir* **17**, 4967 (2001).
93. Kilduff, J., Karanfil, T., Webe, W., Competitive Interactions among Components of Humic Acids in Granular Activated Carbon Adsorption Systems: Effects of Solution Chemistry. *Environ. Sci. Technol*. **30**, 1344 (1996).

94. Summers, R. S., Roberts, P. V., Activated Carbon Adsorption of Humic Substances: I. Heterodisperse Mixtures and Desorption. *J. Colloid Interface Sci.* **122**, 367 (1988).
95. Summers, R. S., Roberts, P. V., Activated Carbon Adsorption of Humic Substances: II. Size Exclusion and Electrostatic Interactions. *J. Colloid. Interface Sci.* **122**, 382 (1988).
96. Kilduff, J., Karanfil, T., Chin, Y., Weber, J. W., Adsorption of Natural Organic Polyelectrolytes by Activated Carbon: A Size-Exclusion Chromatography Study. *Environ. Sci. Technol*. **30**, 1336 (1996).
97. Hollander, A. F., Somasundaran, P., Gryte, C.C., *Adsorption from Aqueous Solution*; Plenum: New York, 1981.
98. Stárek, J., Zukal, A., and Rathouský, J., Comparison of the Adsorption of Humic Acids from Aqueous Solutions on Active Carbon and Activated Charcoal Cloths. *Carbon* **32**, 207 (1994).
99. Snoeyink, V. L., Hai, H. T., Johnson, J. H., Young, J. F., *Chemistry of Water Supply, Treatment and Distribution*; Ann Arbor Sciences, Ann Arbor: MI, 1974.
100. Mecklenburg, W., Schichtenfiltration, U., Layer Filtration-Theory of the Gas Mask. *Z. Electrochem.* **31**, 488 (1925).
101. Jonas, L. A., Rehrmann, J. A., The Kinetics of Adsorption of Organo-Phosphorus Vapors from Air Mixtures by Activated Carbons. *Carbon*, 10, 657 (1972).
102. Lodewyckx, P., Vansant, E. F., Influence of Humidity on Adsorption Capacity From Wheeler–Jonas Model for Prediction of Breakthrough Times of Water Immiscible Organic Vapors on Activated Carbon Beds. *Am. Ind. Hyg. Assoc. J.* **60**, 612, 1999.
103. Claesson, J. O., Fangmark, I., Hammarstrom, L., A Systematic Investigation of the Overall Rate Coefficient in the Wheeler–Jonas Equation for Adsorption on Dry Activated Carbons. *Carbon* **43,** 481 (2005).
104. Yoon, Y. H., Nelson, J. H., Application of Gas Adsorption Kinetics. I. A Theoretical Model for Respirator Cartridge Service Life. *Am. Ind. Hyg. Assoc. J.* **45**, 509 (1984).
105. Lodewyckx, P., Vansant, E. F., Influence of Humidity on the Overall Mass Transfer Coefficient of the Wheeler-Jonas Equation. *Am. Ind. Hyg. Assoc. J.* **61**, 461 (2000).
106. National Institute for Occupational Safety and Health. *Development of improved respirator cartridge and canister test methods by DM Smoot;* Bendix Corp.

Cincinnati, Ohio: Department of Health Education and Welfare; National Institute for Occupational Safety and Health, 1977. p. 60.

107. Jonas, L. A., Rehrmann, J. A., Predictive Equations in Gas Adsorption Kinetics. *Carbon* **11**, 59 (1973).

108. Dubinin, M. M., Fundamentals of the Theory of Adsorption in Micropores of Carbon Adsorbents: Characteristics of Their Adsorption Properties and Microporous Structures. *Carbon* **27**, 457 (1989).

109. Wood, G. O., Stampfer, J. F., Adsorption Rate Coefficients for Gases and Vapors on Activated Carbons. *Carbon* **31**, 195 (1993).

110. Lodewyckx, P., Vansant, E. F., Estimating the Overall Mass Transfer Coefficient K_v of the Wheeler–Jonas Equation: A New and Simple Model. *Am. Ind. Hyg. Assoc. J.* **61**, 501 (2000).

111. Lodewyckx, P., Wood, G. O., Ryu, S. K., The Wheeler–Jonas Equation: A Versatile Tool for the Prediction of Carbon Bed Breakthrough Times: Influence of Humidity on the Overall Mass Transfer Coefficient of the Wheeler-Jonas Equation. *Carbon* **42**, 1351 (2004).

112. Carrasco-Marin, F., Mueden, A., Centeno, T. A., Stoeckli, F., Moreno-Castilla, C., Water Adsorption on Activated Carbons with Different Degrees of Oxidation. *J. Chem. Soc. Faraday Trans.* **93**, 2211 (1997).

113. Jagiello, J., Bandosz, T. J., Schwarz, A. J., Application of Inverse Gas Chromatography at Infinite Dilution to Study the Effects of Oxidation of Activated Carbons. *Carbon* **30**, 62 (1992).

114. Strelko, Jr. V., Malik, D. J., Streat, M., Characterisation of the Surface of Oxidized Carbon Adsorbents. *Carbon* **40**, 95 (2002).

115. Jagiello, J., Bandosz, T. J., Putyera, K., Schwarz, J. A., Determination of Proton Affinity Distributions for Chemical Systems in Aqueous Environments Using a Stable Numerical Solution of the Adsorption Integral Equation. *J. Colloid Interface Sci.* **172**, 341(1995).

116. Salame, I., Bandosz, T. J., Surface Chemistry of Activated Carbons: Combining the Results of Temperature-Programmed Desorption, Boehm, and Potentiometric Titrations. *J. Colloid Interface Sci.* **240**, 252 (2001).

117. Biniak, S., Szymanski, G., Siedlewski, J., Swiatkowski, A., The Characterization of Activated Carbons with Oxygen and Nitrogen Surface Groups. *Carbon* **35**, 1799 (1997).
118. *Handbook of Chemistry and Physics;* Weast, R.C. Ed., CRC Press, 67th edition, Boca Raton, Fl., 1986.
119. Jagiello, J., Bandosz, T. J., Schwarz, J. A., Inverse Gas Chromatographic Study of Activated Carbons: The Effect of Controlled Oxidation on Microstructure and Surface Chemical Functionality. *J. Colloid Interface Sci.* **151**, 433 (1992).
120. Bandosz, T. J., Jagiello, J., Schwarz, J. A., Krzyzanowski, A., Effect of Surface Chemistry on Sorption of Water and Methanol on Activated Carbons. *Langmiur* **12**, 6480 (1996).
121. Moreno-Castilla, C., Carrasco-Marin, F., Mueden, A., The Creation of Acid Carbon Surfaces by Treatment with $(NH_4)_2S_2O_8$. *Carbon* **35**, 1619 (1997).
122. Elsayed, Y., Bandosz, T. J., A Study of Acetaldehyde Adsorption on Activated Carbons. *J. Colloid Interface Sci.* **44**, 242 (2001).
123. Elsayed, Y., Bandosz, T. J., Acetaldehyde Adsorption on Nitrogen-Containing Activated Carbons. *Langmuir* **18**, 3213 (2002).
124. Elsayed, Y., Bandosz, T. J., Effect of Increased Basicity of Activated Carbon Surface on Valeric Acid Adsorption from Aqueous Solution. *Phys. Chem. Chem. Phys.* **5**, 4892 (2003).
125. Elsayed, Y., Bandosz, T. J., Adsorption of Valeric Acid from Aqueous Solution onto Activated Carbons: Role of Surface Basic Sites. *J. Colloid Interface Sci.* **273**, 64 (2004).
126. Karanfil, T., Kilduff, J. E., Role of Granular Activated Carbon Surface Chemistry on the Adsorption of Organic Compounds. 1. Priority Pollutants. *Environ. Sci. Technol.* **33**, 3217(1999).
127. Müller, G., Radke, C. J., Prausnitz, J. M., Adsorption of Weak Organic Electrolytes from Aqueous Solution on Activated Carbon. Effect of pH. *J. Phys. Chem.* **84**, 369 (1980).

128. Müller, G., Radke, C. J., Prausnitz, J. M., Adsorption of Weak Organic Electrolytes from Dilute Aqueous Solution onto Activated Carbon. Part I. Single-solute Systems. *J. Colloid Interface Sci.* **103**, 466 (1985).
129. Müller, G., Radke, C. J., Prausnitz, J. M., Adsorption of Weak Organic Electrolytes from Dilute Aqueous Solution onto Activated Carbon. Part II. Multisolute Systems. *J. Colloid Interface Sci.* **103**, 484 (1985).
130. McCallum, C. L., Bandosz, T. J., McGrother, S. C., Muller, E. A., Gubbins, K. E., A Molecular Model for Adsorption of Water on Activated Carbon: Comparison of Simulation and Experiment. *Langmuir*, **15**, 533 (1999).
131. Iiyama, T., Nishikawa, K., Otowa, T., Kaneko, K., An Ordered Water Molecular Assembly Structure in a Slit-Shaped Carbon Nanospace. *J. Phys. Chem.* **99**, 10075 (1995).
132. Dubinin, M. M., Serpinsky, V. V., Isotherm Equation for Water Vapor Adsorption by Microporous Carbonaceous Adsorbents. *Carbon* **19**, 402 (1981).
133. Do D. D., and Do H. D., A model for water adsorption in activated carbon. *Carbon* **38**, 767 (2000).
134. Salame, I. I., Bandosz, T. J., Experimental Study of Water Adsorption on Activated Carbons. *Langmuir* **15**, 587 (1999).
135. Salame, I. I., Bandosz, T. J., Study of Water Adsorption on Activated Carbons with Different Degrees of Surface Oxidation. *J. Colloid Interface Sci.* **210**, 367 (1999).
136. Derylo-Marczewska, A., Analysis of the Adsorption Equilibrium for the System Dilute Aqueous Solution of Dissociating Organic Substance-Activated Carbon. *Langmuir* **9**, 2344 (1993).
137. Sokoll, R., Hobert, H, Schmuck, I., Thermal Desorption and Infrared Studies of Amines Adsorbed on SiO_2 Al_2O_3, Fe_2O_3, MgO, and CaO I. Diethylamine and Triethylamine. *J. Catal.* **121**, 153 (1990).
138. Veefkind, V., *Shape Selective Synthesis of Alkylamines over Acid Catalysts*. Ph.D. thesis, http://doc.utwente.nl/fid/1108, University of Twente, The Netherlands, 1998.
139. Kenvin, J., Micromeritics application notes #134, September 2003.
140. Smith, P. A., *Open-Chain Nitrogen Compounds*; W.A., Benjamin, Inc.: New York, 1965.

141. El-Sayed, Y., Bandosz, T. J., Role of Surface Oxygen Groups in Incorporation of Nitrogen to Activated Carbons via Ethylmethylamine Adsorption. *Langmuir* **21**, 1282 (2005).
142. Brennan, J. K., Bandosz, T. J., Thomson, K. T., Gubbins, K. E., Water in Porous Carbons. *Colloids and Surfaces A* **187-188**, 539 (2001).
143. Salame, I. I., Bandosz, T. J., Adsorption of Water and Methanol on Micro- and Mesoporous Wood-Based Activated Carbons. *Langmuir* **16**, 5435 (2000).
144. Lodewyckx, P., Vansant, E. F., Water Isotherms of Activated Carbons with Small Amounts of Surface Oxygen. *Carbon* **37**, 1647 (1999).